

Mechanistic Studies of One-Electron Reduced Bipyridine Reactions Relevant to Carbon
Dioxide Sequestration

by

Rajeev Ranjan

A Dissertation Presented in Partial Fulfillment
of the Requirement for the Degree
Doctor of Philosophy

Approved March 2015 by the
Graduate Supervisory Committee:

Ian R. Gould, Co-Chair
Daniel A. Buttry, Co-Chair
Jeff Yarger
Dong-Kyun Seo

ARIZONA STATE UNIVERSITY

May 2015

ABSTRACT

Increasing concentrations of carbon dioxide in the atmosphere will inevitably lead to long-term changes in climate that can have serious consequences. Controlling anthropogenic emission of carbon dioxide into the atmosphere, however, represents a significant technological challenge. Various chemical approaches have been suggested, perhaps the most promising of these is based on electrochemical trapping of carbon dioxide using pyridine and derivatives. Optimization of this process requires a detailed understanding of the mechanisms of the reactions of reduced pyridines with carbon dioxide, which are not currently well known. This thesis describes a detailed mechanistic study of the nucleophilic and Bronsted basic properties of the radical anion of bipyridine as a model pyridine derivative, formed by one-electron reduction, with particular emphasis on the reactions with carbon dioxide. A time-resolved spectroscopic method was used to characterize the key intermediates and determine the kinetics of the reactions of the radical anion and its protonated radical form. Using a pulsed nanosecond laser, the bipyridine radical anion could be generated in-situ in less than 100 ns, which allows fast reactions to be monitored in real time. The bipyridine radical anion was found to be a very powerful one-electron donor, Bronsted base and nucleophile. It reacts by addition to the C=O bonds of ketones with a bimolecular rate constant around $1 \times 10^7 \text{ M}^{-1} \text{ s}^{-1}$. These are among the fastest nucleophilic additions that have been reported in literature. Temperature dependence studies demonstrate very low activation energies and large Arrhenius pre-exponential parameters, consistent with very high reactivity. The kinetics of E2 elimination, where the radical anion acts as a base, and SN2 substitution, where the radical anion acts as a nucleophile, are also characterized by large bimolecular

rate constants in the range ca. $10^6 - 10^7 \text{ M}^{-1} \text{ s}^{-1}$. The pKa of the bipyridine radical anion was measured using a kinetic method and analysis of the data using Marcus theory model for proton transfer. The bipyridine radical anion is found to have a pKa of 40 ± 5 in DMSO. The reorganization energy for the proton transfer reaction was found to be 70 ± 5 kJ/mol. The bipyridine radical anion was found to react very rapidly with carbon dioxide, with a bimolecular rate constant of $1 \times 10^8 \text{ M}^{-1} \text{ s}^{-1}$ and a small activation energy, whereas the protonated radical reacted with carbon dioxide with a rate constant that was too small to measure. The kinetic and thermodynamic data obtained in this work can be used to understand the mechanisms of the reactions of pyridines with carbon dioxide under reducing conditions.

ACKNOWLEDGEMENTS

First of all, I would like to thank my research advisor at ASU: Ian Gould, who brought me to the world of photochemistry and kinetic studies of transients, developed me to be an independent scientific professional, and always inspiring my passion on new research challenges. He is always there to help, provided me an unique opportunity to study at ASU, gave me useful research suggestions, and helped me toward a successful future career. I would like to thank Daniel Buttry, my co-advisor who provided me valuable mentoring during my qualifying exam and continuous inputs throughout my PhD. I would like to thank Don Seo, my committee member who was always there for help. He provided me valuable guidance on my project. I am thankful to him for serving on my committee at a difficult situation. I would like to thank Jeff Yarger for his continuous help and support

I am very grateful to various colleagues and friends at ASU for helping me with my research and leaving me memorable graduate school experiences. People to acknowledge (without a particular order) include: Ashok Kumar, Chris Starr, Tim Lamb, Dan Mahlman, David Nutt and Martha McDowell.

This would not be possible without the tremendous love and support from my wife Shikha, daughter Saina and my family. I would like to give special thanks to my parents and my grandparents for always believing in me, and for always understanding and helping me throughout.

TABLE OF CONTENTS

	Page
LIST OF TABLES.....	vii
LIST OF FIGURES.....	viii
CHAPTER	
1 INTRODUCTION.....	1
1.1 Motivation for CO ₂ Capture and Sequestration.....	1
1.2 Current Status of CO ₂ Capture Technology.....	5
1.3 Electrochemical Systems for CO ₂ Capture.....	7
1.4 Photochemical Electron Transfer Reactions.....	10
1.5 Thesis Overview.....	13
References.....	15
2 EXPERIMENTAL.....	20
2.1 Time-Resolved Absorption Spectroscopy.....	20
2.2 Solvents and Donors.....	22
2.3 CO ₂ Concentration Variation.....	22
2.4 CO ₂ Solubility Measurement in DCE	23
2.5 Kinetic Study with the Carbonyls.....	23
2.6 pKa Study of the Radical Anion.....	24
References.....	25

CHAPTER	Page
3	BIPYRIDINE RADICAL ANION: CHARACTERIZATION AND REACTIVITY TOWARDS CARBONYLS AND HALIDES.....26
	3.1. Introduction.....26
	3.2 Experimental.....27
	3.3. Bipyridine Radical Anion.....28
	3.4 The Reaction of the 4,4'-Bipyridine Radical Anion With Carbonyl Compounds and Electrophiles.....35
	3.5 Bipyridine Radical Anion Kinetics with Alkyl Halides.....41
	3.6 Conclusions.....48
	References.....49
4	REVERSIBLE ELECTROCHEMICAL TRAPPING OF CARBON DIOXIDE USING 4,4'-BIPYRIDINE.....52
	4.1. Introduction.....52
	4.2. Results and Discussion..... 53
	4.2.1. Reversible Trapping of CO ₂ using 4,4'-Bipyridine as an Electrochemical Switch.....53
	4.2.2. Kinetic Studies of the Reaction Between the 4,4'-Bipyridine Radical Anion and Carbon Dioxide..... 57
	4.2.3. Computational Studies of the Reaction Between the 4,4'-Bipyridine Radical Anion and Carbon Dioxide.....62
	4.3. Computational Studies of the Distonic Carbamate Anion Radical Adduct66

CHAPTER	Page
4.4 Summary.....	71
4.5. Experimental.....	72
References.....	75
5 KINETICS AND THERMODYNAMICS OF THE 4,4'-BIPYRIDINE RADICAL ANION AS BRONSTED BASE.....	78
5.1. Introduction.....	78
5.2. Experimental.....	79
5.3 Results and Discussion.....	80
5.3.1. Reaction Kinetics.....	80
5.3.2. Data Fitting.....	82
5.4. Summary.....	88
References.....	89
6 SUMMARY OF CHAPTERS AND OUTLOOK FOR FUTURE WORK.....	92
6.1. Summary of Current Work.....	92
6.2. What Did We Learn About the Bipyridine Radical Anion.....	93
6.3. Recommendations for Future Work.....	93
REFERENCES.....	95

LIST OF TABLES

Table	Page
1. Bimolecular Rate Constants for Reaction of the 4,4'-Bipyridine Radical Anion with Electron Acceptors, and Their Reduction Potentials.....	34
2. Bimolecular Rate Constants, k_r , For Nucleophilic Addition of the Bipyridine Radical Anion With Various Carbonyl Compounds.....	42
3. Effect of Solvent and Water Content on the Bimolecular Rate Constant for Reaction Between the Bipyridine Radical Anion and Cyclohexanone, k_r ...	43
4. Bimolecular rate Constants for the Reaction Between the Bipyridine Radical Anion and Various Alkyl Halides, k_r	46
5. Bimolecular rate Constants for the Reaction Between the 2,2'-Dimethyl-4,4'-bipyridine Radical Anion and Various Alkyl Halides, k_r	47
6. Rate Constants, k_{H^+} , and Thermodynamic Data for Proton Transfer From Phenols and Other Alcohols to the Radical Anion of 4,4'-Bipyridine in Acetonitrile Solvent at Room Temperature.....	81

LIST OF FIGURES

Figure	Page
1. Plot of Global Instrumental Temperature Anomaly vs. Time.....	2
2. Plot of Atmospheric CO ₂ Concentration (ppmv) vs. Time as Measured at Mauna Loa, Hawaii.....	3
3. Scheme 1. Schematic of Post-Combustion Capture.....	5
4. Scheme 2. Overall Proposed Mechanism for the Pyridinium-Catalyzed Reduction of CO ₂ to the Various Products of Formic Acid, Formaldehyde, and Methanol.....	9
5. Orbital Representation of the Oxidation and the Reduction Processes for the Ground State R and Excited State *R.....	12
6. Schematic illustration of the transient absorption apparatus.....	21
7. Scheme 1. Reaction scheme for formation of the separated 4,4'-bipyridine radical anion (Bpy^{•-}) in the time-resolved laser experiments in solution, using either triethylamine or DABCO as the amine electron donor (A).	28
8. Transient absorption spectrum of the 4,4'-bipyridine radical anion in acetonitrile, in the presence of DABCO as an electron donor, at room temperature.....	31
9. The transient absorption spectrum of the radical product of protonation of the 4,4'-bipyridine radical anion in acetonitrile in the presence of triethylamine as the electron donor, at room temperature.....	32

Figure	Page
10. Representative absorbance decay showing decay of the 4,4'-bipyridine radical anion, monitored at 380 nm, in argon purged acetonitrile.....	33
11. Observed pseudo-first order rate constant for decay of the 4,4'-bipyridine radical anion, k_{obs} , as a function of concentration of cyclohexanone.....	36
12. Transient absorption spectra of the distonic carbamate anion radical adduct of the 4,4'-bipyridine radical anion with cyclohexanone, in acetonitrile, in the presence of DABCO in 100mM cyclohexanone solution, at room temperature.....	37
13. Arrhenius plot of the rate constant for reaction of cyclohexanone with the bipyridine radical anion in acetonitrile.....	39
14. Transient absorption spectra of the bipyridine radical adduct in acetonitrile, measured 100 ns after excitation of the bipyridine in the presence of DABCO in 60 mM t-butyl bromide solution, at room temperature.....	45
15. Cyclic voltammetry of 10 mM 4,4'-bipyridine in N-butyl-N-methylpyrrolidinium bis(trifluoromethylsulfonyl)imide ionic liquid solvent at room temperature.....	56
16. Scheme 1. Reaction scheme for formation of the separated 4,4'-bipyridine radical anion (Bpy^{•-}) in the time-resolved laser experiments in solution, using either triethylamine or DABCO as the amine electron donor (A)	58

Figure	Page
17. Transient absorption spectra of (left) the 4,4'-bipyridine radical anion in acetonitrile, (center) the radical product of protonation of the radical anion in acetonitrile measured in the presence of triethylamine, and (right) the distonic carbamate anion radical adduct in dichloromethane in the presence of DABCO in a CO ₂ saturated solution, all at room temperature.....	59
18. Observed pseudo-first order rate constant for decay of the 4,4'-bipyridine radical anion, k_{obs} , as a function of concentration of carbon dioxide. The inset is an Arrhenius plot for the reaction rate constant.....	60
19. Electronic energy (including the free energy of solvation contribution) as a function of the N–C bond length for reaction of bipyridine radical anion with carbon dioxide, $r_{\text{N-C}}$. The inset shows the smooth change in the O–C–O bond angle, as a function of decreasing $r_{\text{N-C}}$, from 180° in the reactants to 129.8° in the adduct.....	64
20. Computed free energies and structures for stationary points along the reaction coordinate for the reaction of the bipyridine radical anion with carbon dioxide to give the distonic carbamate anion radical adduct showing formation of a bimolecular complex prior to the transition state.	65
21. Computed free energies and structures for stationary points along the reaction coordinate for decarboxylation of the oxidized product of addition of the 4,4'-bipyridine radical anion and carbon dioxide, to give neutral bipyridine and carbon dioxide, showing formation of a bimolecular complex after the transition state for bond cleavage.....	68

22. Electronic energy (including the free energy of solvation contribution) as a function of the N–C bond length for the fragmentation reaction of the oxidized bipyridine radical anion with carbon dioxide, $r_{\text{N-C}'}$, showing formation of a bimolecular complex after the transition state to form the neutral 4,4'-bipyridine and carbon dioxide.70
23. Absorbance decay showing decay of the 4,4'-bipyridine radical anion, monitored at 380 nm, in the presence of 2mM trimethyl phenol. The smooth curve through the data represents the best first order kinetic fit, corresponding to a first order rate constant for decay of $9 \times 10^6 \text{ s}^{-1}$. Inset shows the spectra of bipyridine radical anion obtained by the proton transfer from phenol derivatives to bipyridine radical anion.....83
24. Log of the rate constant for bimolecular proton transfer from phenol and aliphatic alcohol proton donors to the radical anion of 4,4'-bipyridine, in acetonitrile at room temperature. The solid curve through the data points corresponds to a best fit according to Eqns 1, with $\lambda = 2.0 \text{ eV}$, $\text{pKa}(\mathbf{Bpy}^{\bullet-}\text{-H}) = 31$ and $k_{\text{diff}} = 1.1 \times 10^{10} \text{ s}^{-1}$ and $k_{\text{diff}} = 2.2 \times 10^{10} \text{ s}^{-1}$88

CHAPTER 1

INTRODUCTION

1.1 Motivation for CO₂ Capture and sequestration

Climate change associated with increasing concentrations of greenhouse gases such as carbon dioxide in the atmosphere poses a serious threat to human-kind, and has been the subject of increasing concern in the scientific community over the last 30 years.¹ Figure 1.1 shows the global mean land ocean temperature from 1880 to 2005, that illustrates a clear increase with time.² This increase in terrestrial temperature with time is commonly referred to as global warming. Increasing concentrations of atmospheric CO₂ have been linked to this observed increase in atmospheric temperature.³

The natural carbon cycle exchanges CO₂ with the oceans and vegetation.⁴ When the cycle is balanced, the amount of carbon entering the atmosphere is equal to the carbon absorbed from the atmosphere.^{5,6} Carbon dioxide concentrations in the atmosphere have been rising constantly since the industrial revolution,⁷ however, see Figure 1.2. Petroleum products and other fossil fuels have become a major energy source due to their high energy content and ready availability. The dependency on fossil fuels as energy sources has grown with increases in population and global industrialization.⁸ Burning of fossil fuels creates carbon dioxide which results into a net increase of carbon dioxide in the atmosphere. Figure 1.2 shows measurements taken at the Mauna Loa Observatory in Hawaii that show how human activity has resulted in a clear trend of rising atmospheric CO₂ concentration.⁷ Greenhouse gases

**Plot of instrumental temperature anomaly vs time
(temperature average from 1961-1990)**

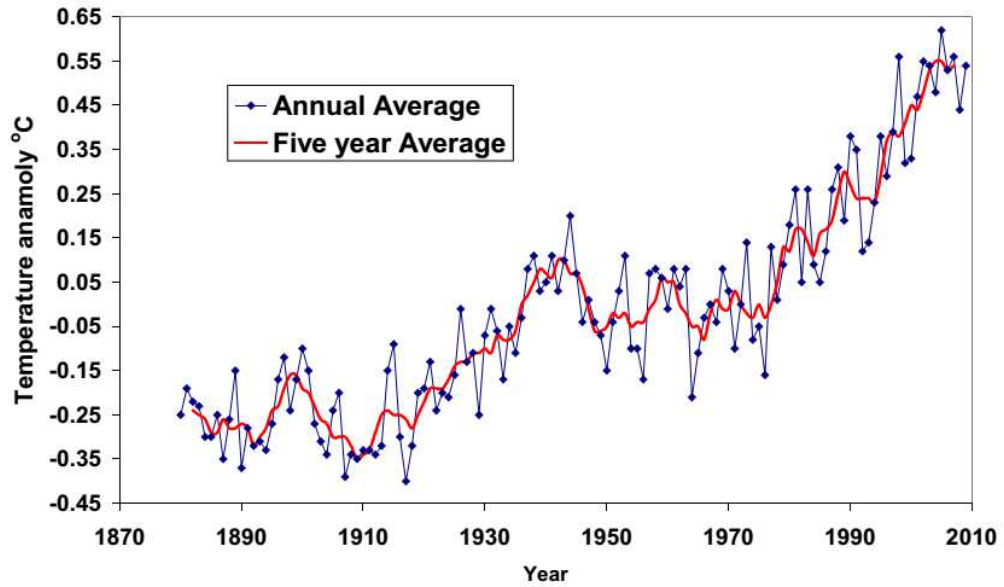


Figure 1.1. Plot of global instrumental temperature anomaly vs. time (Data from reference 2).

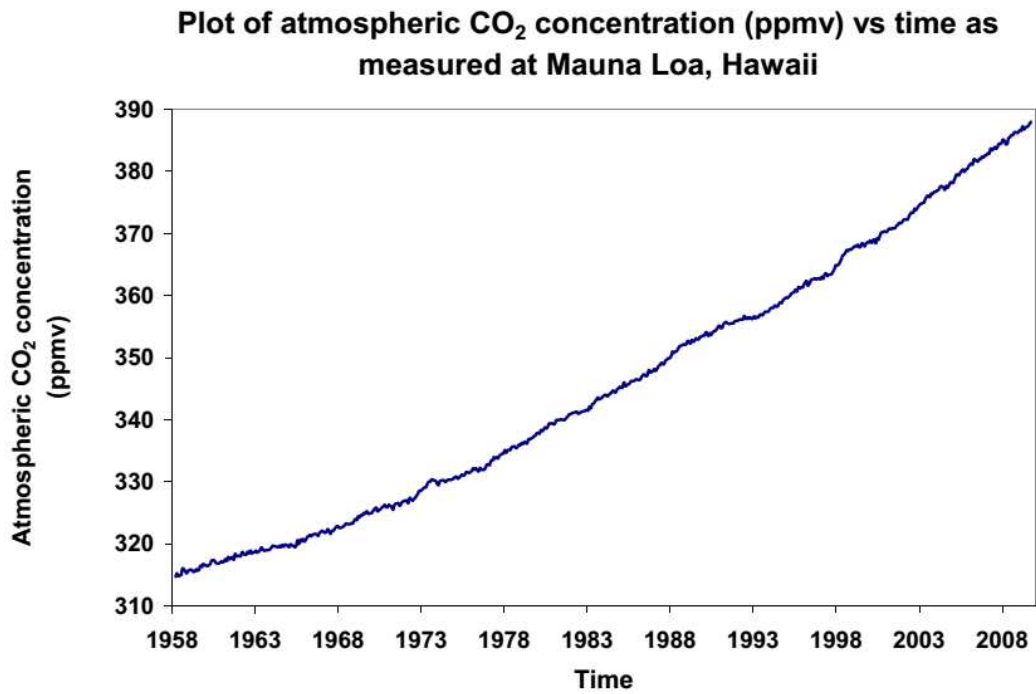


Figure 1.2. Plot of the atmospheric CO₂ concentration (ppmv) vs. time, measured at Mauna Loa, Hawaii (Data from reference 7).

such as carbon dioxide absorb a portion of the infrared radiation that is reflected from earth that results in an increase in temperature at the Earth's surface.^{9,10}

In the US, energy-related sources accounted for 98% of the total CO₂ emissions in 2007, with electricity generation being the major contributor (40% of the total).¹¹ EIA predicts that CO₂ emissions from electricity generation in the US will account for 43% of the total US emissions in 2030.¹² Because it is the major contributor to the generation of CO₂, it is understandable that electric power generation has been the primary focus of CO₂ mitigation technologies.

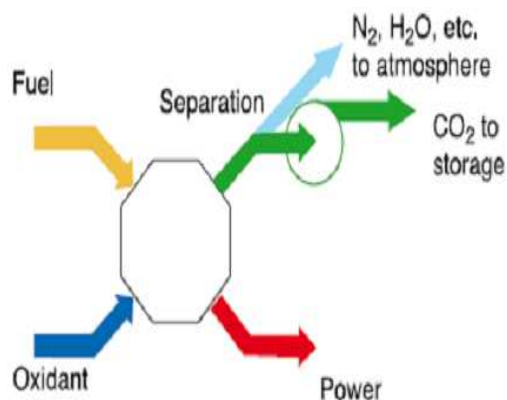
The climate changes associated with global warming are dangerous because they will affect weather patterns,¹³ and will increase melting of polar ice caps that in turn will result in increased sea levels, which represents a major threat to the inhabitants of coastal areas.¹ All of the consequences of climate change are not well understood, however.¹⁴

In an effort to decrease the rate of global warming, many research groups around the world are working to find cost-effective methods for sequestration of atmospheric carbon dioxide,¹⁵⁻¹⁹ and in particular from flue gases from power plants.²⁰⁻²³ A closely related area of research is directed towards finding methods for removal of carbon dioxide by chemical reduction to form value-added products such as methanol or even methane.²⁴⁻³² The chemistry of carbon dioxide is thus a major scientific issue of the early 21st century.

1.2 Current status of CO₂ capture technology

Mineralization has also been discussed as a method to capture CO₂.^{33,34} In this case, CO₂ is reacted with a variety of inorganic species (typically oxides or hydroxides) under high temperature and/or high pressure conditions to produce a carbonate-containing or bicarbonate-containing mineral. These processes tend to consume large amounts of energy, however, and are generally irreversible in a practical sense (i.e. they are reversible only with input of very large amounts of thermal energy).

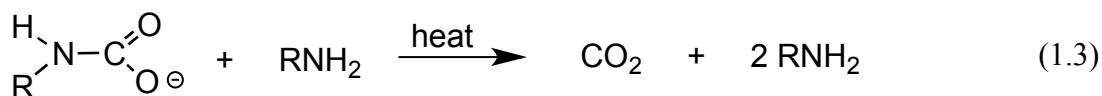
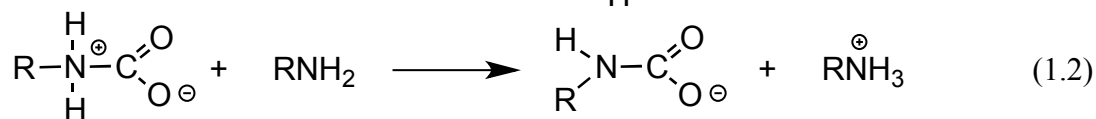
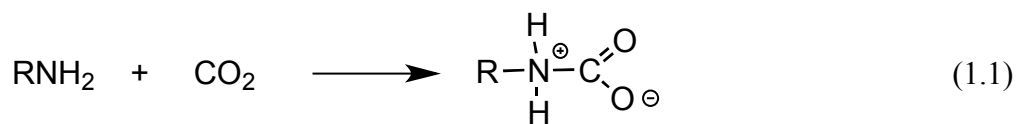
In power plant post-combustion separation technology, CO₂ is isolated by passing the flue gas through a continuous scrubbing system, which consists of an absorber and a desorber. The absorption processes use a chemical reaction of CO₂ with a trapping agent. After trapping, the absorbed CO₂ is released by initiating a reverse



Scheme 1.1. Schematic diagram for post-combustion capture of carbon dioxide

chemical reaction that breaks the covalent bond to the carbon dioxide. The CO₂ separated by this method is then compressed for further processing, and the solvent and trapping agent are regenerated and recycled back into the absorption chamber, Scheme 1.1.

The most commercially viable technology for carbon dioxide capture uses solution phase or immobilized amines. Several plant scale demonstrations using this technology, first patented in 1930, have now been reported.³⁵ Monoethanolamine has been identified as a good candidate amine. Carbon dioxide can react with aqueous monoethanolamine (MEA) to form an intermediate zwitterion structure, Eqn 1.1.³⁶ This intermediate then reacts with another equivalent of MEA via deprotonation to form a stable complex of protonated MEA and MEA carbamate anion, Eqn 1.2, which is the conjugate base anion of the carbamic acid.



Desorption of the carbon dioxide requires re-protonation and endothermic carbon-nitrogen bond cleavage, Eqn 1.3. Heat energy is thus required, and steam is usually used to drive CO₂ liberation from the aqueous amine. This results in a significant energy requirement in addition to the energy required to compress the CO₂ for storage. As

discussed in a recent NETL report (DOE/NETL-2009/1366), the energy required for this process comprises approximately 40% of total plant output and increases the cost of electricity by approximately 85%.³⁷ Thus, in spite of much study, amine scrubbing has not been widely implemented because of the poor energetics of the carbon dioxide release process. A better approach could be to engineer a system in which both the absorption and desorption steps are energetically favorable.

1.3 Electrochemical systems for CO₂ capture

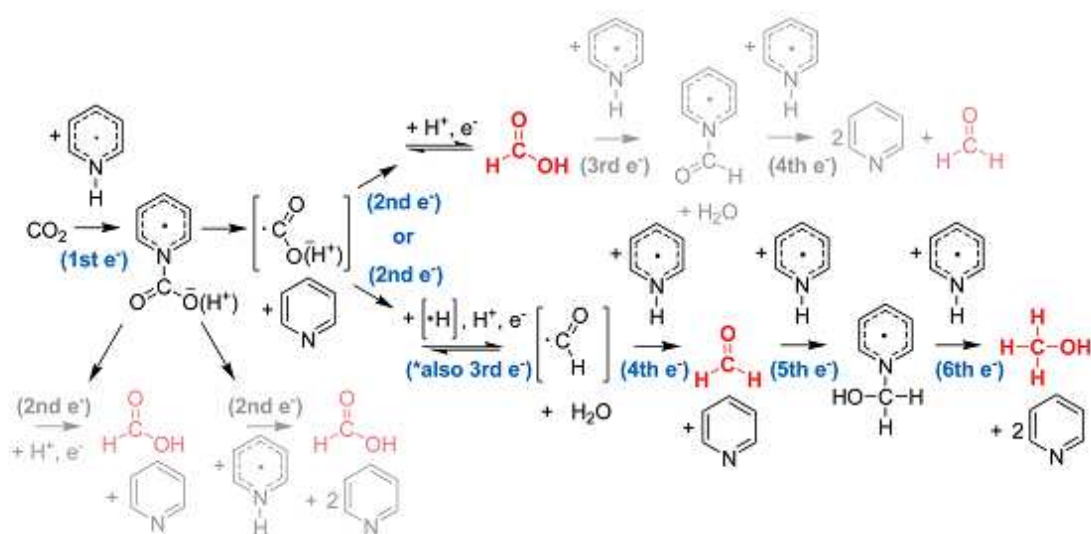
In order for both the trapping and release processes to be energetically favorable, an additional chemical process is required that can "switch" the driving force. Such a switch could provide potential energy in various forms, for example, via a photochemical or electrochemical process. Because power plants produce electricity, an electrochemical switch is clearly attractive.

There are a few isolated previous reports of the use of electrochemical methods to capture CO₂ or to effect its separation from other gases. In one of the earliest reports in 1989 Mizen and Wrighton described the binding of CO₂ to 9,10-phenanthrenequinone dianions prepared electrochemically by reduction of the parent quinone.³⁸ Specifically, they showed that in the presence of CO₂, the quinone was reduced by a single two electron step, generating a dianion that captured two equivalents of CO₂. Oxidation of the quinone dianion-CO₂ adduct (an organic carbonate) released the CO₂ and regenerated the quinone. In a much later 2003 report Scovazzo et al. described CO₂ binding to a different quinone derivative, 2,6-di-*t*-butyl-1,4-benzoquinone.³⁹ They modeled the behavior expected for CO₂ binding based on various values for the binding constant describing the

equilibrium between CO₂ and the reduced form of the quinone to form the adduct. They also demonstrated electrochemical separation of carbon dioxide based on this chemistry, although not with a cell design that would be scalable to be useful industrially. Finally, in 2011 Stern et al. modeled the thermodynamics of this type of electrochemical separation process based on reduced quinone capture agents.⁴⁰ They showed that the energetics of the process are very attractive if the process can be run as a two stage process (i.e. if capture occurs at the cathode as a consequence of reduction, and release simultaneously occurs at the anode as a consequence of oxidation).

Recent reports also describe electrochemical^{16,17,18} and photochemical^{24,25,28} systems that reduce CO₂ to formate, formaldehyde and methanol, using N-heterocyclic compounds. Semiconductor materials and transition metal based catalysts have also been used to reduce CO₂ to monoxide and other reduced forms.⁴¹⁻⁴⁸ The Bocarsely group has studied the pyridinium cation as an electrochemical catalyst for reduction of CO₂ to methanol on a palladium electrode.¹⁵ Although a mechanism has been proposed,^{15,49} see Scheme 1.2, the exact details have still not been completely confirmed. Nevertheless, it is clear that a one electron reduced pyridinium ion is involved in a process that can also involve up to 6 electrons in sequential steps.

An interesting step in this mechanism is formation of a new covalent bond between the pyridinyl nitrogen and the carbon atom of CO₂. This is interesting since it suggests a possible method for CO₂ trapping based on this new covalent bond formation, that can be initiated electrochemically. This observation forms the basis for the work described in



Scheme 1.2. Overall Proposed Mechanism for the Pyridinium-Catalyzed Reduction of CO₂ to the Various Products of Formic Acid, Formaldehyde, and Methanol.¹⁵

this thesis. A pyridine radical anion formed by one-electron reduction can, in principle, be used to trap carbon dioxide, and if the carbon dioxide can be released upon on electron oxidation, then a reversible trapping system for CO₂ could be developed.

1.4 Photochemical Electron Transfer Reactions

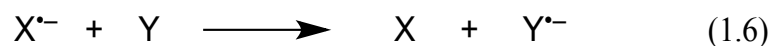
Charge separation and electron transfer play a crucial role in many photochemical processes.⁵⁰ Photoinduced charge transfer between a neutral electron donor (D) and electron acceptor (A) can result in formation of an exciplex, which is an excited state charge-transfer complex that may have varying degrees of charge transfer, or may result in complete transfer and the formation of the radical cation of the donor (D^{•+}) and radical

anion of the acceptor ($A^{\bullet-}$).⁵⁰ In an electron transfer process, the excited state may act as the electron donor, Eqn 1.4, or as the electron acceptor, Eqn 1.5.

The kinetics of the electron transfer process are dictated by the total free energy change associated with the electron transfer. Because no chemical bonds are broken or



made in electron transfer reactions, an exergonic electron transfer reaction, i.e. for which the change in the Gibbs free energy is negative, will usually also be exothermic. The free energy change associated with a ground state electron transfer reaction, Eqn 1.6,



can be determined as the difference in the relevant redox potentials. For the example reaction shown in Eqn 6, the free energy of the reaction is thus shown in Eqn 1.7.

$$\Delta G_{\text{et}} = E_{\text{red}}^Y - E_{\text{red}}^X \quad (1.7)$$

For a photoinduced electron transfer reaction, the excited state energy is also taken into account, and so for the reaction shown in Eqn 4, the reaction free energy, Eqn 1.8.

$$\Delta G_{\text{et}}^* = (E_{\text{ox}}^D - E_{\text{red}}^A) - E_{\text{ex}}^D \quad (1.8)$$

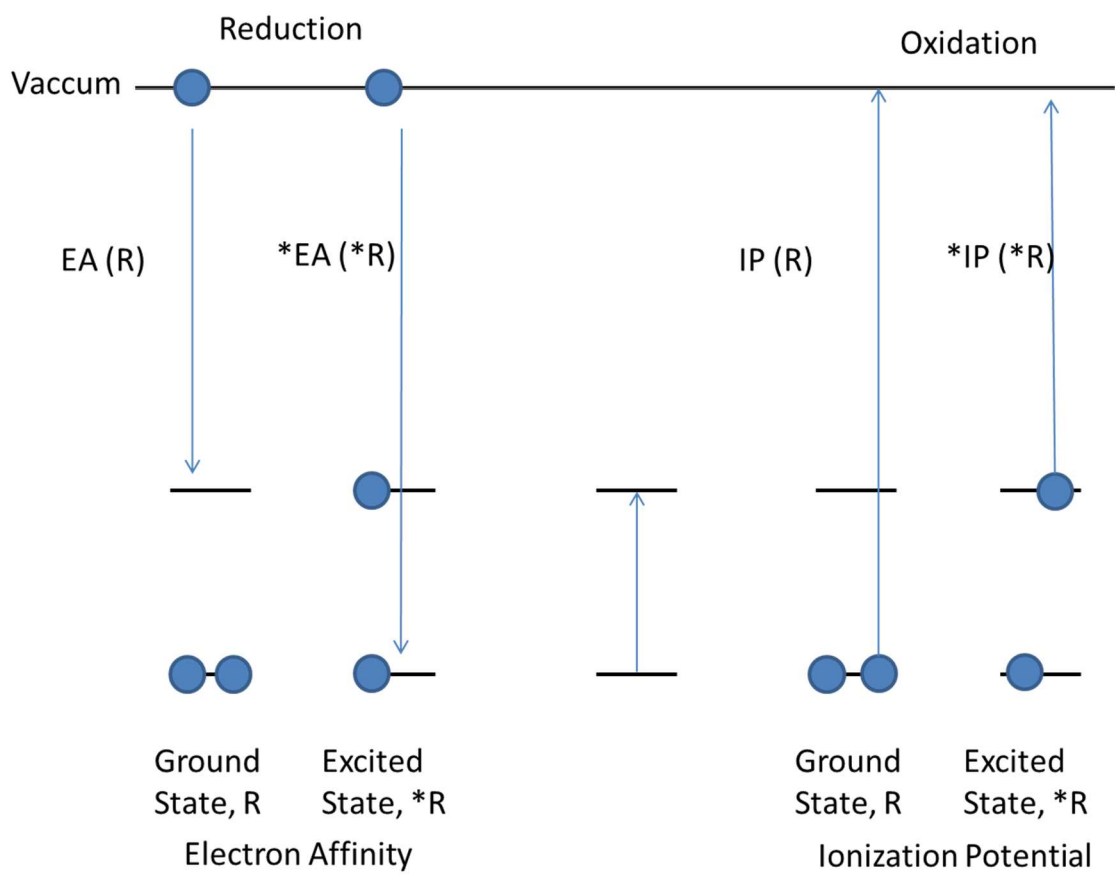


Figure 1.3. Orbital representation of the oxidation and the reduction processes for the ground state R and excited state *R. (adapted from reference 51)

Excited state species in either singlet or triplet excited state are always better oxidizing and reducing agents compared to ground states. A molecular orbital diagram that illustrates this is shown in Figure 1.3. The ionization potential of the ground state R is smaller than the ionization potential of the excited state *R. The electron affinity of the ground state R is less negative than the electron affinity of the excited state *R.

As shown in Figure 1.3, electron affinity for the excited state *R is more negative as a consequence of transfer of an electron from the lower energy HOMO to the higher energy LUMO. Similarly, less energy is needed to remove an electron from the LUMO orbital to the vacuum, resulting in a lower ionization potential for the excited state *R.

1.5 Thesis Objective and Overview

In this thesis describes a detailed study of analogue of simple pyridine. 4,4'-Bipyridine, in its one-electron reduced radical anion form could be potentially used as a catalyst for CO₂ capture and subsequent release in electrochemical systems. Apart from the Bocarsly work, which did not include kinetic measurements of individual rate processes, the kinetics of the reaction between the pyridine based radical anions and carbon dioxide have not been investigated. The bipyridine radical anion would be expected to be very reactive as a one-electron reductant, as a Bronsted base and as a nucleophile, and characterizing these various reactivities will be important for any practical application of reduced bipyridine. In this work, we have studied the kinetics of the reaction between the bipyridine radical anion and carbon dioxide using photochemical methods. We have also characterized the kinetics of the reactions of the

bipyridine radical anion as a nucleophile and a Bronsted base with a range of electrophiles and Bronsted acids. This thesis describes a detailed characterization of bipyridine radical anion and its various chemical reactions using the nanosecond pulsed laser spectroscopic technique.

In Chapter 2, experimental techniques, conditions and details have been discussed. Chapter 3 describes the characterization of bipyridine radical anion, its nucleophilic addition reactions to carbonyl systems and the temperature dependent kinetics, and elimination reactions of bipyridine with alkyl halides. Chapter 4 describes the details of the kinetics of the bipyridine radical anion addition to CO₂, thermodynamic parameters and kinetics details. Measurement of the radical anion pK_a is described in chapter 5. In chapter 6, we have summarized our findings and scope of this study and suggest future work.

References:

1. Climate Change 2001: Synthesis Report. A Contribution of Working Groups I, II, and III to the Third Assessment Report of the Intergovernmental Panel on Climate Change (Ed.: R. T. Watson), Cambridge University Press, New York, 2001.
2. Goddard Institute of Space Studies NASA. 2009 [cited 2009 November 12]; Available from: <http://data.giss.nasa.gov/gistemp/graphs/fig.A2.txt>.
3. M. M. Halmann, M. Steinberg, Greenhouse Gas Carbon Dioxide Mitigation, Lewis, New York, 1999
4. Doney, S. C.; Fabry, V. J.; Feely, R. A.; Kleypas, J. A. *Annu. Rev. Mar. Sci.* 2009, 1, 169.
5. Geider, R. J.; *Global Change Biol.* 2001, 7, 849.
6. Beer, C.; *Science* 2010, 329, 834.
7. Earth System Research Laboratory Global Monitoring Division. 2009 [cited 2009 November 12]; Available from: ftp://ftp.cmdl.noaa.gov/ccg/co2/trends/co2_mm_mlo.txt.
8. Henni, A.; Li, J.; Tontiwachwuthikul, P. *Ind. Eng. Chem. Res.* 2008, 47, 2213-2220.
9. Wood, R.W. (1909). "Note on the Theory of the Greenhouse". *Philosophical Magazine* 17: 319–320.
10. "Introduction to Atmospheric Chemistry, by Daniel J. Jacob, Princeton University Press, 1999. Chapter 7, "The Greenhouse Effect"

11. Energy Information Administration, *Electric Power Annual 2007: A Summary*. 2009: Washington, D.C.
12. Energy Information Administration, *International Energy Outlook*. 2009: Washington, D.C.
13. United Nations Environment Programme and the Climate Change Secretariat (UNFCCC): "Climate Change Information Kit", July 2002.
14. Doney, S. C.; Fabry, V. J.; Feely, R. A.; Kleypas, J. A. *Annu. Rev. Mar. Sci.* 2009, 1, 169.
15. Barton, C. E.; Lakkaraju, P. S.; Rampulla, D. M.; Morris, A. J.; Abelev, E.; Bocarsly, A. B. *J. Am. Chem. Soc.* 2010, 132, 11539.
16. Seshadri, G.; Lin, C.; Bocarsly, A. B.; *J. Electroanal. Chem.* 1994, 372, 145.
17. Barton, E. E.; Rampulla, D. M.; Bocarsly, A. B.; *J. Am. Chem. Soc.* 2008, 130, 6342.
18. Bocarsly, A. B.; Gibson, Q. D.; Morris, A. J.; L'Esperance, R. P.; Detweiler, Z. M.; Lakkaraju, P. S.; Zeitler, E. L.; Shaw, T. W.; *ACS Catal.* 2012, 2, 1684.
19. de Tacconi, N. R.; Chanmanee, W.; Dennis, B. H.; MacDonnell, F. M.; Boston, D. J.; Rajeshwar, K. *Electrochem. Solid State* 2011, 15, B5.
20. Kondure, P. B.; Vaidya, P. D.; Kenig, E. Y.; *Environ. Sci. Technol.* 2010, 44, 2138–2143

21. Pani, F.; Gaunand, A.; Cadours, R.; Bouallou, C.; Richon, D.; J. Chem. Eng. Data 1997, 42, 353-359
22. Rochelle, G.T., Amine Scrubbing for CO₂ Capture. Science, 2009. 325(5948): 1652-1654.
23. Danckwerts, P. V. (1979). "The Reaction of Carbon Dioxide with Ethanolamines." Chem. Engr. Sci. 34: 443.
24. Morris, A. J.; Meyer, G. J.; Fujita, E. Molecular Approaches to the Photocatalytic Reduction of Carbon Dioxide for Solar Fuels. Acc. Chem. Res. 2009, 42, 1983-1994
25. Fujita, E. Photochemical Carbon Dioxide Reduction with Metal Complexes. Coord. Chem. Rev. 1999, 185, 373-384.
26. Takeda, H.; Ishitani, O. Development of Efficient Photocatalytic Systems for CO₂ Reduction Using Mononuclear and Multinuclear Metal Complexes Based on Mechanistic Studies. Coord. Chem. Rev. 2010, 254, 346-354.
27. Liang, Y. T.; Vijayan, B. K.; Gray, K. A.; Hersam, M. C. Minimizing Graphene Defects Enhances Titania Nanocomposite Based Photocatalytic Reduction of CO₂ for Improved Solar Fuel Production. Nano Lett. 2011, 11, 2865-2870.
28. Tsai, C. W.; Chen, H. M.; Liu, R. S.; Asakura, K.; Chan, T. S.; Ni@NiO Core-Shell Structure-Modified Nitrogen-Doped InTaO₄ for Solar-Driven Highly Efficient CO₂ Reduction to Methanol. J. Phys. Chem. C 2011, 115, 10180-10186.

29. Izumi, Y. Recent Advances in the Photocatalytic Conversion of Carbon Dioxide to Fuels with Water and/or Hydrogen Using Solar Energy and Beyond. *Coord. Chem. Rev.* 2013, 257, 171–186.
30. Aurian-Blajeni, B.; Halmann, M.; Manassen, J. Electrochemical Measurement on the Photoelectrochemical Reduction of Aqueous Carbon Dioxide on p-Gallium Phosphide and p-Gallium Arsenide Semiconductor Electrodes. *Sol. Energy. Mater.* 1983, 8, 425–440.
31. Halmann, M. Photoelectrochemical Reduction of Aqueous Carbon Dioxide on p-type Gallium Phosphide in Liquid Junction Solar Cells. *Nature*, 1978, 275, 115.
32. Kaneco, S.; Katsumata, H.; Suzuki, T.; Ohta, K. Photoelectrochemical Reduction of Carbon Dioxide at p-type Gallium Arsenide and p-type Indium Phosphide Electrodes in Methanol. *Chem. Eng. J.* 2006, 116, 227–231.
33. Choi, S., Drese, J.H., & Jones, C.W., Adsorbent Materials for Carbon Dioxide Capture from Large Anthropogenic Point Sources. *Chemsuschem* 2 (9), 796-854 (2009).
34. Wolf, G.H., Chizmeshya, A.V.G., Diefenbacher, J., & McKelvy, M.J., In situ observation of CO₂ sequestration reactions using a novel microreaction system. *Environmental Science & Technology* 38 (3), 932-936 (2004).
35. Rubin, E. S., A. B. Rao, et al. (2004). Comparative Assessment of Fossil Fuel Power Plants with CO₂ Capture and Storage. 7th International Conference on Greenhouse Gas Control Technologies, Vancouver, Canada.
36. Danckwerts, P. V. (1979). "The Reaction of Carbon Dioxide with Ethanolamines." *Chem. Engr. Sci.* 34: 443.

37. National Energy Technology Laboratory Report, Research and Development Goals for CO₂ Capture Technology, DOE/NETL-2009/1366 (2011).
38. Mizen, M.B. & Wrighton, M.S., Reductive Addition of CO₂ to 9,10-Phenanthrenequinone. *Journal of the Electrochemical Society* 136 (4), 941-946 (1989).
39. Scovazzo, P., Poshusta, J., DuBois, D., Koval, C., & Noble, R., Electrochemical separation and concentration of < 1% carbon dioxide from nitrogen. *Journal of the Electrochemical Society* 150 (5), D91-D98 (2003).
40. Stern, M.C. *et al.*, Electrochemically Mediated Separation for Carbon Capture. *Energy Procedia* 4, 860-867 (2011).
41. Fischer, B.; Eisenberg, R. J. *Am. Chem. Soc.* 1980, 102, 7361
42. Tinnemans, A. H. A.; Koster, T. P. M.; Thewissen, D. H. M. W.; Mackor, A. M. *Recl. TraV. Chim. Pays-Bas.* 1984, 103, 288.
43. Pearce, D. J.; Pletcher, D.J. *Electroanal. Chem.* 1986, 197, 317.
44. Beley, M.; Collin, J. P.; Ruppert, R.; Sauvage, J. P.J. *Chem. Soc., Chem. Commun.* 1984, 1315.
45. Beley, M.; Collin, J. P.; Ruppert, R.; Sauvage, J. P.J. *Am. Chem. Soc.*, 1986, 108, 7461.
46. Ishida, H.; Tanaka, K.; Tanaka, T. *Chem. Lett.* 1985, 405.

47. Ishida, H.; Tanaka, H.; Tanaka, K.; Tanaka, T. *J. Chem. Soc., Chem. Commun.* 1987, 131.
48. Ishida, H.; Tanaka, K.; Tanaka, T. *Organometallics* 1987, 6, 181.
49. Yan, Y.; Gu, J.; Bocarsly, A.B.; *Aerosol and Air Quality Research*, 14: 515–521, 2014
50. G. J. Kavarnos, *Fundamentals of Photoinduced Electron Transfer*, VCH Publishers, New London, CT, 1999, p. 359.
51. Nicholas J. Turro, *Modern Molecular Photochemistry of Organic Molecules*, University Science Books, 2010, p. 418.

CHAPTER 2

EXPERIMENTAL

2.1 Time-Resolved Absorption Spectroscopy

Time resolved absorption spectra were recorded using a nanosecond pulsed laser system.^{1,2} A simplified schematic representation of the apparatus is shown in Figure 2.1. A neodymium-doped yttrium aluminium garnet; (Nd:Y₃Al₅O₁₂) YAG laser (Quantel, Brilliant B) was used as the excitation source. This laser emits 1064 nm light which is frequency doubled to 532 nm light and then doubled again to 266 nm. The 266 nm light is used to excite the bipyridine to the first excited singlet state, which then intersystem crosses to the triplet state. The laser was operated in Q-switched mode, meaning an electro-optical switch is inserted into the optical cavity, maximizing the neodymium ion excited state population inversion prior to cavity opening. The pulse width is approximately 3 - 4 nanoseconds in the 266 nm pulse.

The 266nm laser light beam was separated from the 1064nm and 532 nm light using a prism, and was focused by the means of lenses onto the sample solutions that have optical densities adjusted to be ca.0.7 – 1.0 in a 1-cm path length optical cuvette. Laser induced changes in transmitted light intensity in the solution were used to monitor the formation and decay of transient species. The analyzing light is a 150 Watt pulsed xenon lamp (Osram XBO-150), that provides essentially continuous output through the UV and visible regions. The laser beam and the analyzing xenon lamp light were focused into the center of the sample cell to generate a sufficient concentration of transient species.

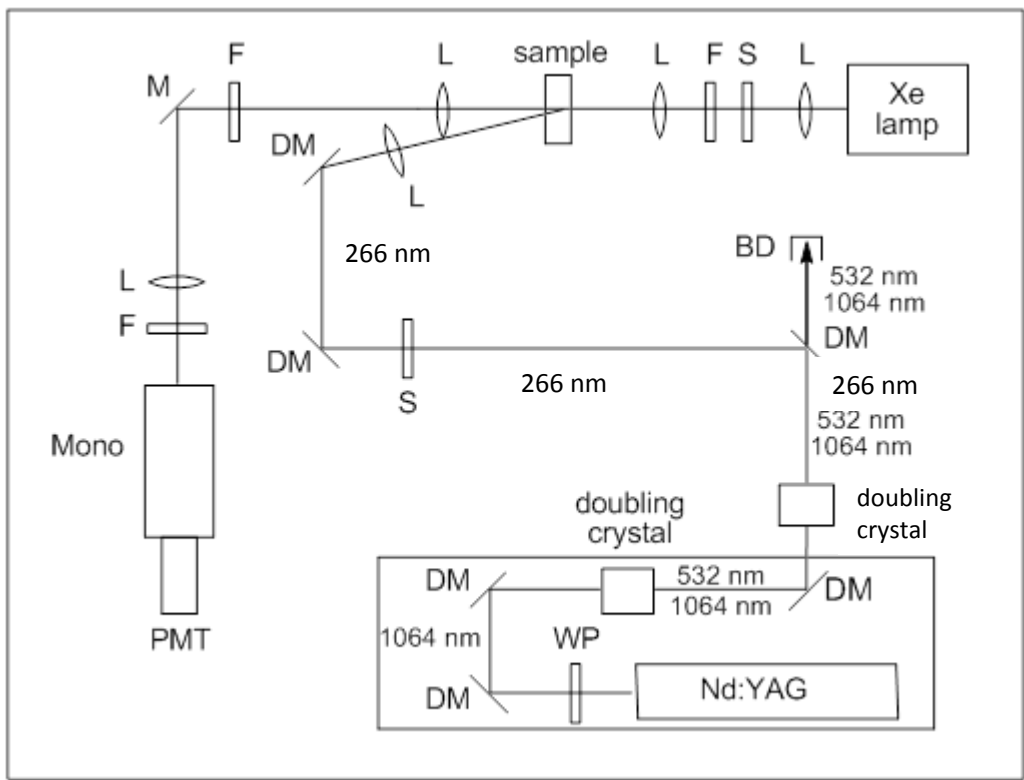


Figure 2.1. Schematic diagram of the transient absorption apparatus. M = mirror, DM = dielectric coated mirror, F = filter, L = lens, BD = beam dump, S = shutter, WP = wave plate, PMT = photomultiplier tube, Mono = monochromator, Nd:YAG = Neodymium YAG laser.

An electronic shutter prevented the analyzing light to enter the sample when not required. The analyzing light was passed through an Instruments SA model H-20 monochromator. Changes in light intensity were detected using a Hamamtsu model R4840 photomultiplier tube. The output is terminated into 50 Ohms and monitored as voltage as a function of time using a Tektronix DSA 601 digital signal analyzer. The waveform data are transferred to a PC for conversion into optical density data as a function of time, and for kinetic analysis.

2.2 Solvents and Donors

Acetonitrile and 1,2-dichloroethane (DCE) was used as the solvents and were obtained from Sigma Aldrich. The solvents were dried with 4 Angstrom molecular sieves (8-12 mesh) for 72 hours before the experiment to reduce the water content. Sieves were present in the cuvettes throughout the experiments to minimize the interference of dissolved water. 4,4'-Bipyridine (BPy) and 1,4-Diazabicyclo[2.2.2]octane (DABCO) was obtained from Sigma Aldrich and used as such.

1 mM solutions of 4,4'-bipyridine were analyzed in acetonitrile or 1,2-dichloroethane solvent in 1-cm cuvettes equipped with arms for purging with nitrogen or carbon dioxide gas. 2mM DABCO or triethylamine were used as the donors.

2.3 CO₂ Concentration

The carbon dioxide concentration in the dichloroethane solutions was varied by purging with a mixture of CO₂ and argon. Balloons filled with argon were weighed and then varying quantities of carbon dioxide were additionally added to the balloons, which

were then weighed again. Ideal gas behavior was assumed in order to calculate the weight percentage of CO₂ in the mixtures in the balloons, which were then used to purge the sample solutions.

2.4 CO₂ solubility measurement in Dichloroethane

The solubility of carbon dioxide in DCE was measured using gravimetric analysis. DCE saturated with CO₂ was mixed with an excess aqueous Ba(OH)₂ solution. The precipitated BaCO₃ was filtered, dried and weighed, and the amount of CO₂ was determined assuming one mole of carbon dioxide per mole of BaCO₃. The solubility of carbon dioxide at all of the temperatures used to generate the Arrhenius plot was determined in the same way. The solubilities obtained this way were 303 mM, 252 mM, 93 mM and 46 mM at 10°C, 25°C, 45°C and 68°C, respectively.

2.5 Kinetic study with the carbonyls and alkyl halides

The kinetics of the reactions between the 4,4'-bipyridine radical anion and the carbonyl compounds (cyclohexanone, cycloheptanone, acetic Anhydride, 3-pentanone, Pentanal, di-t-butyl ketone, acetophenone, butyrolactone, Ethyl acetate) were measured using the time-resolved nano-second laser spectroscopic technique. Acetic anhydride, 3-pentanone and pentanal was purified by the methods described elsewhere.³ Apart from these, all of the chemicals were received from Sigma-Aldrich and were used as received. The bipyridine triplet state was generated in-situ by irradiating the 1 mM solutions of 4,4'-bipyridine in acetonitrile using pulsed 266 nm laser excitation. DABCO was used as an electron donor to donate an electron to the excited triplet bipyridine to form the

radical anion, which could be observed with an absorbance maximum at 380 nm. The rate of decay of the radical anion was measured in the presence of the carbonyls at different concentration. The pseudo-first order rate constant for decay of the radical anion decay were plotted as a function of the concentration of the carbonyl to give the bimolecular rate constant as the slope.

The kinetics of the reactions between the bipyridine radical anion and alkyl halides were measured in the same way. *t*-butyl Bromide, 2-bromobutane, 1-bromobutane, 1-iodobutane, 1-chlorobutane, iodomethane and methyl-*p*-toluenesulfonate were obtained from Sigma-Aldrich, and were used as received.

2.6 pKa of the 4,4'-Bipyridine Radical Anion

The pKa of bipyridine radical was estimated by measuring the kinetics of its reaction with a series of phenol derivatives. *p*-Nitrophenol, *p*-trifluoromethylphenol, 2-fluorophenol, 3-fluorophenol, phenol, *p*-cresol, *p*-methoxyphenol, trimethylphenol, hexafluoroisopropanol and trifluoroethanol was received from Sigma-Aldrich and was used as such for the experiments.

Bipyridine triplet state was generated in-situ by irradiating the 1 mM solutions of 4,4'-bipyridine in acetonitrile using 266 nm laser shots. DABCO was used as a donor which donates an electron to the excited triplet bipyridine molecule to form the radical anion which could be observed with a maxima at 380 nm. Decay rate of the radical anion was studied in the presence of carbonyls at different concentration. Rate of the radical anion decay at different concentration of the carbonyls were plotted to obtain the bimolecular rate constants as the slopes.

References:

1. Herkstroeter, W. G.; Gould, I. R. In *Physical Methods of Chemistry Series*, 2nd ed.; Rossiter, B., Baetzold, R., Eds.; Wiley: New York, 1993; Vol. 8, p 225.
2. Lorance, E. D.; Kramer, W. H.; Gould, I. R. *J. Am. Chem. Soc.*, 2004, *126*, 14071.
3. Armarego, W. L. F.; Chai, C. L. L.; *Purification of Laboratory Chemicals*, Elsevier, 2013, p. 105

CHAPTER 3

BIPYRIDINE RADICAL ANION: CHARACTERIZATION AND REACTIVITY TOWARDS CARBONYLS AND ALKYL HALIDES

3.1 Introduction

Pyridine and its derivatives have been the subject of much current interest as potential catalysts for useful chemistry of carbon dioxide.¹ Two main areas of research focus on the conversion of CO₂ to liquid fuels,² and the chemical trapping of CO₂ for sequestration.³ These two processes are fundamentally related by formal reduction of carbon dioxide, either by one-electron transfer, formal hydrogen addition, or covalent bond formation to a nucleophile. Of these, the reactions of CO₂ with nucleophiles, in particular amines, have been extensively studied.⁴ Several electrochemical and photochemical systems have now been described that can convert CO₂ to formate, formaldehyde and methanol in the presence of N-heterocyclic compounds.⁵⁻¹³ The electrochemical reduction of CO₂ to methanol using the aromatic amine pyridine as a catalyst has recently been reported by Bocarsly et al.¹⁴ This process is related to ethanolamine capture of CO₂ in that nucleophilic addition of pyridine to the carbonyl carbon of CO₂ may be an important step in the mechanism.¹⁴

One-electron reduction of 4,4'-bipyridine generates a radical anion, which should be strongly nucleophilic, and could be used to trap carbon dioxide via bond formation to the carbonyl carbon. The mechanisms of the carbon dioxide trapping and release reactions will be described elsewhere in this thesis. In this chapter, we describe studies that characterize the bipyridine radical anion quantitatively in terms of its nucleophilicity and Bronsted basicity. The radical anion is generated in situ in

homogeneous solution and studied using time-resolved nano-second laser transient spectroscopy. We have studied the nucleophilic addition of the radical anion of 4,4'-bipyridine with a variety of carbonyl compounds. Bipyridine radical anion can also behave as a strong base, and we have found that it can be used to perform E2 elimination reactions with alkyl halides, that can occur in competition with nucleophilic substitution. These two processes for alkyl halides have been characterized kinetically and are discussed.

3.2 Experimental

Acetonitrile was used as the solvent and was obtained from Sigma Aldrich. Acetonitrile was dried with 4 Å molecular sieves (8-12 mesh) for 72 hours before the experiment to reduce the water content. Sieves were present in the cuvettes throughout the experiments to minimize the interference of dissolved water. 4,4'-bipyridine (BPY) and 1,4-Diazabicyclo[2.2.2]octane (DABCO) was obtained from Sigma Aldrich and used as such.

1 mM solutions of 4,4'-bipyridine were analyzed in acetonitrile in 1-cm cuvettes equipped with arms for purging with argon or carbon dioxide gas. 2mM DABCO was used as the donors.

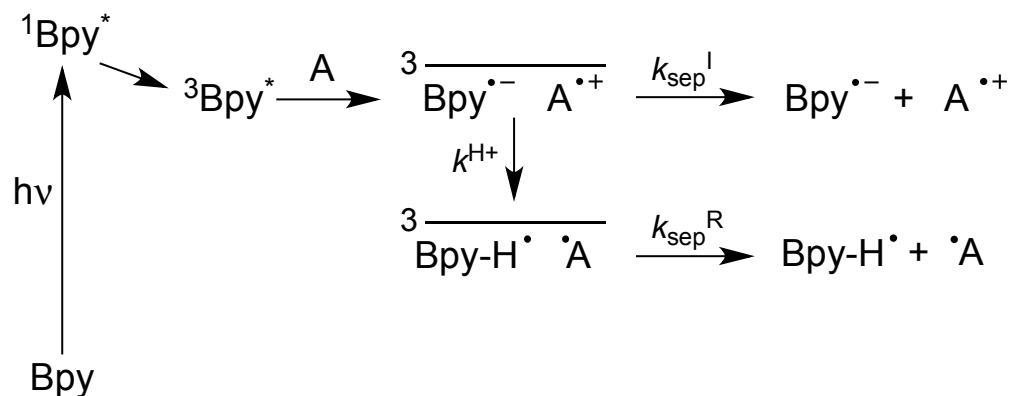
The kinetics of the reaction between the bipyridine radical anion and carbonyl compounds (cyclohexanone, cycloheptanone, acetic anhydride, 3-pentanone, pentanal, di-t-butyl ketone, acetophenone, butyrolactone, ethyl acetate) were measured using the time-resolved nano-second laser spectroscopic technique. Acetic anhydride, 3-pentanone and pentanal was purified by the methods described previously.¹⁵ All of the chemicals

received from Sigma-Aldrich and were used as received. The bipyridine triplet state was generated in-situ by irradiating 1 mM solutions of 4,4'-bipyridine in acetonitrile using a nanosecond pulsed 266 nm laser. DABCO was used as an electron donor to the excited triplet bipyridine to form the bipyridine radical anion, which could be observed with an absorbance maximum at 380 nm. The decay rate of the radical anion was measured in the presence of carbonyls as electrophiles at different concentration. The pseudo first order rate constant for decay of the radical anion decay at different concentrations of the electrophiles were plotted to obtain the bimolecular rate constants as the slopes.

The rate constants for reaction between the bipyridine radical anion and alkyl halides were obtained in the same way. *t*-Butyl bromide, 2-bromobutane, 1-bromobutane, 1-iodobutane, 1-chlorobutane, iodomethane and methyl-*p*-toluenesulfonate as electrophiles were used as received from Sigma-Aldrich.

3.3 The 4,4'-Bipyridine Radical Anion

As shown previously,¹⁶ one-electron reduction of the first excited triplet state of bipyridine (**Bpy**) using amines (**A**) as the electron donor results in formation of a triplet geminate bipyridine radical anion (**Bpy^{•-}**)/amine radical cation (**A^{•+}**) pair, Scheme 3.1. When triethylamine is the donor, proton transfer within the geminate radical ion pair can occur, k^{H^+} , to form the bipyridyl radical (**Bpy[•]-H**) and an α -amino radical (**A[•]**), Scheme I. Separation within this geminate pair, k_{sep}^R , yields these freely diffusing radicals. With DABCO as the electron donor **A**, however, proton transfer in the geminate pair is much slower and separation of the radical ions occurs, k_{sep}^I , to generate a freely diffusing



Scheme 3.1. Reaction scheme showing formation of the separated 4,4'-bipyridine radical anion (**Bpy^{•-}**) for pulsed laser excitation in solution, using either triethylamine or DABCO as the amine electron donor (**A**). Proton transfer in the triplet geminate radical ion pair (k^{H^+}) competes with separation, k_{sep} .

bipyridine radical anion (**Bpy**^{•-}) and the DABCO radical cation (**A**^{•+}). The **Bpy**^{•-} ($\lambda_{\text{max}} = 380 \text{ nm}$) and **Bpy**^{•-}-H ($\lambda_{\text{max}} = 365 \text{ nm}$) are distinguishable on the basis of their absorption spectra, Figure 3.1 and Figure 3.2. **Bpy**^{•-} is a powerful one-electron donor and Bronsted base, and the time-resolved decay of the radical anion in fluid solution is pseudo-first order, presumably due to reaction with solvent impurities, or slow reaction with the solvent itself. The measured lifetime of the **Bpy**^{•-} is 1.2 μs in argon-purged acetonitrile. Figure 3.3 shows an example absorbance decay for the bipyridine radical anion in argon purged acetonitrile. The first order rate constant was measured to be $5 \times 10^5 \text{ s}^{-1}$ in this case.

Because the absorption spectra of the radical anion and the radical were similar, we performed experiments to assign the absorptions observed in the transient absorption on the basis of chemical reactivity. Because the radical anion is a strong one-electron donor, it should react rapidly with electron acceptors. The rate constants for reaction of the transient with absorption maximum at 380 nm generated in the presence of DABCO as the electron donor were obtained for reaction with tetracyanobenzene, dicyanobenzene, stilbene and oxygen. These data are summarized in Table 3.1, together with the relevant reduction potentials. The reduction potentials for each of the acceptors is less negative than that of 4,4'-bipyridine itself, Table 3.1, which means that electron transfer to each should be exothermic. Indeed, rate constants close to the diffusion controlled limit are observed, consistent with exothermic electron transfer. In addition, with tetracyanobenzene the radical anion of the acceptor was observed after the reaction as a transient absorption, confirming the mechanism of reaction as electron

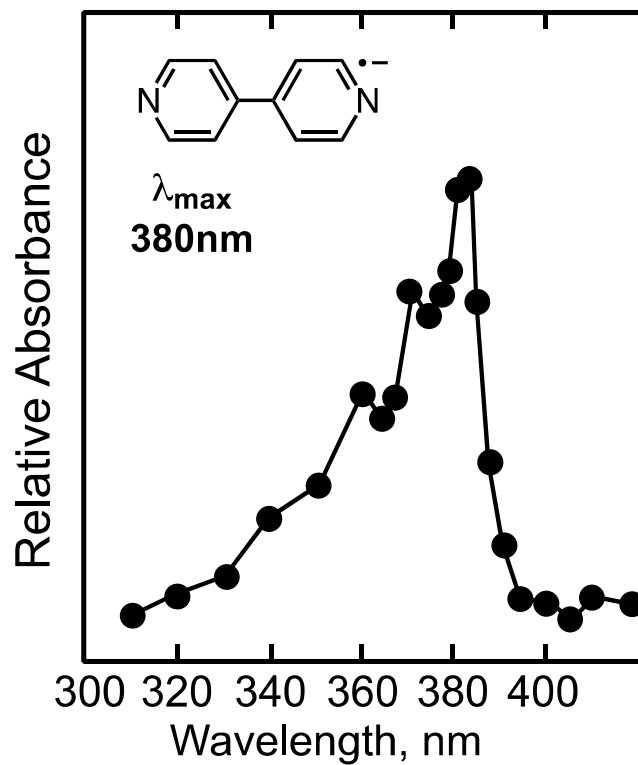


Figure 3.1. Transient absorption spectrum of the 4,4'-bipyridine radical anion in acetonitrile, measured 200 ns after pulsed laser excitation of the bipyridine in the presence of DABCO as an electron donor, at room temperature.

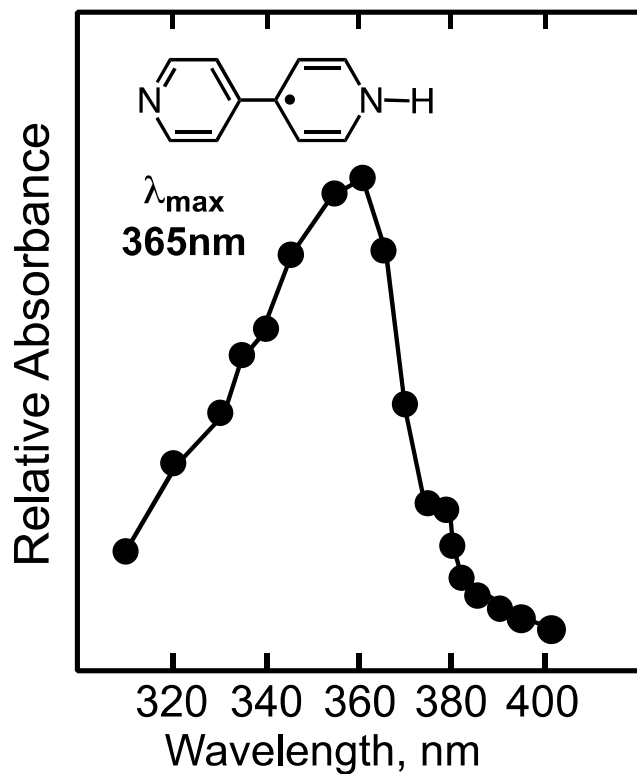


Figure 3.2. The transient absorption spectrum of the radical product of protonation of the 4,4'-bipyridine radical anion in acetonitrile, measured 200 ns after pulsed laser excitation of the bipyridine, in the presence of triethylamine as the electron donor, at room temperature.

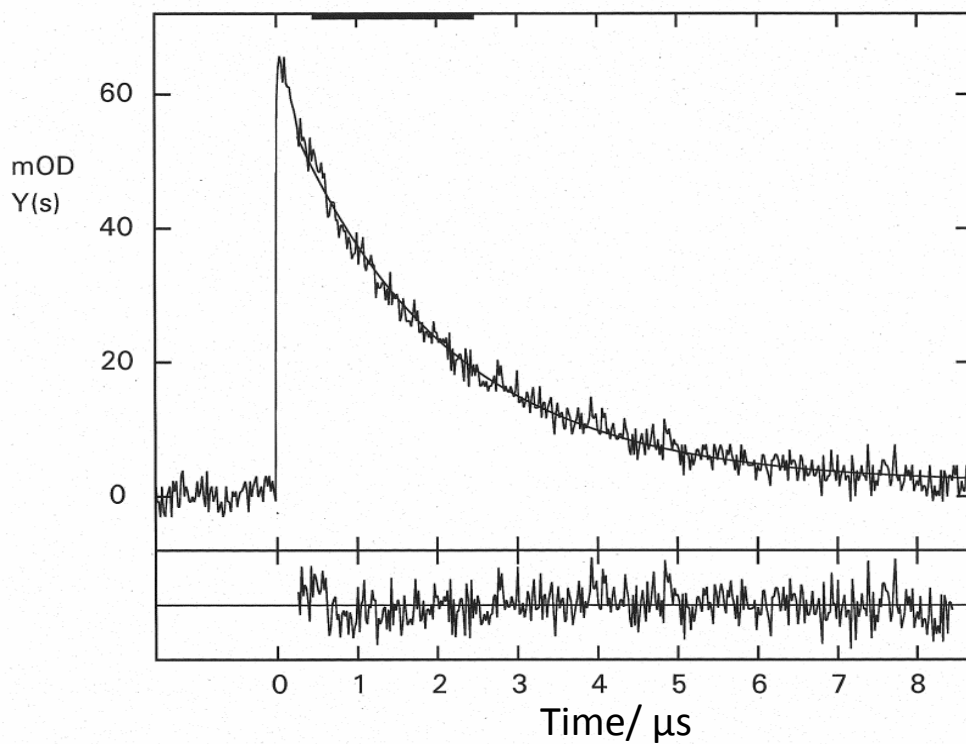


Figure 3.3. Representative absorbance decay showing decay of the 4,4'-bipyridine radical anion, monitored at 380 nm, in argon purged acetonitrile. The smooth curve through the data represents the best first order kinetic fit, corresponding to a first order rate constant for decay of $5 \times 10^5 \text{ s}^{-1}$ and a lifetime of $1.9 \mu\text{s}$.

Table 3.1. Bimolecular Rate Constants for Reaction of the 4,4'-Bipyridine Radical Anion with Electron Acceptors, and Their Reduction Potentials

Substrate	Rate Const (k) M⁻¹ s⁻¹	Reduction Potential V vs. SCE
Oxygen	1 x 10 ¹⁰	-0.40 V
Tetracyanobenzene	9 x 10 ⁹	-0.65V
Dicyanobenzene	5 x 10 ⁹	-1.60 V
4,4'-Bipyridine		-1.80 V

transfer. The same reactivity was not observed when the absorbance at 365 nm was monitored using triethylamine as the donor, where the protonated radical was expected to absorb. We conclude that the absorbance at 380 nm is exclusively due to the 4,4'-bipyridine radical anion and that the absorbance of the protonated radical form can readily be distinguished at 365 nm.

3.4 The Reaction of the 4,4'-Bipyridine Radical Anion With Carbonyl Compounds and Electrophiles

Nucleophilicity is a fundamental property of an organic reactant. Nucleophilicity is the kinetic ability of a structure to act as a Lewis base, which is a basic concept for formation of new covalent bonds in organic chemistry. The nucleophilicities of very few organic radical anions have been described in the literature, however. Because of the importance of pyridine radical anions in carbon dioxide reduction and sequestration, we have characterized its nucleophilicity with a variety of electrophiles. Cyclohexanone was chosen as an archetype carbonyl electrophile and reaction with the bipyridine radical anion was readily observed in acetonitrile. A plot of the pseudo-first order rate constant for decay of the bipyridyl radical anion (**Bpy**^{•-}) as a function of cyclohexanone concentration yields a bimolecular rate constant for reaction of $1.3 \times 10^7 \text{ M}^{-1} \text{ s}^{-1}$, Figure 3.4, Table 3.2. After reaction with CO₂, the absorption spectrum of the **Bpy**^{•-} is replaced by a new spectrum with absorption maximum at 370 nm, Figure 3.5. Even though this new species and the radical **Bpy**[•]-H have similar absorption spectra, Figure 2, it is apparent that the new species is not simply a radical derived from bipyridine because it

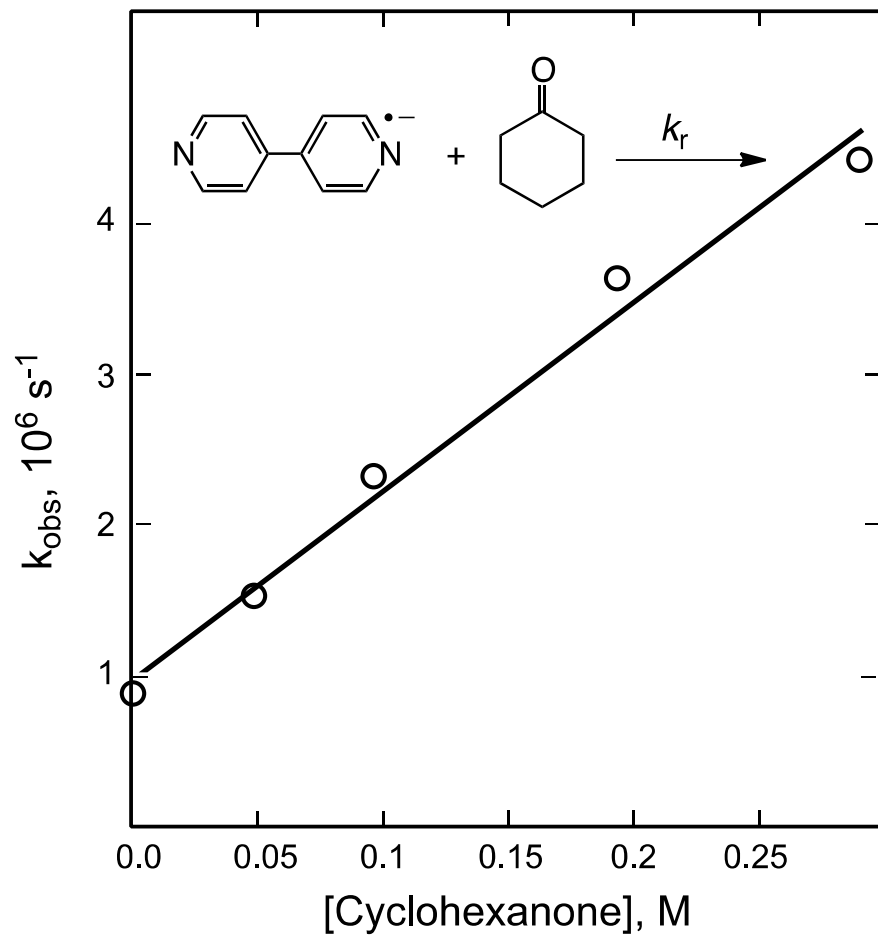


Figure 3.4. Observed pseudo-first order rate constant for decay of the 4,4'-bipyridine radical anion, k_{obs} , as a function of concentration of cyclohexanone. The bimolecular rate constant for reaction is given by the slope as $1.3 \pm 0.2 \times 10^7 \text{ M}^{-1} \text{ s}^{-1}$.

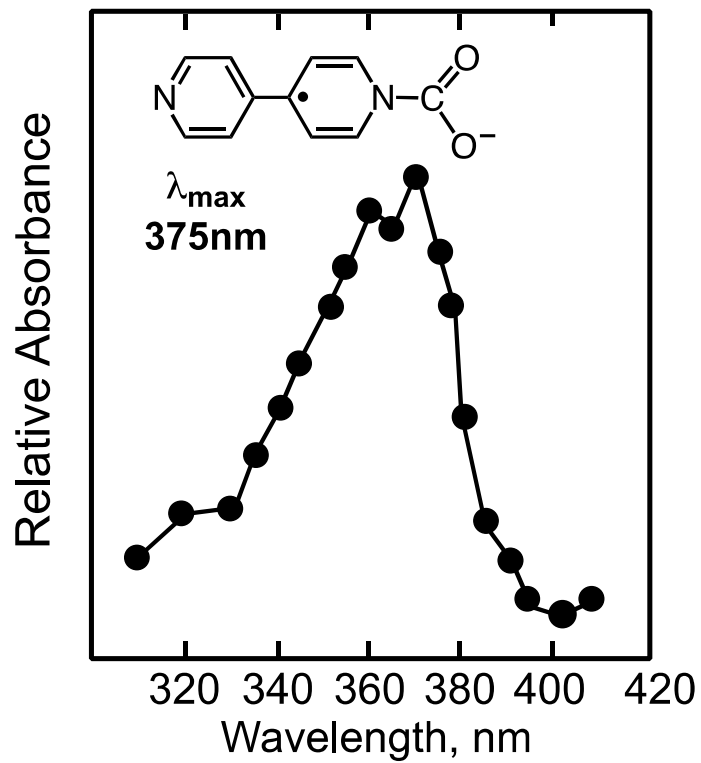
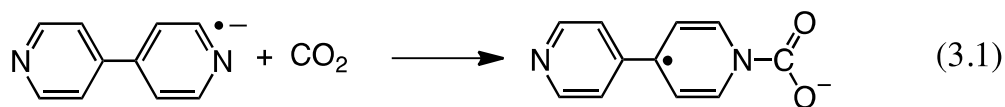


Figure 3.5. Transient absorption spectra of the distonic carbamate anion radical adduct of the 4,4'-bipyridine radical anion with cyclohexanone, in acetonitrile, measured 100 ns after excitation of the bipyridine in the presence of DABCO in 100mM cyclohexanone solution, at room temperature.

reacts with dissolved oxygen more slowly than does the radical, and in contrast to the radical, it is long lived on the timescale of the experiment. Its lifetime is greater than 10 ms and is in fact too long to be measured with the experimental apparatus. We assign this new species to the product of nucleophilic addition of one of the bipyridyl nitrogens to the carbonyl carbon, Eqn. 3.1.



The rate constant of $1.3 \pm 0.2 \times 10^7 \text{ M}^{-1} \text{ s}^{-1}$ represents a very fast nucleophilic addition to cyclohexanone,¹⁷ and is consistent with a low barrier for reaction. The temperature dependence of the rate constant was measured over the temperature range 3°C - 70°C. An Arrhenius plot of the bimolecular rate constant for reaction of **Bpy**^{•-} with cyclohexanone is shown in Figure 3.6. The Arrhenius activation energy is 18.8 ± 2.0 kJ/mol and the pre-exponential factor is $3.2 \pm 1 \times 10^{10} \text{ s}^{-1}$. The experimental uncertainties in these values are large because of the restricted temperature range of the measurements. Nevertheless, it is clear that the reaction has a small barrier.

The kinetics of the reactions of the bipyridine radical anion with a variety of carbonyl electrophiles are summarized in Table 3.2. It is evident that the anhydride reacts almost two times faster than cyclohexanone. 3-Pentanone, pentanal, di-*t*-butyl ketone and cycloheptanone react with BPy radical anion with similar rate constants. This is exactly the behavior expected for nucleophilic addition to a carbonyl, where anhydrides are more

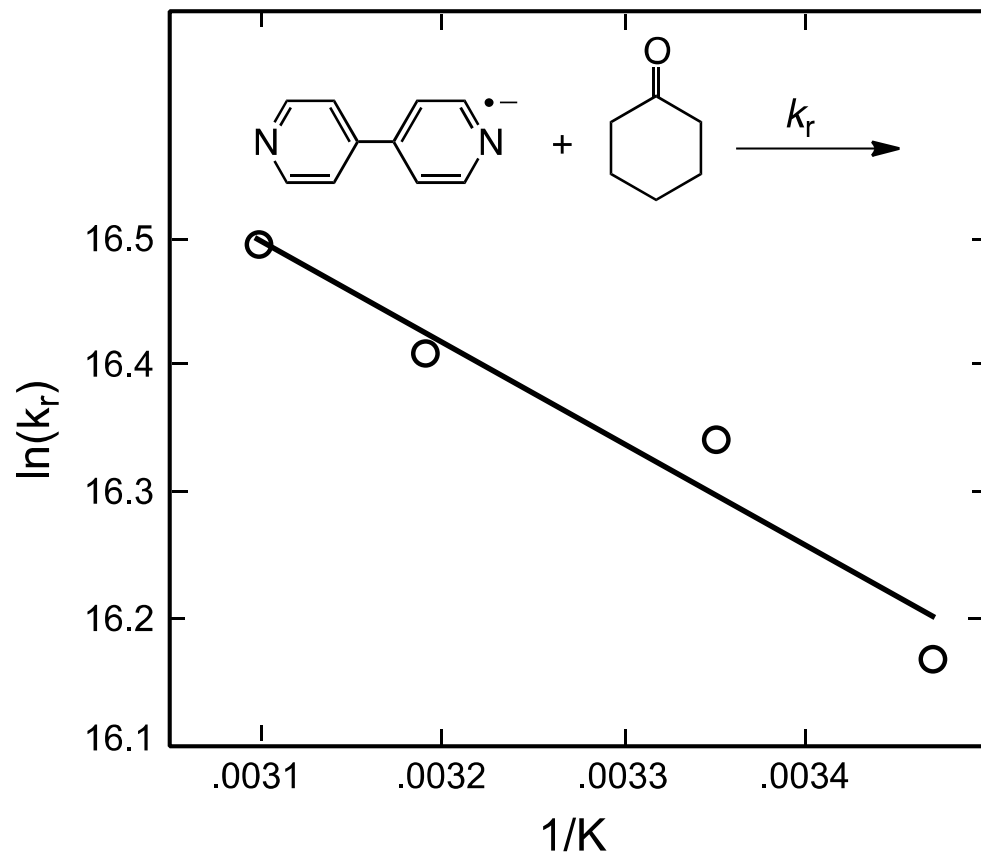


Figure 3.6. Arrhenius plot of the rate constant for reaction of cyclohexanone with the bipyridine radical anion in acetonitrile.

reactive than aldehydes and ketones, and aldehydes and ketones react at similar rates. Similarly, acetophenone reacts more slowly than cyclohexanone, again consistent with the conventional understanding of nucleophilic addition to carbonyls. The partial positive charge on the carbonyl carbon in acetophenone is delocalized into the benzene ring, thus decreasing reactivity. Esters exhibit very low reactivity and the rate constants in these cases are lower than our detection limit of $10^5 \text{ M}^{-1}\text{s}^{-1}$.

Aldehydes are often observed to act as slightly weaker electrophiles than ketones, but in these experiments they are not distinguishable on the basis of their rate constants, Table 3.2. However, the rate constants measured here are among the fastest that have yet been recorded for nucleophilic attack on carbonyl structures, and consequently the reactivity/selectivity principle suggests that small differences may not be discernable, especially for reactions with very low activation barriers. Nevertheless, the rate trends observed are clearly consistent with nucleophilic addition of a pyridyl nitrogen to the carbonyl carbon in these reactions, which confirms the bipyridine radical anion as being among the most reactive nucleophiles yet studied. Furthermore, the observation of a long product of the addition reaction to cyclohexanone provides a spectroscopic signature for nucleophilic addition that is distinct from the radical formed by protonation, Figures 3.2 and 3.5.

Nucleophilicity is often susceptible to solvent effects, and because we are interested in the chemistry of the bipyridine radical anion in various conditions, even perhaps in aqueous environments, we studied the kinetics of the reaction with cyclohexanone in different solvents with varying water content. In DMSO and acetonitrile the rate constants were essentially the same. This may not be surprising since

they are both high dielectric constant solvents that do not hydrogen bond. However in dichloroethane solvent, the water content was found to have a significant effect on the rate constant. In less polar solvents, the reactivity of nucleophiles is often diminished in the presence of hydrogen-bonding structures. In the presence of hydrogen bonding, the nucleophilic electrons are decreased in energy as a result of the electrostatic effect, and the nucleophilic atom may have larger radii due to hydration which reduces the nucleophilic strength.

3.5 Bipyridine radical anion kinetics with alkyl halides

BPy radical anions are strong nucleophiles as demonstrated in the previous section pertaining to high rate constants towards the carbonyl compounds. Another aspect of this radical anion, the basicity, has not been explored much in detail.¹⁸ We explored the basicity of the BPy radical anion here in detail.

We also studied the kinetics of the reaction between the bipyridine radical anion and alkyl halides. Alkyl halides represent classic cases of electrophiles that can undergo competitive electrophilic reactions, specifically electrophilic reactions resulting in substitution, and Bronsted acidic reactions resulting in elimination. Table 3.4 summarizes the rate constants for several of these reactions. A plot of the pseudo-first order rate constant for decay of the bipyridyl radical anion (**Bpy^{•-}**) as a function of t-butyl bromide concentration yields a bimolecular rate constant for reaction of $4.7 \times 10^6 \text{ M}^{-1} \text{ s}^{-1}$. After reaction with t-butyl bromide, the absorption spectrum of the **Bpy^{•-}** is replaced by a new

Table 3.2. Bimolecular Rate Constants, k_r , For Nucleophilic Addition of the Bipyridine Radical Anion With Various Carbonyl Compounds

Carbonyl	k_r ($M^{-1}s^{-1}$)
Cyclohexanone	1.3×10^7
Cycloheptanone	1.3×10^7
Acetic Anhydride	3.0×10^7
3-pentanone	1.5×10^7
Pentanal	1.4×10^7
di-t-butyl ketone	1.6×10^7
acetophenone	6.5×10^6
butyrolactone	$\leq 5 \times 10^5$
Ethyl acetate	$\leq 5 \times 10^5$

Table 3.3. Effect of Solvent and Water Content on the Bimolecular Rate Constant for Reaction Between the Bipyridine Radical Anion and Cyclohexanone, k_r

Solvent	Water Content	k_r ($M^{-1}s^{-1}$)
Dichloroethane	20 ppm	2.0×10^7
Dichloroethane	160 ppm	5.9×10^6
DMSO	280 ppm	1.9×10^6
DMSO	40 ppm	1.9×10^6
Acetonitrile	320 ppm	1.3×10^7
Acetonitrile	80 ppm	$1.5 * 10^7$

spectrum with absorption maximum at 365 nm, Figure 3.7. This new species and the radical **Bpy[•]-H** have similar absorption spectra, Figure 3.2. This confirms formation of BPy radical by abstraction of a proton from t-butyl bromide, i.e., in this case the bipyridine radical anion is acting as a Bronsted base. No product was isolated but the spectra are consistent with an E2 elimination reaction between the radical anion and t-butyl bromide. Depending upon the structure of the alkyl halide, SN2 and E2 elimination reactions were observed.

Iodomethane reacts with the bipyridine radical anion with a bimolecular rate constant of $1.3 \times 10^6 \text{ M}^{-1} \text{ s}^{-1}$. E2 elimination is not a feasible reaction with methyl iodide, and so this bimolecular rate constant most likely corresponds to SN2 substitution. Spectra of the transients observed at the end of the reaction do not appear to be those of a single product.

The bimolecular rate constants for reaction of the bipyridine radical anion with t-butyl bromide, 2-bromobutane and 1-bromobutane (Table 3.4), clearly indicates E2 elimination in each case. It is well known that E2 reactions are fastest for tertiary halides and slowest for primary halides. Reaction with 1-bromobutane and 1-chlorobutane was too slow to be measured using our experimental apparatus. Although rate constants could not be determined, this behavior is again consistent with known reactivities of primary halides in SN2 reactions.

We also studied the reactivity of alkyl halides with substituted bipyridine, 2,2'-dimethyl-4,4'-bipyridine. We expected the bimolecular rate constants for both SN2 and E2 reactions to be slower for this structure compared to the parent bipyridine due to

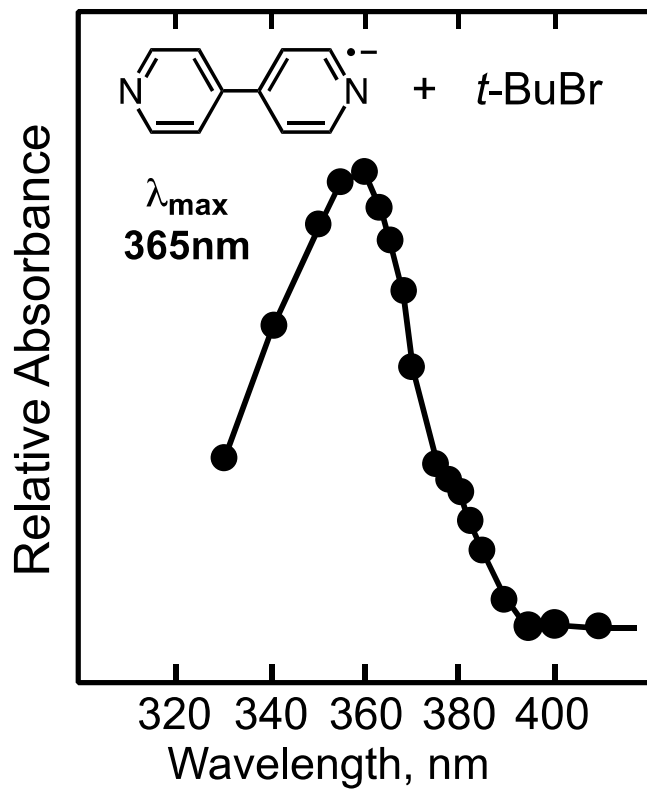


Figure 3.7. Transient absorption spectra of the bipyridine radical adduct in acetonitrile, measured 100 ns after excitation of the bipyridine in the presence of DABCO in 60 mM t-butyl bromide solution, at room temperature.

Table 3.4. Bimolecular rate Constants for the Reaction Between the Bipyridine Radical Anion and Various Alkyl Halides, k_r .

Substrate	k_r ($M^{-1}s^{-1}$)
t-butyl Bromide	4.7×10^6
2-bromobutane	1.7×10^6
1-bromobutane	$\leq 5 \times 10^5$
iodobutane	1.1×10^6
bromobutane	$\leq 5 \times 10^5$
chlorobutane	$\leq 5 \times 10^5$
iodomethane	1.3×10^6
Methyl – p-toluenesulfonate	1.3×10^7

Table 3.5. Bimolecular rate Constants for the Reaction Between the 2,2'-Dimethyl-4,4'-bipyridine Radical Anion and Various Alkyl Halides, k_r .

Substrate	k_r ($M^{-1}s^{-1}$)
t-butyl Bromide	5.1×10^6
iodobutane	4.2×10^7
iodomethane	7.2×10^6

steric hindrance. To our surprise, we observed an increase in bimolecular rate constant, in particular for the alkyl iodides. This suggests that the rate-determining step in this case may be one-electron transfer from the radical anion to the halides. The additional methyl substituents will result in a more negative reduction potential for this bipyridine, which will make it a more powerful one-electron reductant. Such reaction behavior suggests that the mechanism has switched to the SRN1 reaction in which the rate-determining step is electron transfer to the halide, which undergoes bond cleavage to form an alkyl radical which then reacts with substitution being the overall result.¹⁹

3.6 Conclusion:

The bipyridine radical anion was found to be a very powerful one-electron donor, Bronsted base and nucleophile. It reacts by nucleophilic addition to the C=O bonds of ketones with a bimolecular rate constants around $1 \times 10^7 \text{ M}^{-1} \text{ s}^{-1}$. These are among the fastest nucleophilic additions that have been reported in the literature. Temperature dependence studies demonstrate very low activation energies and large Arrhenius pre-exponential parameters, consistent with very high reactivity. The kinetics of E2 elimination, where the radical anion acts as a base, and SN2 substitution, where the radical anion acts as a nucleophile, are also characterized by large bimolecular rate constants in the range ca. $10^6 - 10^7 \text{ M}^{-1} \text{ s}^{-1}$. These studies provide the basis for detailed investigations of the nucleophilic reaction of the 4,4'-bipyridine radical anion with carbon dioxide, discussed in Chapter 4. The Bronsted basicity of the bipyridine radical anion is further investigated both thermodynamically and kinetically in Chapter 5.

References:

1. a) Dell'Amico, D. B.; Calderazzo, F.; Labella, L.; Marchetti, F.; Pampaloni, G. *Chem. Rev.* 2003, 103, 3857- 3898. b) Jessop, P. G.; Joó, F.; Tai, C. C. *Coord. Chem. Rev.* 2004, 248, 2425-2442. c) Sakakura, T.; Choi, J. C.; Yasuda, H. *Chem. Rev.* 2007, 107, 2365-2387. d) Mikkelsen, M., Jorgensen, M.; Krebs, F. C. *Energy Environ. Sci.* 2010, 3, 43–81.
2. a) Kumar, B.; Llorente, M.; Froehlich, J.; Dang, T.; Sathrum, A.; Kubiak, C. P. *Annu. Rev. Phys. Chem.*, 2012, 63, 541-569. b) Centi, G.; Perathoner, S. *Catal. Today* 2009, 148, 191–205.
3. a) Aresta, M. *Carbon Dioxide Recovery and Utilization*; Kluwer Academic Publishers: Dordrecht, 2010. b) Metz, B., Davidson, O., De Coninck, H., Loos, M. & Meyer, L. *Carbon Dioxide Capture and Storage*; Cambridge University Press: Cambridge UK, 2005.
4. a) Villiers, C.; Dognon, J.-P.; Pollet, R.; Thuory, P.; Ephritikhine, M. *Angew. Chem. Int. Ed.* 2010, 49, 3465 –3468. b) Ma, J.; Zhang, X.; Zhao, N.; Al-Arifi, A. S. N.; Aouak, T.; Al-Othman, Z. A.; Xiao, F.; Wei, W.; Sun, Y. J. *Mol. Catal. A* 2010, 315, 76-81. c) McGhee, W.; Riley, D.; Christ, K.; Pan, Y.; Parnas, B. J. *J. Org. Chem.* 1995, 60, 2820–2830. d) McGhee, W.; Riley, D. *J. Org. Chem.* 1995, 60, 6205-6207. e) Hooker, J. M.; Reibel, A. T.; Hill, S. M.; Schueller, M. J.; Fowler, J. S. *Angew. Chem. Int. Ed.* 2009, 48, 3482-3485.
5. Morris, A. J.; Meyer, G. J.; Fujita, E. Molecular Approaches to the Photocatalytic Reduction of Carbon Dioxide for Solar Fuels. *Acc. Chem. Res.* 2009, 42, 1983–1994
6. Fujita, E. Photochemical Carbon Dioxide Reduction with Metal Complexes. *Coord. Chem. Rev.* 1999, 185, 373–384.
7. Takeda, H.; Ishitani, O. Development of Efficient Photocatalytic Systems for CO₂ Reduction Using Mononuclear and Multinuclear Metal Complexes Based on Mechanistic Studies. *Coord. Chem. Rev.* 2010, 254, 346–354.

8. Liang, Y. T.; Vijayan, B. K.; Gray, K. A.; Hersam, M. C. Minimizing Graphene Defects Enhances Titania Nanocomposite-Based Photocatalytic Reduction of CO₂ for Improved Solar Fuel Production. *Nano Lett.* 2011, 11, 2865–2870.
9. Tsai, C. W.; Chen, H. M.; Liu, R. S.; Asakura, K.; Chan, T. S.; Ni@NiO Core–Shell Structure-Modified Nitrogen-Doped InTaO₄ for Solar-Driven Highly Efficient CO₂ Reduction to Methanol. *J. Phys. Chem. C* 2011, 115, 10180–10186.
10. Izumi, Y. Recent Advances in the Photocatalytic Conversion of Carbon Dioxide to Fuels with Water and/or Hydrogen Using Solar Energy and Beyond. *Coord. Chem. Rev.* 2013, 257, 171–186.
11. Aurian-Blajeni, B.; Halmann, M.; Manassen, J. Electrochemical Measurement on the Photoelectrochemical Reduction of Aqueous Carbon Dioxide on p-Gallium Phosphide and p-Gallium Arsenide Semiconductor Electrodes. *Sol. Energy Mater.* 1983, 8, 425–440.
12. Halmann, M. Photoelectrochemical Reduction of Aqueous Carbon Dioxide on p-type Gallium Phosphide in Liquid Junction Solar Cells. *Nature* 1978, 275, 115.
13. Kaneco, S.; Katsumata, H.; Suzuki, T.; Ohta, K. Photoelectrochemical Reduction of Carbon Dioxide at p-type Gallium Arsenide and p-type Indium Phosphide Electrodes in Methanol. *Chem. Eng. J.* 2006, 116, 227–231.
14. a) Barton, E. E.; Rampulla, D. M.; Bocarsly, A. B. *J. Am. Chem. Soc.* 2008, 130, 6342–6344. b) Barton Cole, E.; Lakkaraju, P. S.; Rampulla, D. M.; Morris, A. J. Abelev, E.; Bocarsly, A. B. *J. Am. Chem. Soc.* 2010, 132, 11539–11551. c) Morris, A. J.; McGibbon, R. T.; Bocarsly, A. B. *ChemSusChem*, 2011, 4, 191–196.
15. Armarego, W. L. F.; Chai, C. L. L.; Purification of Laboratory Chemicals, Elsevier, 2013, p. 105

16. Ebersson, L. E. *Electron Transfer Reactions in Organic Chemistry*; Springer-Verlag: New York, 1988.
17. Sakakura, T., Choi, J.-C.; Yasuda, H. *Chem. Rev.* **2007**, *107*, 2365–2387.
18. Keith, J. A.; Carter, E. A.; *J. Am. Chem. Soc.* 2012, *134*, 7580–7583
19. a) Ashby, E.C. *Acc. Chem. Res.*, 1988, *21* (11), pp 414–421. b) Rossi, R. A. *Acc. Chem. Res.* 1982, *15*, 164-170. c) Bunnett, J. F.; Kim, J. K. *J. Am. Chem. Soc.* 1970, *92*, 7463-7464.

CHAPTER 4
REVERSIBLE ELECTROCHEMICAL TRAPPING OF CARBON DIOXIDE
USING 4,4'-BIPYRIDINE

4.1 Introduction

In response to dwindling fossil fuel energy resources and the growing global warming problem, the chemistry of carbon dioxide has been the subject of substantial current recent research activity.¹ Two main areas of research focus on the conversion of CO₂ to liquid fuels,² and chemical trapping of CO₂ for sequestration.³ These two processes are fundamentally related by formal reduction of carbon dioxide, either by one-electron transfer, formal hydrogen addition, or covalent bond formation to a nucleophile. Of these, the reactions of CO₂ with nucleophiles, in particular amines have been extensively studied.⁴ Systems that use nucleophiles such as ethanolamine and other amines have been developed for industrial-scale reversible carbon dioxide trapping applications.⁵ Covalent bond formation followed by deprotonation forms a carbamate anion, the deprotonated form of a carbamic acid. Thermal decomposition of such a carbamate anion liberates carbon dioxide and an amine,⁵ although the energy cost of the CO₂ liberation process represents a limitation to its use in reversible carbon dioxide trapping schemes.⁶

Electrochemical reduction of CO₂ to methanol using the aromatic amine pyridine as a catalyst has recently been reported by Bocarsly et al.⁷ This process is related to ethanolamine capture of CO₂ in that nucleophilic addition of pyridine to the carbonyl carbon of CO₂ may be an important step in the mechanism,⁷ although the details are still under investigation.⁸

A method of CO₂ trapping and release that does not require substantial thermal input in either direction would clearly be of interest. Electrochemical methods for reduction of CO₂ to generate useful high-value structures have received a lot of attention,^{2,9} but reversible electrochemical trapping of CO₂ has not yet been extensively studied, and no kinetic studies have been reported.

Here we demonstrate a method for reversible trapping of CO₂ using 4,4'-bipyridine that uses electrochemistry to switch between a structure that covalently bonds carbon dioxide, initiated by one-electron reduction of the 4,4'-bipyridine, and one that releases carbon dioxide and neutral bipyridine upon oxidation. Both the reaction that traps the carbon dioxide and the reaction that liberates the carbon dioxide are exergonic and both proceed with low reaction energy barriers. The mechanisms of the carbon dioxide trapping and release reactions are explored in detail, both experimentally and computationally. The trapping and release of carbon dioxide over more than twenty cycles is demonstrated at room temperature.

4.2 Results and Discussion

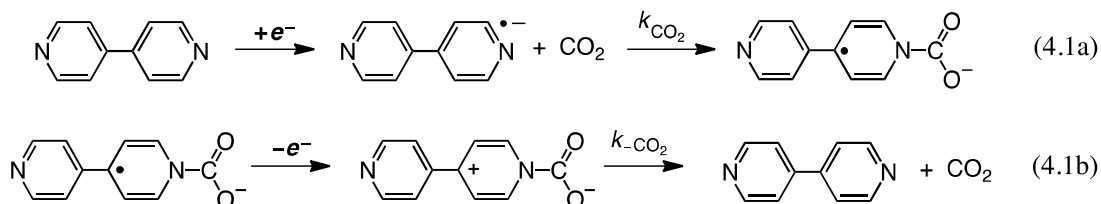
4.2.1. Reversible Trapping of CO₂ using 4,4'-Bipyridine as an Electrochemical Switch.

One-electron reduction of 4,4'-bipyridine in the ionic liquid N-butyl-N-methylpyrrolidinium bis(trifluoromethylsulfonyl)imide as the electrolyte in a nitrogen atmosphere is reversible, demonstrating that the bipyridine radical anion is stable on the millisecond timescale under the experimental conditions. Electrochemical experiments were performed by a colleague, Jarred Olsen. The reduction potential is -2.3 V vs

ferrocene as an internal reference, Figure 4.1. In the presence of a saturated solution of carbon dioxide the electrochemical behavior changes dramatically, Figure 4.1. The cathodic peak shifts to lower potential, ca. -2.05 V vs. ferrocene, presumably as a result of rapid reaction of the bipyridine radical anion with carbon dioxide to form an adduct. The current density also increases, presumably due to the higher diffusion coefficient of carbon dioxide in the ionic liquid compared to bipyridine. Oxidation of the bipyridine radical anion is now absent in the reverse wave. Instead, an oxidation wave that is ca. 700 mV less negative than the reduction wave is observed; this wave must correspond to a reaction product, presumably the bipyridine radical anion/carbon dioxide adduct. Attempts to replace the carbon dioxide with nitrogen again after electrochemical cycling were unsuccessful due to the high solubility of CO₂ in the ionic liquid. However, the electrochemical behavior in the presence of carbon dioxide is reproducible and the same reduction and re-oxidation waves are observed for over 20 cycles, during which period all of the dissolved bipyridine would have been consumed if the reactions were not reversible (the maximum number of repeatable cycles has not been determined).

These observations are consistent with reversible electrochemical reactions. Protonation of the neutral or electrochemically activated bipyridine by acid (such as carbonic acid derived from the reaction of water with CO₂) can be ruled out since the concentration of water (determined by Karl-Fischer titration) in solution is less than the detection limit of the instrument (1.5mM), and separate experiments involving protonation of the bipyridine resulted in irreversible passivation of the electrode interface during voltammetric measurements. The reaction between the bipyridine radical anion and carbon dioxide is presumably nucleophilic addition to the carbonyl carbon to form a

carbamate anion, Eq. 4.1a, that also has a single non-bonding electron associated with the bipyridine π -system. One possible electron configuration is shown in Eq. 4.1a, which is consistent with the results of the computations, which suggest that the non-bonding electrons is associated with a π^* M.O. on the bipyridine and not on the carboxyl. Oxidation of this distonic carbamate anion pyridyl radical is most easily envisioned as occurring at the pyridyl radical rather than the carboxylate, as shown in Eq. 4.1b. This is because the pyridyl radical is an α -amino radical,¹⁰ which are known to have much lower oxidation potentials than carboxylate anions,¹¹ although biradical electron configurations corresponding to carboxylate oxidation should undoubtedly also be considered, see below.



In support of the assignment of the product of the reaction between the bipyridine radical anion and CO_2 to the distonic carbamate anion radical shown in Eq. 1a, the oxidation potentials for substituted pyridyl radicals are usually found to be between ca. -1.0 and ca. -1.5 V versus ferrocene,¹² consistent with the oxidation wave observed in Figure 4.1.

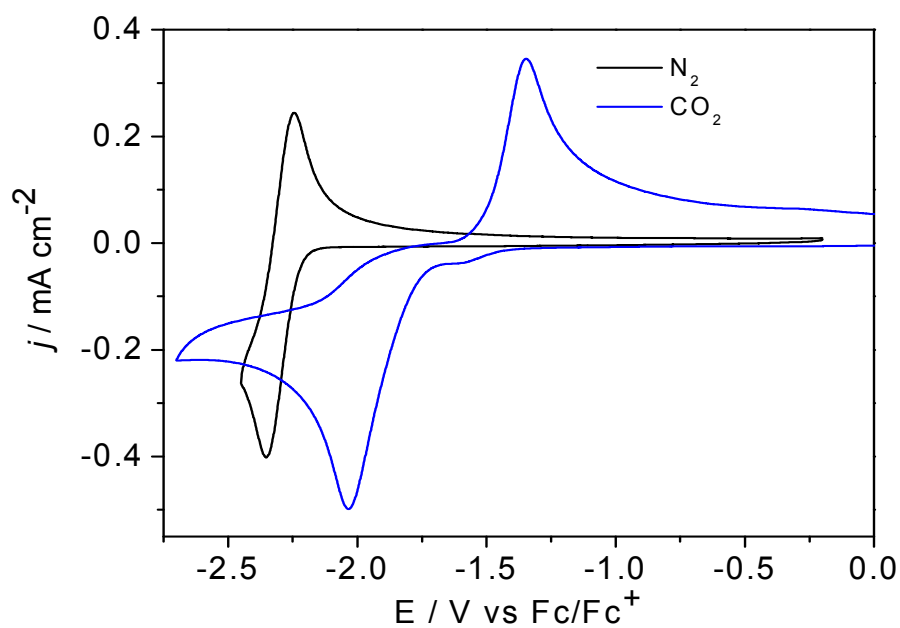
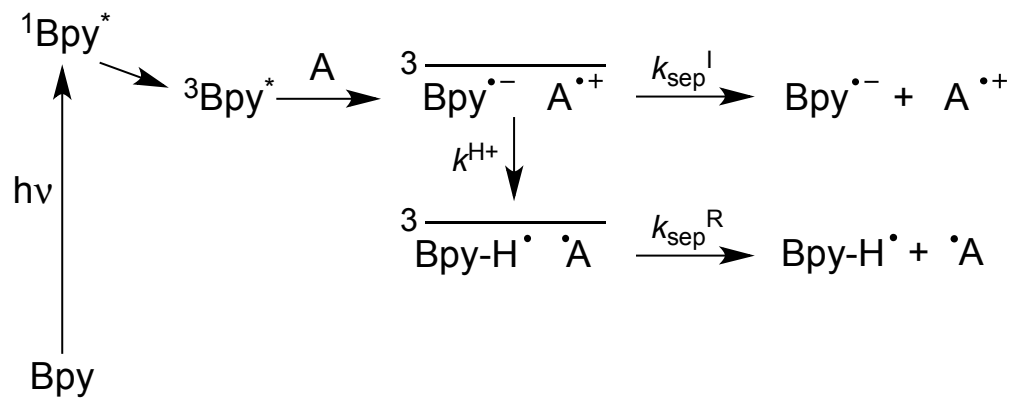


Figure 4.1. Cyclic voltammetry of 10 mM 4,4'-bipyridine in N-butyl-N-methylpyrrolidinium bis(trifluoromethylsulfonyl)imide ionic liquid solvent at room temperature (black curve) purged with nitrogen gas, and (blue curve) purged with carbon dioxide gas, using a glassy carbon working electrode and platinum counter electrode with ferrocene as an internal reference. (Experiment performed by Jarred Olsen)

4.2.2. Kinetic Studies of the Reaction Between the 4,4'-Bipyridine Radical Anion and Carbon Dioxide.

The kinetics of the 4,4'-bipyridine radical anion reaction with CO₂ were studied using transient absorption spectroscopy. As shown previously,¹¹ one-electron reduction of the first excited triplet state of bipyridine (**Bpy**) using amines (**A**) as the electron donor results in formation of a triplet geminate bipyridine radical anion (**Bpy**^{•-})/amine radical cation (**A**^{•+}) pair, Scheme I. When triethylamine is the donor, proton transfer within the geminate radical ion pair can occur, k^{H^+} , to form the bipyridyl radical (**Bpy**[•]-**H**) and an α -amino radical (**A**[•]), Scheme 4.1. Separation within this geminate pair, k_{sep}^R , yields these freely diffusing radicals. With DABCO as the electron donor **A**, however, proton transfer in the geminate pair is much slower and separation of the radical ions occurs, k_{sep}^I , to generate a freely diffusing bipyridine radical anion (**Bpy**^{•-}) and the DABCO radical cation (**A**^{•+}). The **Bpy**^{•-} ($\lambda_{max} = 380$ nm) and **Bpy**[•]-**H** ($\lambda_{max} = 365$ nm) are readily distinguished on the basis of their absorption spectra, Figure 4.2. **Bpy**^{•-} is a powerful one-electron donor and Bronsted base, and the time-resolved decay of the radical anion in fluid solution is pseudo-first order, presumably due to reaction with solvent impurities, or slow reaction with the solvent itself. The measured lifetime of the **Bpy**^{•-} is 1.2 μ s and 0.9 μ s in argon-purged acetonitrile and dichloroethane, respectively.

Attempts to react **Bpy**^{•-} with CO₂ in acetonitrile solution failed due to formation of acidic species via reaction of CO₂ with residual water in the solvent that resulted only in protonation of the radical anion with formation of the bipyridyl radical (**Bpy**[•]-**H**) with absorption maximum at 365 nm.¹² However, reaction with CO₂ was readily observed in



Scheme 4.1. Reaction scheme for formation of the separated 4,4'-bipyridine radical anion (**Bpy**^{•-}) in the time-resolved laser experiments in solution, using either triethylamine or DABCO as the amine electron donor (**A**). Proton transfer in the triplet geminate radical ion pair (k^{H^+}) competes with separation, k_{sep} .

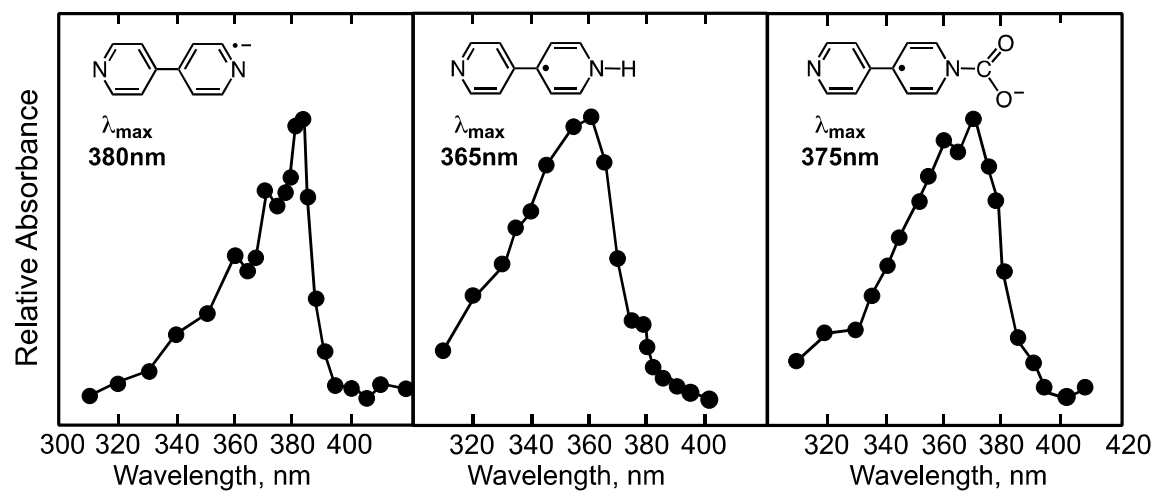


Figure 4.2. Transient absorption spectra of (left) the 4,4'-bipyridine radical anion in acetonitrile, measured 200 ns after pulsed laser excitation of the bipyridine in the presence of DABCO, (center) the radical product of protonation of the radical anion in acetonitrile measured 200 ns after pulsed laser excitation of the bipyridine in the presence of triethylamine, and (right) the distonic carbamate anion radical adduct in dichloromethane, measured 100 ns after excitation of the bipyridine in the presence of DABCO in a CO₂ saturated solution, all at room temperature.

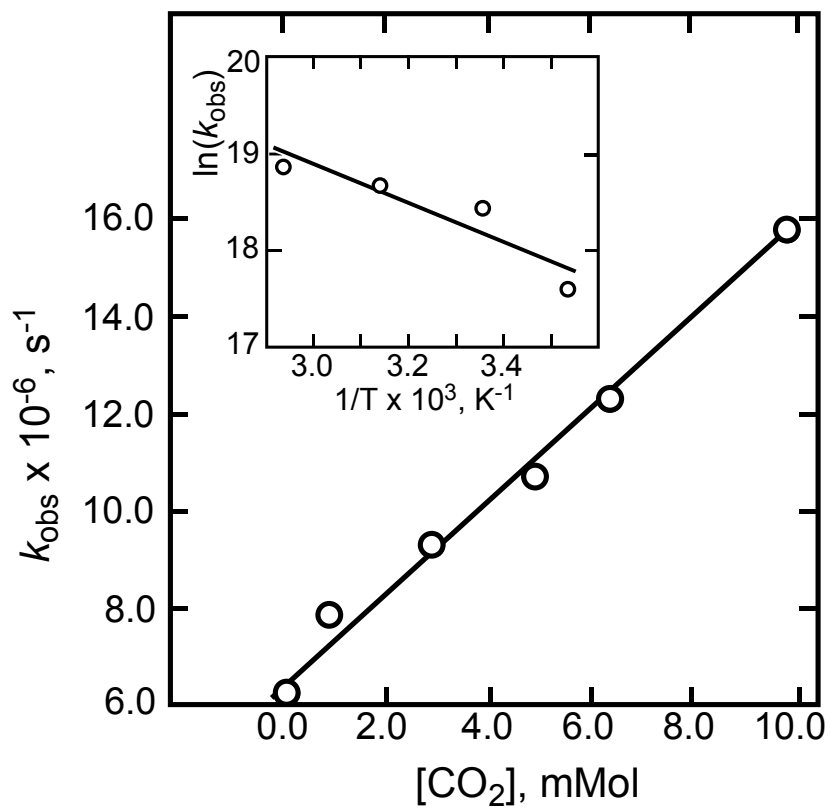


Figure 4.3. Observed pseudo-first order rate constant for decay of the 4,4'-bipyridine radical anion, k_{obs} , as a function of concentration of carbon dioxide. The bimolecular rate constant for reaction is given by the slope as $9.2 \pm 0.2 \times 10^7 \text{ M}^{-1} \text{ s}^{-1}$. The inset is an Arrhenius plot for the reaction rate constant.

dried dichloroethane (see the Experimental section for details). A plot of the pseudo-first order rate constant for decay of the bipyridyl radical anion (**Bpy^{•-}**) as a function of CO₂ concentration yields a bimolecular rate constant for reaction of $9.2 \times 10^7 \text{ M}^{-1} \text{ s}^{-1}$, Figure 3. After reaction with CO₂, the absorption spectrum of the **Bpy^{•-}** is replaced by a new spectrum with absorption maximum at 375 nm. Even though this new species and the radical **Bpy[•]-H** have similar absorption spectra, Figure 4.3, it is apparent that the new species is not the radical because it reacts with dissolved oxygen more slowly than the radical, and in contrast to the radical it is long lived on the timescale of the experiment. Its lifetime is greater than 10 ms and is too long to be measured with the experimental apparatus. We assign this new species to the product of nucleophilic addition of one of the bipyridyl nitrogens to the carbonyl carbon, Eqn. 4.1a. Support for this assignment comes from computational studies, described below.

To the best of our knowledge, the rate constant of $9.2 \pm 0.2 \times 10^7 \text{ M}^{-1} \text{ s}^{-1}$ represents the largest reported for a nucleophilic addition to CO₂,¹³ and is consistent with a low barrier for reaction. The temperature dependence of the rate constant was measured over the temperature range 10°C - 68°C. An Arrhenius plot of the bimolecular rate constant for reaction of **Bpy^{•-}** with CO₂ is included as an insert in Figure 4.3. The Arrhenius activation energy is $16.7 \pm 2.0 \text{ kJ/mol}$ and the pre-exponential factor is $7.4 \pm 3 \times 10^{10} \text{ s}^{-1}$. The experimental uncertainties in these values are large because of the restricted temperature range of the measurements, but more importantly because the change in solubility of the CO₂ over the temperature range was larger than the change in the reaction rate constant (see Experimental section). Nevertheless, it is clear that the

reaction has a small barrier. The activation free energy at 300K corresponds to 27.7 ± 2.0 kJ/mol.

4.2.3. Computational Studies of the Reaction Between the 4,4'-Bipyridine Radical Anion and Carbon Dioxide

Computational analysis was performed by Edward D. Lorange, our collaborator at Vanguard University. The reaction between the **Bpy**^{•-} and CO₂ was studied computationally with Gaussian09 (see Experimental section), using the M06-2X hybrid meta-GGA density functional with the aug-cc-pVDZ basis, which has been found by Truhlar to give good results for kinetic studies.¹⁴ The solvent was included using IEFPCM as implemented in Gaussian 09. The adduct structure was first obtained, and a potential energy scan conducted lengthening the bipyridyl nitrogen-CO₂ carbonyl (N-C) bond length, $r_{\text{N-C}}$, to locate the transition state and any intermediates. When stationary points (minima or first-order saddle points) were located, they were then optimized without bond length restrictions and the free energy computed, including electrostatic and non-electrostatic solvation contributions. These free energies were then used with transition state theory to compute the reaction rate.

In addition to the N-C bond length, the most significant molecular parameters that change are the O-C-O angle in the carboxyl, α , and the length of the carbon-carbon bond that joins the rings in the bipyridyl (the inter-ring C-C bond). The O-C-O bond angle changes smoothly as the linear carbon dioxide transforms into a carboxylate as it is attacked by the bipyridyl radical anion, Figure 4.4. In the bipyridyl radical anion, the inter-ring C-C bond is stretched, presumably to increase the space over which the extra

electron is spread. In the course of the reaction the charge density in the bipyridyl radical anion is shifted toward the more electronegative oxygen atoms and generally diffused into larger molecular orbitals and the inter-ring C-C bond shortens. The initial ring shape in the bipyridyl radical anion is distorted as a consequence of populating the bipyridyl LUMO π^* orbital. The attacking (*proximal*) ring is brought into a more regular hexagonal shape in the adduct, presumably due to a shift in electron density away from the distorting π^* orbital.

In addition to the transition state, an energy minimum was found corresponding to a pre-reaction complex, Figure 4.4, within the single-solvent-cavity region of the N-C bond stepping ($< 3.4 \text{ \AA}$), it seems likely that it represents a real complex and not an artifact of the solvation method being used at extreme separations. The relevant free energies are summarized in Figure 4.5. The existence of a pre-reaction complex raises the question of whether the slower step in the reaction is formation of the complex or the actual nucleophilic addition; the computation predicts that it will be the formation of the complex. The free energy barrier from the complex to the nucleophilic addition transition state is 6.65 kJ/mol, yielding a rate constant (at 25°C, assuming a transmission coefficient of unity) of $4.2 \times 10^{11} \text{ M}^{-1} \text{ s}^{-1}$, while the barrier to forming the complex from isolated reactants is 26.9 kJ/mol, yielding a bimolecular rate constant of $1.2 \times 10^7 \text{ M}^{-1} \text{ s}^{-1}$, which is remarkably close to the experimentally measured value of $9.2 \times 10^7 \text{ M}^{-1} \text{ s}^{-1}$.

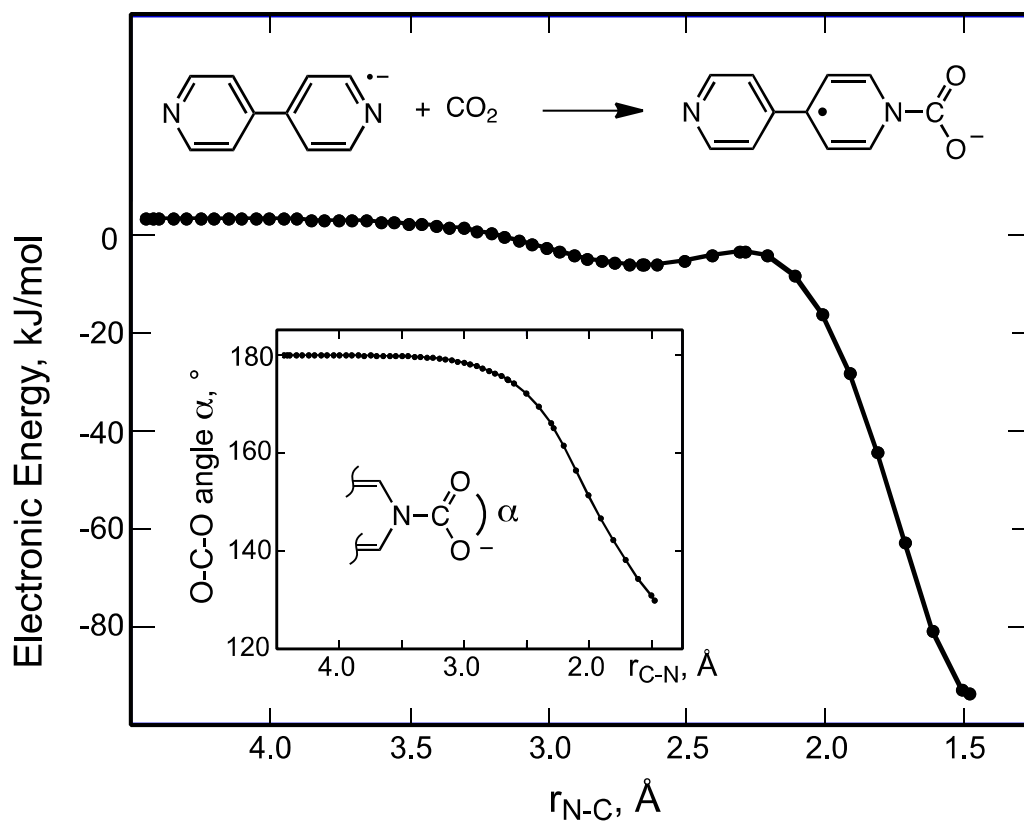


Figure 4.4. Electronic energy (including the free energy of solvation contribution) as a function of the N–C bond length for reaction of bipyridine radical anion with carbon dioxide, r_{N-C} , showing formation of a weak bimolecular complex before the transition state to form the distonic carbamate anion radical adduct. The inset shows the smooth change in the O–C–O bond angle, α , as a function of decreasing r_{N-C} , from 180° in the reactants to 129.8° in the adduct.

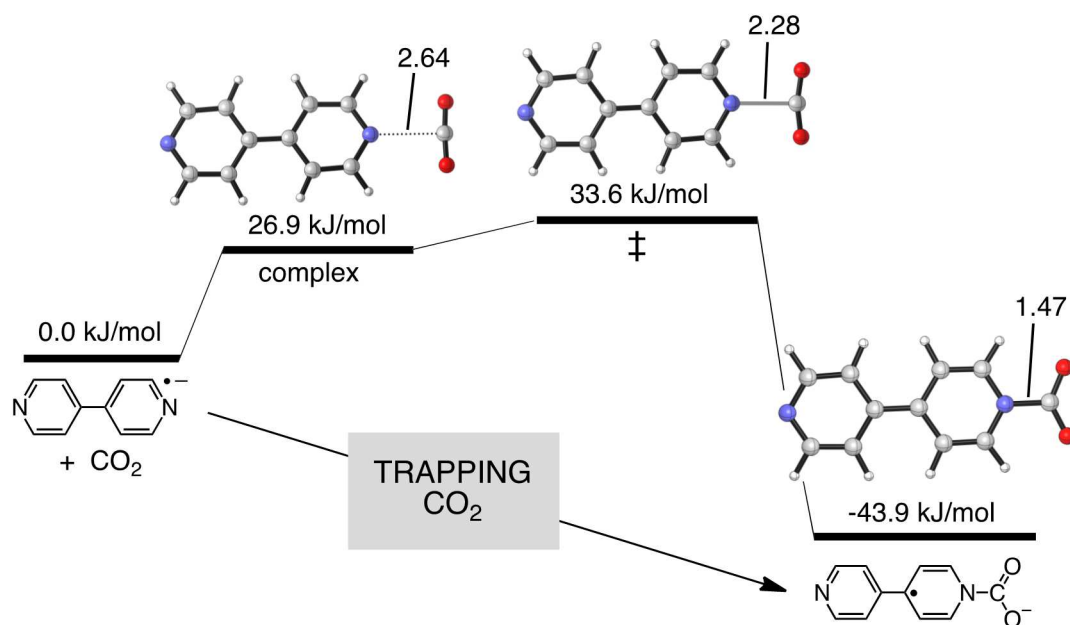


Figure 4.5. Computed free energies and structures for stationary points along the reaction coordinate for the reaction of the bipyridine radical anion with carbon dioxide to give the distonic carbamate anion radical adduct (see text and experimental section for details), showing formation of a bimolecular complex prior to the transition state. The energies are relative to the sum of the solvated free energies of 4,4'-bipyridyl radical anion and carbon dioxide, the indicated bond lengths are in Å.

In turn this strongly supports the proposal that the reaction of the bipyridine radical anion with carbon dioxide under both electrochemical and photochemical conditions is formation of the carbamate radical ion adduct, Eqn 4.1a.

The overall reaction is computed to be exergonic, by 43.9 kJ/mol. It is also computed to be exothermic, the reaction enthalpy is -88.3 kJ/mol, and the computed reaction entropy is -149.1 J/K.mol, which is not unusual for a reaction that forms one chemical species from two.¹⁵

4.3. Computational Studies of the Distonic Carbamate Anion Radical Adduct

The carbamate product of addition of the 4,4'-bipyridine radical anion to carbon dioxide has radical character, and although it is fairly stable in solution on a seconds timescale, based on the reversible cyclic voltammetry, Figure 4.1, attempts to isolate it failed, presumably due to reaction with oxygen. The kinetics of the oxidative decarboxylation could not, therefore, be directly measured using pulsed laser techniques. The oxidized adduct can be described in terms of biradical or zwitterion electron configurations, depending upon whether oxidation is considered to take place formally at the radical center or at the carboxylate anion. As mentioned above, the oxidation potentials of conjugated amino radicals are known to be lower than the carboxylate anion,^{10,11} and the computed structure of the oxidized adduct is a ground state singlet (using an unrestricted method), so we draw the oxidized adduct as a zwitterion, Eq. 1b. Decarboxylation of the formal zwitterion thus closely resembles the known decarboxylation reaction of the radical cations of aniline carboxylates, which are known

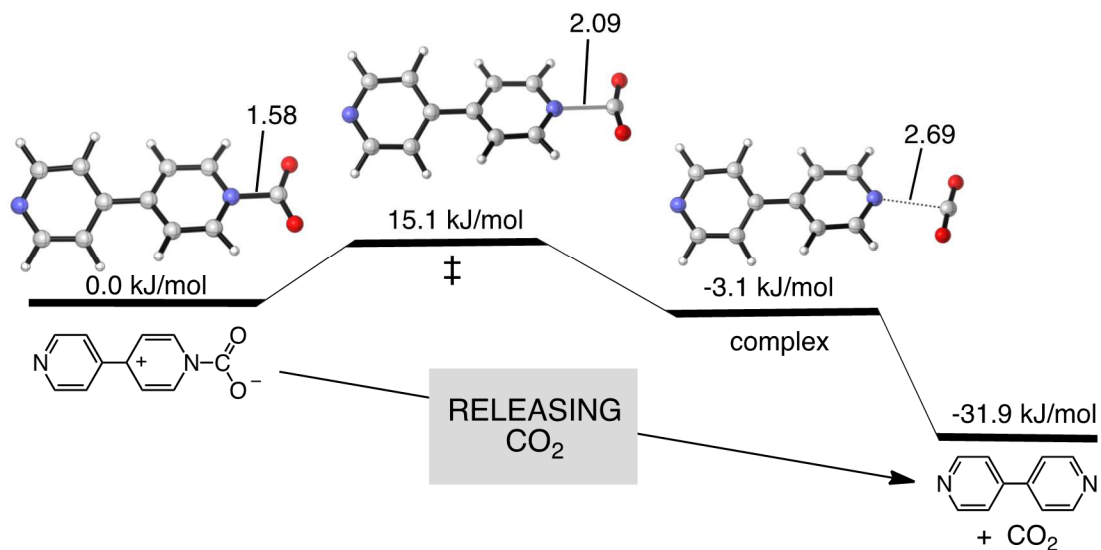


Figure 4.6. Computed free energies and structures for stationary points along the reaction coordinate for decarboxylation of the oxidized product of addition of the 4,4'-bipyridine radical anion and carbon dioxide, to give neutral bipyridine and carbon dioxide (see text and experimental section for details), showing formation of a bimolecular complex after the transition state for bond cleavage. The energies are relative to the free energy of the oxidized and solvated adduct, the indicated bond lengths are in Å.

to be exergonic and fast.¹⁶ Another one-electron-oxidized electron configuration is a biradical, Eqn. 4.1b, and because mixing of electron configurations is required for decarboxylation,^{16,17} this state could also be important in controlling the reaction kinetics. Decarboxylation of the biradical resembles fragmentations in other pyridyl radicals, which are known to be fast.¹⁷ In addition, we have also shown previously that density functional theory can accurately predict the kinetics of fragmentation of pyridyl radicals.^{17a,b} We thus expect that density functional theory should provide a good description of the kinetics of the oxidation decarboxylation of the adduct.

The fragmentation of the oxidized adduct was studied using the same methods and parameters as the nucleophilic addition of the bipyridyl radical anion described above, Figure 4.6.

The structure of the oxidized adduct was determined and a potential energy scan conducted by lengthening the bipyridyl nitrogen-CO₂ carbonyl bond length, $r_{\text{N-C}'}$, where the prime symbol distinguishes the fragmentation reaction from the bond formation reaction above. As with bond formation, a bimolecular complex was found, except that from the perspective of fragmenting the zwitterionic adduct, this is a *post-reaction* complex rather than a pre-reaction complex, Figure 4.7. At larger separation distances than the complex, the electronic energy profile was very insensitive to $r_{\text{N-C}'}$, and was at the same time quite sensitive to the relative orientations of the CO₂ and the bipyridyl long axis and the nearest pyridine plane. Consequently, the transition state for the formation of the CO₂-bipyridyl complex was not located. Separation of the fragments from the complex is exergonic, Figure 4.6, therefore we equate formation of the complex

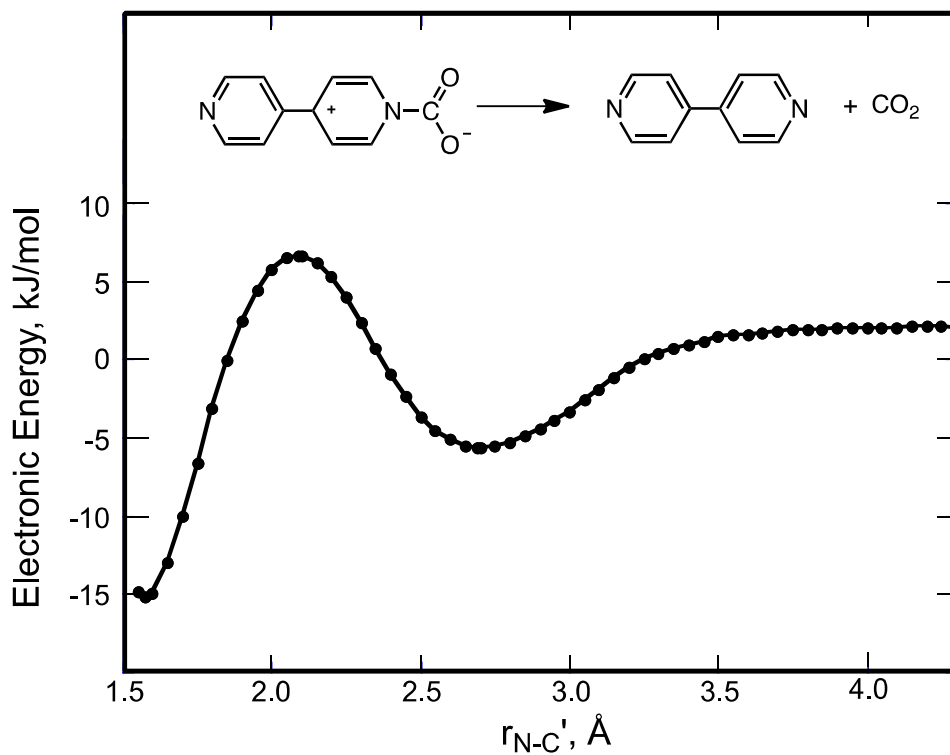


Figure 4.7. Electronic energy (including the free energy of solvation contribution) as a function of the N–C bond length for the fragmentation reaction of the oxidized bipyridine radical anion with carbon dioxide, $r_{N-C'}$, showing formation of a bimolecular complex after the transition state to form the neutral 4,4'-bipyridine and carbon dioxide. Although the electronic energy in the products is higher than that in the reactant, the reaction is exergonic, see Figure 4.5.

with the rate-determining step for overall reaction. The free energy gap from the zwitterion to the transition state is 15.1 kJ/mol, which yields a rate constant (at 25°C, assuming a transmission coefficient of unity) of $1.4 \times 10^{10} \text{ s}^{-1}$. This rate constant is very much in the range of rate constants for fragmentation in related systems.^{16,17} The overall reaction is computed to be exergonic, by 31.9 kJ/mol, although in this case the reaction is slightly endothermic: the reaction enthalpy is 9.79 kJ/mol. However, the reaction entropy is highly favorable, 139.8 J/K.mol (as expected for a reaction that converts one chemical species into two), which results in an overall fast reaction.

4.4. Summary

Trapping of carbon dioxide using the radical anion of 4,4'-bipyridine, formed electrochemically, is exothermic, exergonic and has a low barrier for reaction. The 4,4'-bipyridine radical anion/carbon dioxide adduct can be oxidized to a species that undergoes decarboxylation to release carbon dioxide in a reaction that, although is slightly endothermic, is exergonic and is expected to be very fast. Each process involves the addition or removal of a single electron and the electrochemical switching voltage between trapping and release is only ca. 700 mV. The energetic requirements for trap and release are thus quite minimal.

4.5. Experimental

1. Electrochemistry. The ionic liquid N-butyl-N-methylpyrrolidinium bis(trifluoromethylsulfonyl)imide was used as both the solvent and the electrolyte, and was synthesized according to literature.¹⁸ The ionic liquid was dried under vacuum with heating until the water content was <20ppm, determined by Karl Fischer titration. The electrochemical apparatus was a modified H-cell, customized to enable titration with the inert (N₂) or reactive (CO₂) gases without introducing O₂ and atmospheric moisture. The working electrode (3-millimeter diameter glassy carbon, CH Instruments) was placed in one chamber of the apparatus, and separate platinum wires (serving as counter and quasi-reference electrodes, respectively) were both confined in the chamber opposite to the working electrode; ferrocene was used as an internal reference. A 10mM solution of 4,4'-bipyridine in the ionic liquid was prepared inside a Vac Atmospheres glovebox (<1ppm H₂O, O₂). All voltammograms were recorded at 50 mV/s with a CH Instruments 618 potentiostat.

2. Photochemistry. The transient absorption apparatus was as described previously.^{17c} The excitation source was a frequency-quadrupled (266 nm) Quantel Brilliant B Ng:YAG laser. 1 mM solutions of 4,4'-bipyridine were analyzed in acetonitrile or 1,2-dichloroethane solvent in 1-cm cuvettes equipped with arms for purging with nitrogen or carbon dioxide gas. The dichloroethane solvent was dried for 72 hours using activated molecular sieves. Sieves were present in the cuvettes throughout the experiments to minimize the interference of dissolved water. 2mM DABCO or triethylamine were used as the donors.

The carbon dioxide concentration in the dichloroethane solutions was varied by purging with a mixture of CO₂ and argon. Balloons filled with argon were weighed and then varying quantities of carbon dioxide were additionally added to the balloons, which were then weighed again. Ideal gas behavior was assumed in order to calculate the weight percentage of CO₂ in the mixtures in the balloons, which were then used to purge the sample solutions. The solubility of carbon dioxide in DCE was measured by gravimetric analysis. DCE saturated with CO₂ was mixed with an excess aqueous Ba(OH)₂ solution. The precipitated BaCO₃ was filtered, dried and weighed, and the amount of CO₂ was determined assuming one mole of carbon dioxide per mole of BaCO₃. The solubility of carbon dioxide at all of the temperatures used to generate the Arrhenius plot was determined in the same way. The solubilities obtained this way were 303 mM, 252 mM, 93 mM and 46 mM at 10°C, 25°C, 45°C and 68°C, respectively.

3. Computations. Calculations were performed using Gaussian09 Rev. A.02,¹⁹ running on a 64-bit Macintosh BSD Unix system. We found, after some preliminary exploration and in particular trials with B3LYP that the M06-2X hybrid meta-GGA density functional would be the best compromise between computational time and accuracy. The M06 family of functionals, and esp. the M06-2X hybrid, are well-known for their accuracy in standard main-group thermochemical and kinetic applications while having a significant improvement in long-range interaction accuracy.²⁰ We used this method with the aug-cc-pVDZ basis;²¹ the M06-2X method with the aug-cc-pVDZ basis has been assessed for kinetics by Truhlar and co-workers and they found that it has a mean signed

error for nucleophilic substitution of -0.01 kcal/mol and for unimolecular and association reactions of -0.37 kcal/mol (*those being the two most applicable categories*).¹⁴

There was some question as to how best to include the solvent in the modeling since it seemed counterproductive to use a low-accuracy solvent model with a high-accuracy electronic structure method; however, this issue has been addressed by Truhlar and co-workers, who determined that for solution phase kinetics the use of a solvation method is important but the quality of the method is generally not largest contribution to the error.²² We therefore chose the integral equation formalism implementation of the polarizable continuum method in Gaussian09 (IEFPCM) with acetonitrile at 25°C and 1 atm pressure. At very long distances, this method predicts that separate cavities will exist for the two reacting particles.

References:

1. a) Dell'Amico, D. B.; Calderazzo, F.; Labella, L.; Marchetti, F.; Pampaloni, G. *Chem. Rev.* 2003, 103, 3857- 3898. b) Jessop, P. G.; Joó, F.; Tai, C. C. *Coord. Chem. Rev.* 2004, 248, 2425-2442. c) Sakakura, T.; Choi, J. C.; Yasuda, H. *Chem. Rev.* 2007, 107, 2365-2387. d) Mikkelsen, M., Jorgensen, M.; Krebs, F. C. *Energy Environ. Sci.* 2010, 3, 43–81.
2. a) Kumar, B.; Llorente, M.; Froehlich, J.; Dang, T.; Sathrum, A.; Kubiak, C. P. *Annu. Rev. Phys. Chem.*, 2012, 63, 541-569. b) Centi, G.; Perathoner, S. *Catal. Today* 2009, 148, 191–205.
3. a) Aresta, M. *Carbon Dioxide Recovery and Utilization*; Kluwer Academic Publishers: Dordrecht, 2010. b) Metz, B., Davidson, O., De Coninck, H., Loos, M. & Meyer, L. *Carbon Dioxide Capture and Storage*; Cambridge University Press: Cambridge UK, 2005.
4. a) Villiers, C.; Dognon, J.-P.; Pollet, R.; Thuory, P.; Ephritikhine, M. *Angew. Chem. Int. Ed.* 2010, 49, 3465 –3468. b) Ma, J.; Zhang, X.; Zhao, N.; Al-Arifi, A. S. N.; Aouak, T.; Al-Othman, Z. A.; Xiao, F.; Wei, W.; Sun, Y. *J. Mol. Catal. A* 2010, 315, 76-81. c) McGhee, W.; Riley, D.; Christ, K.; Pan, Y.; Parnas, B. *J. Org. Chem.* 1995, 60, 2820–2830. d) McGhee, W.; Riley, D. *J. Org. Chem.* 1995, 60, 6205-6207. e) Hooker, J. M.; Reibel, A. T.; Hill, S. M.; Schueller, M. J.; Fowler, J. S. *Angew. Chem. Int. Ed.* 2009, 48, 3482-3485.
5. Metz, B. *IPCC Special Report on Carbon Dioxide Capture and Storage*; Cambridge University Press: Cambridge, 2005.
6. Freguia, S.; Rochelle, G. T. *AIChE J.* 2003, 49, 1676– 168. b) Kim, I.; Svendsen, H. F. *Ind. Eng. Chem. Res.* 2007, 46, 5803-5809. c) Davison, J. *Energy* 2007, 32, 1163– 1176.

7. a) Barton, E. E.; Rampulla, D. M.; Bocarsly, A. B. *J. Am. Chem. Soc.* 2008, *130*, 6342–6344. b) Barton Cole, E.; Lakkaraju, P. S.; Rampulla, D. M.; Morris, A. J. Abelev, E.; Bocarsly, A. B. *J. Am. Chem. Soc.* 2010, *132*, 11539–11551. c) Morris, A. J.; McGibbon, R. T.; Bocarsly, A. B. *ChemSusChem*, 2011, *4*, 191–196.
8. Keith, J. A.; Carter, E. A. *J. Am. Chem. Soc.*, 2012, *134*, 7580-7583.
9. a) Constantin, C.; Saveant, J.-M. *Chem. Soc. Rev.* 2013, *42*, 2423-2436. b) Gattrell, M.; Gupta, N.; Co, A. *J. Electroanal. Chem.* 2006, *594*, 1-19. c) Hori, Y. in *Modern Aspects of Electrochemistry*, Vol. 42; Vayenas, C.; White, R. E.; Gamboa-Adelco, M. E. (Eds.), Springer: New York, 2008, p. 89. d) Qiao, J.; Liu, Y.; Hong, F.; Zhang, J. *Chem. Soc. Rev.* 2014, *43*, 631-675.
10. a) Wayner, D. D.; McPhee, D. J.; Griller, D. *J. Am. Chem. Soc.* 1988, *110*, 132-137. b) Griller, D.; Wayner, D. D. *M. Pure Appl. Chem.* 1989, *61*, 717-724.
11. a) Poizat, O.; Buntinx, G.; Valat, P.; Wintgens, V.; Bridoux, M. *J. Phys. Chem.* 1993, *97*, 5905-5910. b) Poizat, O.; Buntinx, G.; Ventura, M.; Lautie, M. F. *J. Phys. Chem.* 1991, *95*, 1245-1253. c) Buntinx, G.; Valat, P.; Wintgens, V.; Poizat, O. *J. Phys. Chem.* 1991, *95*, 9347-9352.
12. Wosinska, Z. M.; Stump, F. L.; Ranjan, R.; Lorance, E. D.; Finley, G. N.; Patel, P. P.; Khawaja, M. A.; Odom, K. L.; Kramer, W. H.; Gould, I. R. *Photochem. Photobiol.*, 2014, *90*, 313-328.
13. Sakakura, T., Choi, J.-C.; Yasuda, H. *Chem. Rev.* 2007, *107*, 2365–2387.

14. Zheng, J. J.; Zhao, Y.; Truhlar, D. G. *J. Chem. Theory Comput.*, **5**, (2009) 808–821.
15. Moore, J. W.; Pearson, R. G. *Kinetics and Mechanism*, 3rd ed.; John Wiley: New York, 1981.
16. Gould, I. R.; Lenhard, J. R.; Farid, S. *J. Phys. Chem. A*. 2004, *108*, 10949-10956.
17. a) Lorange, E. D., Hendrickson, K., Gould, I. R. *J. Org. Chem.*, 2005, *70*, 2014-2020. b) Lorange, E. D.; Gould, I. R. *J. Phys. Chem. A*. 2005, *109*, 2912. c) Lorange, E. D.; Kramer, W. H.; Gould, I. R. *J. Am. Chem. Soc.*, 2004, *126*, 14071. d) Gould, I. R.; Shukla, D.; Giesen, D.; Farid, S. *Helv. Chim. Acta*, 2001, *84*, 2796-2812.
18. Appetecchi G. B.; Scaccia S.; Tizzani C.; Alessandrini F.; Passerini S. *J. Electrochem. Soc.* 2006, *153*, A1685–A1691.
19. Gaussian 09, Revision A.02, M. J. Frisch, G. W. Trucks, H. B. Schlegel, G. E. Scuseria, M. A. Robb, J. R. Cheeseman, G. Scalmani, V. Barone, B. Mennucci, G. A. Petersson, H. Nakatsuji, M. Caricato, X. Li, H. P. Hratchian, A. F. Izmaylov, J. Bloino, G. Zheng, J. L. Sonnenberg, M. Hada, M. Ehara, K. Toyota, R. Fukuda, J. Hasegawa, M. Ishida, T. Nakajima, Y. Honda, O. Kitao, H. Nakai, T. Vreven, J. A. Montgomery, Jr., J. E. Peralta, F. Ogliaro, M. Bearpark, J. J. Heyd, E. Brothers, K. N. Kudin, V. N. Staroverov, R. Kobayashi, J. Normand, K. Raghavachari, A. Rendell, J. C. Burant, S. S. Iyengar, J. Tomasi, M. Cossi, N. Rega, J. M. Millam, M. Klene, J. E. Knox, J. B. Cross, V. Bakken, C. Adamo, J. Jaramillo, R. Gomperts, R. E. Stratmann, O. Yazyev, A. J. Austin, R. Cammi, C. Pomelli, J. W. Ochterski, R. L. Martin, K. Morokuma, V. G. Zakrzewski, G. A. Voth, P. Salvador, J. J. Dannenberg, S. Dapprich, A. D. Daniels, O. Farkas, J. B.

Foresman, J. V. Ortiz, J. Cioslowski, and D. J. Fox, Gaussian, Inc., Wallingford CT, 2009.

20. Zhao, Y.; Truhlar, D. G. *Theor. Chem. Acc.* 2008, *120*, 215-241.
21. Dunning, T. H. *J. Chem. Phys.* 1989, *90*, 1007-1023. b) Kendall, R. A.; Dunning, T. H.; Harrison, R. J. *J. Chem. Phys.* 1992, *96*, 6796-806. c) Woon, D. E.; Dunning, T. H. *J. Chem. Phys.* 1993, *98*, 1358-1371. d) Peterson, K. A.; Woon, D. E.; Dunning, T. H. *J. Chem. Phys.* 1994, *100*, 7410-7415. e) Wilson, A. K.; van Mourik, T.; Dunning, T. H. *J. Mol. Struct. (Theochem)* 1996, *388*, 3393-49. f) Davidson, E. R. *Chem. Phys. Lett.* 1996, *260*, 514-518.
22. a) Truhlar, D. G.; Pliego, J. R. in *Continuum Solvation Models in Chemical Physics: From Theory to Applications*, Mennucci, B.; Cammi, R. (Eds.); Wiley: Chichester, 2008. p.338-365 (esp. 357-8). b) Raspert, G.; Nguyen, M. T.; Kelly, S.; Hegarty, A. F. *J. Org. Chem.* 1998, *63*, 9669-9677. c) Cavalli, A.; Masetti, M.; Recantini, M.; Prandi, C.; Guarna, A.; Occhiato, E. G. *Chem. Eur. J.* 2006, *12*, 2836-2845.

CHAPTER 5

KINETICS AND THERMODYNAMICS OF THE 4,4'-BIPYRIDINE RADICAL ANION AS A BRONSTED BASE

5.1 Introduction

One electron reduction of an organic molecule forms a radical anion, which compared to the corresponding neutral species is potentially a much stronger Brønsted base, Lewis base, one-electron reductant and nucleophile.¹ Quantitative studies of the Brønsted basicity of a variety of organic radical anions have now been reported.² Brønsted basicity and nucleophilicity are molecular properties that are often competitive, a famous example being the competition between substitution and elimination reactions of alkyl halides.³ Nucleophilicity is defined kinetically, whereas Brønsted basicity is usually defined thermodynamically, in terms of pKa. When nucleophilicity and Brønsted basicity are competitive, a kinetic comparison of these two properties would be more useful in order to understand or even predict which would dominate. The kinetics of proton transfer reactions have traditionally been described using transition state theory,⁴ however, transition state theory has no predictive capability.

However, classical Marcus theory has also been extensively applied to proton transfer reactions.⁵ Because Marcus theory connects the kinetics of proton transfer with the thermodynamics of the reaction, knowing the pKa values of the acid and base could in theory allow prediction of the reaction kinetics, if the intrinsic barrier, or reaction reorganization energy is known. Although quantum mechanical effects become important for highly exothermic proton transfer reactions,^{4,6} particularly in the so-called

inverted region, where the reaction rates decrease with driving force,^{7,8} the simple classical theory is useful for thermally activated proton transfers.⁹

We are interested in the competition between nucleophilicity and Bronsted basicity because the reactions of one-electron reduced pyridines have recently been found to be useful in applications that either reversibly trap carbon dioxide,¹⁰ or convert it into higher value reduced forms such as methanol.¹¹ In the latter example the reactions appear to involve mainly the protonated reduced pyridine, and in the former, protonation of the pyridine radical anion competes with the desired nucleophilic addition reaction. Quantitative studies of the nucleophilic reactions of the pyridine radical anions have recently been completed,¹² but quantitative measurements of the Bronsted basicity of these species have not yet been reported. In fact, although equilibrium pKa measurements of several transient radical anions have been made,¹³ there have been only a few reports of kinetics studies that allow the determination of reorganization energies for proton transfer to organic radical anions.^{8,9,14} Here we report quantitative measurements of the pKa of the radical anion of 4,4'-bipyridine and also the reorganization energy for proton transfer from phenols as proton donors.

5.2 Experimental

Transient absorption. The kinetics of the proton transfer reactions were measured using pulsed laser transient absorption. The apparatus has been described previously.¹⁵ The excitation source was a frequency-quadrupled (266 nm) Quantel Brilliant B Ng:YAG laser. 1 mM solutions of 4,4'-bipyridine were analyzed in acetonitrile solvent in 1-cm cuvettes equipped with arms for purging with argon gas. The concentration of the DABCO electron donor was 2 mM. The decay kinetics of the bipyridine radical

anion were measured at 380 nm. All chemicals and the solvent were obtained from Sigma-Aldrich and were used as received.

5.3 Results and Discussion

5.3.1. Reaction Kinetics. The kinetics of the proton transfer reactions were measured using pulsed laser transient absorption spectroscopy. As demonstrated previously,¹⁶ one-electron reduction of the first excited triplet state of bipyridine (**Bpy**) using **DABCO** as the electron donor results in formation of a triplet **Bpy^{•-}/DABCO^{•+}** pair. Separation of the radical ions in the polar acetonitrile is rapid and efficient,¹⁷ and freely diffusing **Bpy^{•-}** is formed within 50 ns of the laser pulse. The **Bpy^{•-}** is a strong one-electron donor and Bronsted base, and the time-resolved decay of the radical anion in acetonitrile is pseudo-first order rather than second order via recombination with the **DABCO^{•+}**. The decay is presumably due to reaction with solvent impurities, or slow reaction with the solvent itself. The measured lifetime of the **Bpy^{•-}** under the experimental conditions is 1.2 μ s in argon-purged acetonitrile.

The observed rate constant for pseudo-first order decay of the **Bpy^{•-}** at 380 nm was measured as a function of added proton donor. Plots of the observed rate constant as a function of concentration of the added proton donor were linear, and from the slopes the bimolecular rate constant for proton transfer were obtained, Table 1.

Table 1. Rate Constants, k_{H^+} , and Thermodynamic Data for Proton Transfer From Phenols and Other Alcohols to the Radical Anion of 4,4'-Bipyridine in Acetonitrile Solvent at Room Temperature.

Proton Donor	pKa ^a	k_{H^+} ^b ($10^8 \text{ M}^{-1} \text{ s}^{-1}$)	ΔG_{H^+} ^c (kJ/mol)
<i>p</i> -nitrophenol	10.8	100	61.62
<i>p</i> -trifluoromethylphenol	15.3	43	87.30
<i>o</i> -fluorophenol	15.6	25	89.01
<i>m</i> -fluorophenol	15.8	33	90.15
phenol	18	12	102.70
<i>p</i> -cresol	18.9	16	107.84
<i>p</i> -methoxyphenol	19.1	12	108.98
2,4,6-trimethylphenol	~20	6.5	114.12
hexafluoroisopropanol	17.9	13.5	102.14
trifluoroethanol	23.5	0.47	134.091

^a pKa values in DMSO solvent, from refs 18 and 19.

^b Bimolecular rate constant for proton transfer in acetonitrile.

^c Free energy change associated with proton transfer from the alcohol to the **Bpy**^{•-} in DMSO solvent, assuming a pKa for the **Bpy**^{•-} of 40 in DMSO.

Substituted phenols were used as the proton donors since the pKa values for these structures can be readily varied over a fairly wide range, so that the driving force for proton transfer to the **Bpy**^{•-} can be correspondingly varied. The use of substituted phenols has been described previously by Jaworski et al.¹⁴ Two other alcohols were used as proton donors, hexafluoroisopropanol and trifluoroethanol, see below.

Reaction with phenol derivatives were readily observed in acetonitrile. A kinetic trace of the decay of bipyridine radical anion in the presence of 2mM trimethyl phenol have been shown in Figure 5.1. After reaction with phenol and its derivatives, the absorption spectrum of the **Bpy**^{•-} is replaced by a new spectrum with absorption maximum at 360 nm, Figure 5.1. This new species and the radical **Bpy**[•]-H have same absorption spectra. It is apparent that the new species is the radical formed by the proton transfer from phenol derivatives to the bipyridine radical anion.

From the known pKa values of the phenols, it is apparent that the stronger Bronsted acids donate protons to the **Bpy**^{•-} with larger rate constants, as expected. The strongest proton donor, *p*-nitrophenol, reacts with the **Bpy**^{•-} with a rate constant that is very close to the diffusion controlled limit.²⁰ All other rate constants are lower due to less energetically favorable proton transfer.

5.3.2. Data Fitting. The kinetic data were fitted using a version of Marcus theory. The important features of Marcus theory and the assumptions made in the analysis of the current data are as follows.⁵ The reactants and products are modeled as intersecting parabolic potential energy surfaces with a reaction coordinate that mainly reflects the

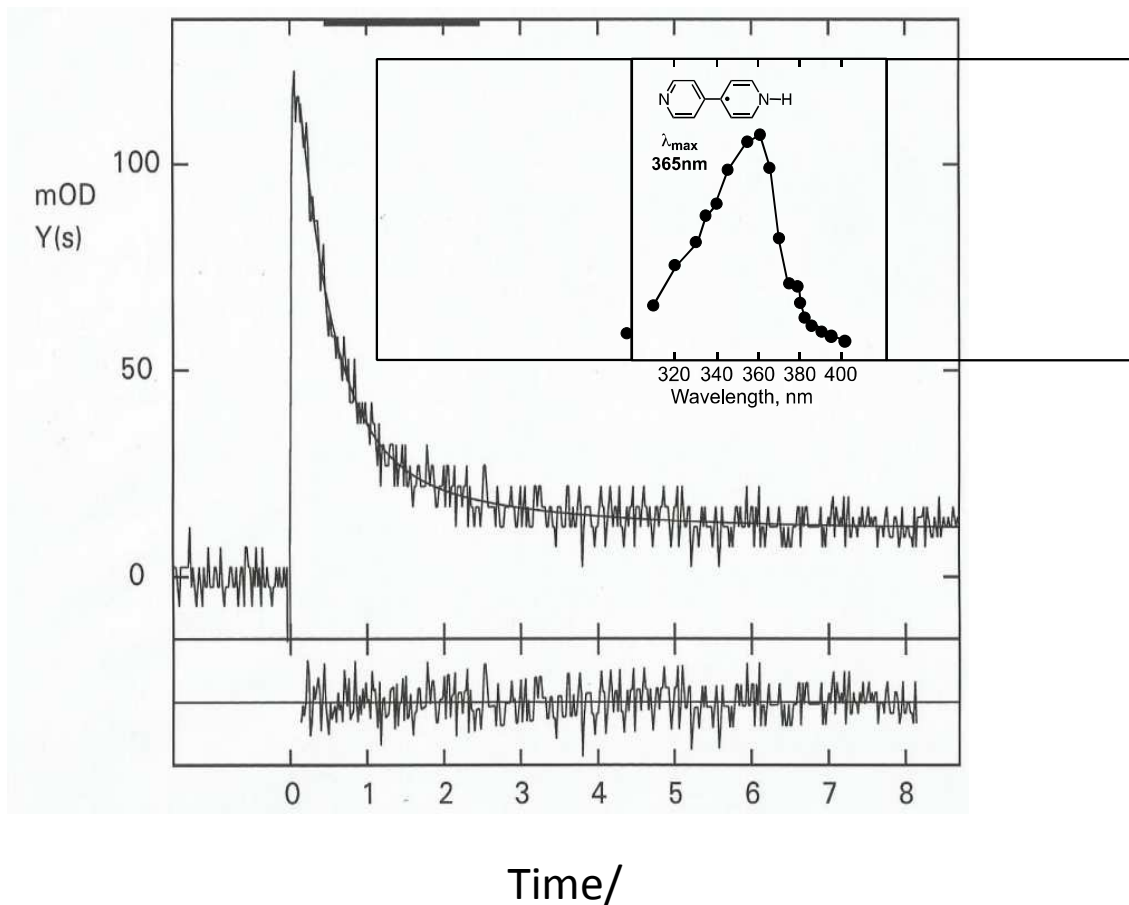


Figure 5.1. Absorbance decay showing decay of the 4,4'-bipyridine radical anion, monitored at 380 nm, in the presence of 2mM trimethyl phenol. The smooth curve through the data represents the best first order kinetic fit, corresponding to a first order rate constant for decay of $9 \times 10^6 \text{ s}^{-1}$. Inset shows the spectra of bipyridine radical anion obtained by the proton transfer from phenol derivatives to bipyridine radical anion.

reorganization of the solvent molecules in response to the change in molecular charges as the proton is transferred. The curves are parabolic as a consequence of the continuum of possible solvation states. The reaction activation energies, ΔG^\ddagger , are related to the reaction free energies, ΔG , via the reaction reorganization, λ Eqn 5.1a, which is a measure of the energy required to reorganize all of the nuclei to allow reaction to proceed. The major contributor to the reorganization energy is usually associated with the required solvent motion, λ_s , and this is the assumption behind the parabolic energy surfaces. Reorganization of the nuclei of the reactants also contributes to the total reorganization energy, λ_v , Eqn 5.1b. The high frequency vibrations associated with these nuclear motions are quantized and should be treated separately.^{5,6,21} However, by analogy to electron transfer reactions, the influence of the high frequency contributions to the reaction kinetics can only be detected in the inverted region,^{6,21,22} and for thermally activated proton transfer reactions, therefore, it is reasonable to combine λ_s and λ_v into a total effective reorganization energy λ since they can't be separated experimentally anyway, Eqns. 5.1a, 5.1b.

$$\Delta G^\ddagger = \frac{(\lambda + \Delta G)^2}{4\lambda} \quad (5.1a)$$

$$\lambda = \lambda_s + \lambda_v \quad (5.1b)$$

$$k_{H^+}^E = kT/h \text{ Exp}(-\Delta G^\ddagger/RT) \quad (5.1c)$$

$$\Delta G = -2.303 RT (\text{pKa}(\text{Bpy-H}) - \text{pKa}(\text{R-H})) \quad (5.1d)$$

$$k_{H^+} = \frac{k_{\text{diff}}}{1 + (k_{\text{-diff}}/k_{H^+}^E) + \text{Exp}(\Delta G/RT)} \quad (5.1e)$$

Thermally activated proton transfer reactions, i.e. those that are endergonic or close to endergonic can be described by classical adiabatic theory,⁶ thus the measured bimolecular rate constant has the transition state theory form of Eqn 5.1c. The proton transfer reactions studied are shown schematically in Eqn. 5.2. The **Bpy**^{•-} reacts with a generic proton donor, **R-H**, to give the protonated conjugate acid of the radical anion, **Bpy**[•]-**H**, and the conjugate base anion of the acid, **R**⁻. The free energy change for this reaction is determined by the difference in the pKas for the two acids, **Bpy**[•]-**H** and **R-H**, Eqn 5.1d.



The reorganization energy can be obtained from fitting the observed bimolecular rate constant, k_{H+} , rate constant as a function of the reaction free energy, ΔG . In the absence of an intrinsic barrier associated with λ , a plot of the logarithm of k_{H+} versus ΔG will be essentially linear, with a Boltzmann slope of $1/RT$.²³ Deviations from this linear behavior are increasingly observed with increasing λ . As the reactions become less endergonic with stronger acids **R-H**, these bimolecular reactions eventually approach the diffusion controlled limit, at which point the kinetics appear to have no information about the proton transfer process. However, the deviations from Boltzmann behavior are greatest at the turn over from highly endergonic to the diffusion controlled limit.²⁴ Thus, reactions that approach the diffusion controlled limit are the most informative with

respect to determining reorganization energies. Most previous studies of the kinetics of proton transfer reactions have been of reactions that are much slower than this.^{9,14}

The observed bimolecular rate constant for proton transfer, k_{H^+} , is related to the unimolecular rate constant for proton transfer in the encounter complex between the reactants, $k_{H^+}^E$, and the diffusion controlled rate constant, k_{diff} , as shown in Eqn. 5.1e. The diffusion controlled rate constant for bimolecular encounter, k_{diff} , can be estimated to be ca. $1.5 \times 10^{10} \text{ M}^{-1} \text{ s}^{-1}$ under the reaction conditions,²⁰ and this is very close to the measured rate constant for proton transfer for the strongest acid *p*-nitrophenol, Table 5.1. Also included in Eqn. 5.1e is the rate constant for diffusive separation from the encounter complex, k_{-diff} , and the usual assumption is this is twice the value of the rate constant for diffusion controlled encounter,²⁵ i.e. ca. $2.0 \times 10^{10} \text{ s}^{-1}$. Thus, using Eqns. 5.1, the rate constant for the bimolecular reaction of the **Bpy**^{•-} with acids of known pKa is described in terms of the parameters k_{diff} , k_{-diff} , λ and pKa (**Bpy-H**), i.e., essentially only the two unknown parameters of interest, λ and pKa (**Bpy-H**), since k_{diff} and k_{-diff} can be estimated fairly accurately independently.

Fits to the data according to Eqns. 5.1 are shown in Figure 5.2. The best fit to the data is obtained for pKa (**Bpy-H**) = 31 and $\lambda = 2.0 \text{ eV}$. The weak dependence of rate constant on driving force requires a large reorganization energy. The calculated dependence for small λ ($\lambda = 0.2 \text{ eV}$, grey curve, Figure 5.2), shows that the data would have a much stronger dependence on driving force if the reorganization energy was small. Although there are essentially only two adjustable parameters to fit the data, unfortunately they are inter-related in the sense that similar driving force dependencies can be obtained over a

fairly wide range in, for example λ , by making corresponding changes to pKa (**Bpy-H**). For this reason the estimated uncertainties in these two parameters are fairly large, $\lambda = 2.0 \pm 0.3$ eV and pKa (**Bpy-H**) = 31 ± 3 .

The measured pKa is thus large, consistent with the 4,4'-bipyridine radical anion being a very strong Bronsted base. However, because of the large reorganization energy, it is interesting that proton transfer only becomes diffusion controlled when the reaction is exothermic by ca. 120 kJ/mol, Figure 5.2. This behavior allows nucleophilic reactions to compete with protonation even though the base strength is large.

The reorganization energy is very large, however, it is similar to reorganization energies for electron transfer between organic molecules in solvent-separated radical ion pairs in acetonitrile, which range from ca. 1.5 eV to ca.2.0 eV.²⁶ The solvent reorganization energy for electron transfer, λ_s , is typically much larger than the internal vibrational reorganization energy, λ_v . and the charges in charge for proton transfer and electron transfer are the same, thus the reorganization energy obtained seems to be quite reasonable.

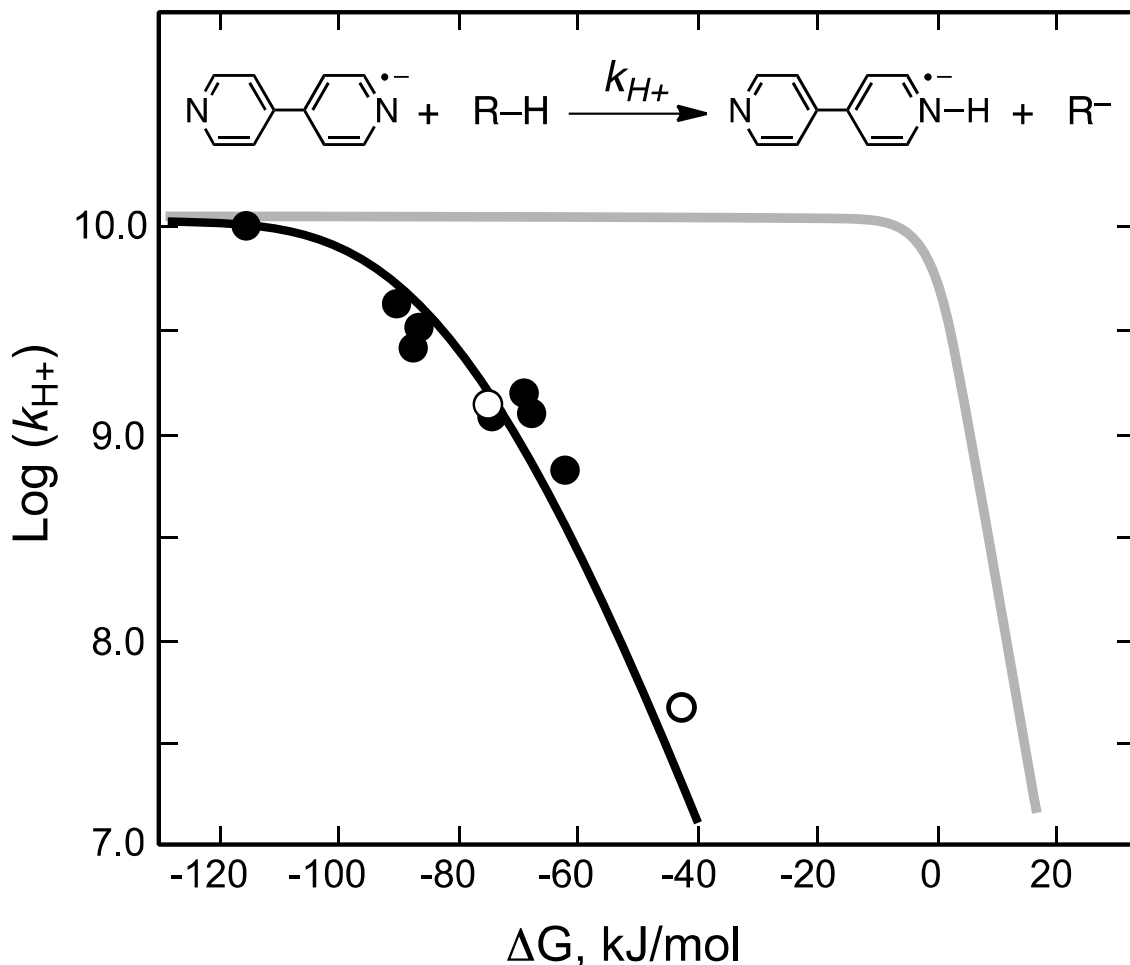


Figure 5.2. Log of the rate constant for bimolecular proton transfer from (closed circles) phenol and (open circles) aliphatic alcohol proton donors to the radical anion of 4,4'-bipyridine, in acetonitrile at room temperature. The solid curve through the data points corresponds to a best fit according to Eqns 1, with $\lambda = 2.0$ eV, $\text{pK}_a(\text{Bpy}^{\bullet-}\text{-H}) = 31$ and $k_{\text{diff}} = 1.1 \times 10^{10} \text{ s}^{-1}$ and $k_{\text{-diff}} = 2.2 \times 10^{10} \text{ s}^{-1}$. The solid grey curve represents a calculated driving force dependence with the same parameters except with $\lambda = 0.2$ eV, showing the dramatic influence of λ at the turnover from diffusion controlled to activated proton transfer.

The pKa of the **Bpy^{•-}-H** conjugate acid of the radical anion is large. The pKa for this structure has previously been estimated using *ab initio* computations to be ca. 20.²⁷ The computation was for water, and it would be expected that the pKa would be smaller in the less polar acetonitrile solvent.

5.4. Summary

For comparison with nucleophilicity, Bronsted basicity needs to be defined kinetically rather than just thermodynamically in terms of pKa. The reorganization energy for the proton transfer reactions of **Bpy^{•-}** are characterized by a large reorganization energy of ca. 2 eV. Consequently, although the **Bpy^{•-}** is a very strong base, it is kinetically less reactive than might be expected on the basis of its pKa. Together with nucleophilicity data collected elsewhere the data reported here allow the complete reactivity of the **Bpy^{•-}** to be quantitatively understood.

References:

1. a) Holy, N. L. *Chem. Rev.*, 1974, 74, 243-277. b) Eberson, L. *Adv. Phys. Org. Chem.* 1982, 18, 79-185. c) Born, M.; Ingemann, S.; Nibbering, N. M. M. *Mass Spec. Revs.* 1997, 16, 181-200
2. See, for example: a) Dorfman, L. M. *Acc. Chem. Res.* 1970, 3, 224-230. b) Hayano, S., Fujihira, M. *Bull. Chem. Soc. Jpn* 1971, 44, 1496. c) Levin, G.; Sutpohen, C.; Szwarc, M. *J. Am. Chem. Soc.* 1972, 94, 2652. d) Levanon, H.; Neta, A.; Trozzolo, A. M. *Chem. Phys. Letts.* 1978, 54, 181-185. e) Cliffel, D. E.; Bard, A. *J. Phys. Chem.* 1994, 98, 8140-8143.
3. Smith, M. M. *March's Advanced Organic Chemistry, 7th Edition*, Wiley: New York, 2013, p 1253.
4. Peters, K. S. *Acc. Chem. Res.* 2009, 42, 89-96.
5. a) Marcus, R. A. *J. Phys. Chem.* 1969, 91, 7224-7225. b) Creutz, C.; Sutin, N. *J. Am. Chem. Soc.* 1988, 110, 2418-2427. c) Albery, W. J. *Ann. Rev. Phys. Chem.* 1980, 31, 227-263.
6. a) Kiefer, P. M.; Hynes, J. T. *J. Phys. Chem. A* 2004, 108, 11809- 11818. b) Kiefer, P. M.; Hynes, J. T. *J. Phys. Chem. A* 2004, 108, 11793- 11808. c) Kiefer, P. M.; Hynes, J. T. *J. Phys. Chem. A* 2003, 107, 9022- 9039. d) Kiefer, P. M.; Hynes, J. T. *J. Phys. Chem. A* 2002, 106, 1850-1861. e) Kiefer, P. M.; Hynes, J. T. *J. Phys. Chem. A* 2002, 106, 1834-1849.
7. a) Peters, K. S.; Cashin, A.; Timbers, P. *J. Am. Chem. Soc.* 2000, 122, 107-113. b) Peters, K. S.; Kim, G. *J. Phys. Chem. A* 2001, 105, 4177- 4181. c) Heeb, L. R.; Peters, K. S. *J. Phys. Chem. A* 2006, 110, 6408-6414.
8. Andrieux, C. P.; Gamby, J.; Hapiot, P.; Saveant, J. M. *J. Am. Chem. Soc.* 2003, 125, 10119-10124.
9. Funston, A. M.; Lyman, S. V.; Saunders-Price, B.; Czapski, G; Miller, J. R. *J. Phys. Chem. B*, 2007, 111, 6895-6902.
10. Ranjan, R.; Olson, J.; Lorance, E. D.; Buttry, D. A.; Gould, I. R. *J. Am. Chem. Soc.*, submitted.

11. a) Barton, E. E.; Rampulla, D. M.; Bocarsly, A. B. *J. Am. Chem. Soc.* 2008, *130*, 6342–6344. b) Barton C., E.; Lakkaraju, P. S.; Rampulla, D. M.; Morris, A. J.; Abelev, E.; Bocarsly, A. B. *J. Am. Chem. Soc.* 2010, *132*, 11539–11551. c) Morris, A. J.; McGibbon, R. T.; Bocarsly, A. B. *ChemSusChem*. 2011, *4*, 191–196.
12. Ranjan, R.; Lorance, E. D.; Gould, I. R., manuscript in preparation.
13. a) Naumov, S.; von Sonntag, C. *Rad. Res.*, 2008, *169*, 355-363. b) Naik, D. B.; Mukherjee, T. *Rad. Phys. Chem.*, 2006, *75*, 42-47. c) Singh, A. K.; Palit, D. K.; Mukherjee, T. *J. Phys. Chem. A*, 2002, *106*, 6084-6093. d) Mohan, H.; Srividya, N.; Ramamurthy, P. *Res. Chem. Inter.* 2000, *26*, 455-467. e) Takacs, E.; Dajka, K.; Wojnarovits, L.; Emmi, S. S. *Phys. Chem. Chem. Phys.*, 2000, *2*, 1431-1433. f) Telo, J. P.; Shohoji, M.; Candida B. L. *J. Chem. Soc. Perkin 2*, 1998, 711-714. g) Shoute, L. C. T.; Mittal, J. P. *J. Phys. Chem.*, 1993, *97*, 8630-8627. h) Parker, V. D.; Tilset, M.; Hammerich, O. *J. Am. Chem. Soc.* 1987, *109*, 7905-6. i) Amatore, C.; Guidelli, R.; Moncelli, M. R.; Saveant, J. M. *J. Electroanal. Chem.*, 1983, *148*, 25-49. j) Neta, P.; Behar, D. *J. Am. Chem. Soc.* 1980, *102*, 4798-802. k) Tolbert, L. M. *J. Am. Chem. Soc.* 1980, *102*, 6808-13. l) Hayon, E.; Simic, M. *J. Am. Chem. Soc.* 1973, *95*, 2433-9.
14. a) Jaworski, J. S. *J. Chem. Soc., Perkin Trans. 2* 1999, 2755-2760. b) Jaworski, J. S.; Cembor, M. *Tetrahedron Lett.* 2000, *41*, 7267-7270. c) Jaworski, J. S.; Cembor, M. *J. Phys. Org. Chem.* 2003, *16*, 655-660.
15. Lorance, E. D.; Kramer, W. H.; Gould, I. R. *J. Am. Chem. Soc.*, 2004, *126*, 14071.
16. a) Poizat, O.; Buntinx, G.; Valat, P.; Wintgens, V.; Bridoux, M. *J. Phys. Chem.* 1993, *97*, 5905-5910. b) Poizat, O.; Buntinx, G.; Ventura, M.; Lautie, M. F. *J. Phys. Chem.* 1991, *95*, 1245-1253. c) Buntinx, G.; Valat, P.; Wintgens, V.; Poizat, O. *J. Phys. Chem.* 1991, *95*, 9347-9352.
17. Gould, I. R.; Mueller, L. J.; Farid, S. *Z. Phys. Chem.* 1991, *170*, 143-157.
18. a) Olmstead, W. N.; Margolin, Z.; Bordwell, F. G. *J. Org. Chem.* 1980, *45*, 3295-3299. b) Bordwell, F. G.; McCallum, R. J.; Olmstead, W. N. *J. Org. Chem.* 1984, *49*, 1424-27.

19. Bordwell, F. G. *Acc. Chem. Res.* 1988, *21*, 456–463.
20. Murov, S. L.; Carmichael, I.; Hug, G. L. *Handbook of Photochemistry, 2nd Edition*; CRC Press: Boca Raton, FL, 1993, p. 207.
21. a) Van Duyne, R. P.; Fischer, S. F. *Chem. Phys.* 1974, *5*, 183. b) Ulstrup, J.; Jortner, J. *J. Chem. Phys.* 1975, *63*, 4358. c) Siders, P.; Marcus, R. A. *J. Am. Chem. Soc.* 1981, *103*, 741.
22. a) Closs, G. L.; Johnson, M. D.; Miller, J. R.; Piotrowiak, P. *J. Am. Chem. Soc.* 1989, *111*, 3751. b) Gould, I. R.; Noukakis, D.; Goodman, J. L.; Young, R. H.; Farid, S. *J. Am. Chem. Soc.* 1993, *115*, 3830. c) Wasielewski, M. R.; Niemcxyk, M. P.; Svec, W. A.; Pewitt, M. B., *J. Am. Chem. Soc.* 1985, *107*, 1080.
23. Sandros, K. *Acta Chem. Scand.* 1964, *18*, 2355
24. a) Scandola, F.; Balzani, V.; Schuster, G. B. *J. Am. Chem. Soc.* 1981, *103*, 2519. b) Farid, S.; Dinnocenzo, J. P.; Merkel, P. B.; Young, R. H.; Shukla, D. *J. Am. Chem. Soc.* 2011, *133*, 4791-4801.
25. North, N. M. *Quart. Rev. Chem. Soc.* 1966, *20*, 421. b) Evans, T. R. *J. Am. Chem. Soc.* 1971, *93*, 2081.
26. Gould, I. R.; Farid, S. *Acc. Chem. Res.* 1996, *29*, 522.
27. Keith, J. A.; Carter, E. A. *J. Am. Chem. Soc.* 2012, *134*, 7580–7583.

CHAPTER 6

SUMMARY OF CHAPTERS AND OUTLOOK FOR FUTURE WORK

6.1. Summary of current work

One of the main themes of the work described in this dissertation is the use of conventional photochemical techniques to obtain a kinetic and mechanistic understanding of bipyridine radical anion properties and reactivity. As detailed in the previous chapters, bipyridine radical anion was successfully synthesized in-situ using a 266 nm monochromatic laser source and its reactivity was studied with various substrates. The decay kinetics of the bipyridine radical anion in the presence of various electrophiles give good insight into the fundamental understanding of the nucleophilic addition reactions. Along with high nucleophilicity, bipyridine radical anion acts as a strong base and facilitates elimination reactions on alkyl halides. We were able to estimate the pKa of the bipyridine radical anion utilizing Marcus's proton transfer theory.

The associated complexity of the CO₂ reaction with bipyridine radical anion was studied in detail. Presence of trace amount of water in the solvent system makes it too difficult to understand and monitor the actual reaction. With dry solvent, we were able to study the CO₂ kinetics with the radical anion.

6.2. What did we learn about the bipyridine radical anion

Bipyridine radical anion has a very small life time, ~ 1 microsecond under argon. It reacts very quickly with O₂, with a bimolecular rate constant of 5×10^8 . In the presence

of trimethylamine as the donor, bipyridine radical is the major product. DABCO, almost exclusively generates radical anions.

Bpy radical anions are very strong nucleophiles and react with cyclohexanone with a bimolecular rate constant of $\sim 1 \times 10^7 \text{ Lmol}^{-1}\text{s}^{-1}$. The reactivity trend with other aldehyde, ketone, anhydride and esters confirms the nucleophilic addition behavior.

Bpy radical anion acts as a strong base and abstracts a proton from alkyl halides to facilitate the E2 mechanism. SN2 mechanism was observed with primary halides. pKa measurement confirms high basic character of the radical anion, ~ 40 in DMSO. Radical anion undergoes diffusion controlled reaction with p-nitrophenol.

Bpy radical anion reacts with CO_2 with a rate constant $\sim 1 \times 10^9 \text{ LMol}^{-1}\text{S}^{-1}$, which is one of the fastest nucleophilic addition reactions studied so far.

6.3. Recommendations for future work

The work described in this thesis contributes to ongoing research towards a plausible and cost-effective method for CO_2 sequestration and trapping. Developing a comprehensive understanding of the reaction mechanism and steps involved will help in fine-tuning the variables for commercial CO_2 trapping. Instead of an electrochemical set-up to supply and withdraw electrons for subsequent trapping and release of CO_2 , research could be directed in employing UV-light as an source of energy to facilitate this process. Bipyridine radical anion is very reactive towards oxygen which limits its application in commercial process. Validating and fine-tuning the catalyst based on the reduction potential would be a step forward towards employing this technique for large scale commercial applications.

REFERENCES

CHAPTER 1

1. Climate Change 2001: Synthesis Report. A Contribution of Working Groups I, II, and III to the Third Assessment Report of the Intergovernmental Panel on Climate Change (Ed.: R. T. Watson), Cambridge University Press, New York, 2001.
2. Goddard Institute of Space Studies NASA. 2009 [cited 2009 November 12]; Available from: <http://data.giss.nasa.gov/gistemp/graphs/Fig.A2.txt>.
3. M. M. Halmann, M. Steinberg, Greenhouse Gas Carbon Dioxide Mitigation, Lewis, New York, 1999
4. Doney, S. C.; Fabry, V. J.; Feely, R. A.; Kleypas, J. A. *Annu. Rev. Mar. Sci.* 2009, 1, 169.
5. Geider, R. J.; et al. *Global Change Biol.* 2001, 7, 849.
6. Beer, C.; et al. *Science* 2010, 329, 834.
7. Earth System Research Laboratory Global Monitoring Division. 2009 [cited 2009 November 12]; Available from: ftp://ftp.cmdl.noaa.gov/ccg/co2/trends/co2_mm_mlo.txt.
8. Henni, A.; Li, J.; Tontiwachwuthikul, P. *Ind. Eng. Chem. Res.* 2008, 47, 2213-2220.
9. Wood, R.W. (1909). "Note on the Theory of the Greenhouse". *Philosophical Magazine* 17: 319–320.
10. "Introduction to Atmospheric Chemistry, by Daniel J. Jacob, Princeton University Press, 1999. Chapter 7, "The Greenhouse Effect""
11. Energy Information Administration, Electric Power Annual 2007: A Summary. 2009: Washington, D.C.

12. Energy Information Administration, International Energy Outlook. 2009: Washington, D.C.
13. United Nations Environment Programme and the Climate Change Secretariat (UNFCCC): "Climate Change Information Kit", July 2002.
14. Doney, S. C.; Fabry, V. J.; Feely, R. A.; Kleypas, J. A. *Annu. Rev. Mar. Sci.* 2009, 1, 169.
15. Barton, C. E.; Lakkaraju, P. S.; Rampulla, D. M.; Morris, A. J.; Abelev, E.; Bocarsly, A. B. *J. Am. Chem. Soc.* 2010, 132, 11539.
16. Seshadri, G.; Lin, C.; Bocarsly, A. B.; *J. Electroanal. Chem.* 1994, 372, 145.
17. Barton, E. E.; Rampulla, D. M.; Bocarsly, A. B.; *J. Am. Chem. Soc.* 2008, 130, 6342.
18. Bocarsly, A. B.; Gibson, Q. D.; Morris, A. J.; L'Esperance, R. P.; Detweiler, Z. M.; Lakkaraju, P. S.; Zeitler, E. L.; Shaw, T. W.; *ACS Catal.* 2012, 2, 1684.
19. de Tacconi, N. R.; Chanmanee, W.; Dennis, B. H.; MacDonnell, F. M.; Boston, D. J.; Rajeshwar, K. *Electrochem. Solid State* 2011, 15, B5.
20. Kondure, P. B.; Vaidya, P. D.; Kenig, E. Y.; *Environ. Sci. Technol.* 2010, 44, 2138–2143
21. Pani, F.; Gaunand, A.; Cadours, R.; Bouallou, C.; Richon, D.; *J. Chem. Eng. Data* 1997, 42, 353-359
22. Rochelle, G. T., Amine Scrubbing for CO₂ Capture. *Science*, 2009. 325(5948): p. 1652-1654.
23. Danckwerts, P. V. (1979). "The Reaction of Carbon Dioxide with Ethanolamines." *Chem. Engr. Sci.* 34: 443.
24. Morris, A. J.; Meyer, G. J.; Fujita, E. Molecular Approaches to the Photocatalytic Reduction of Carbon Dioxide for Solar Fuels. *Acc. Chem. Res.* 2009, 42, 1983–1994

25. Fujita, E. Photochemical Carbon Dioxide Reduction with Metal Complexes. *Coord. Chem. Rev.* 1999, 185, 373–384.
26. Takeda, H.; Ishitani, O. Development of Efficient Photocatalytic Systems for CO₂ Reduction Using Mononuclear and Multinuclear Metal Complexes Based on Mechanistic Studies. *Coord. Chem. Rev.* 2010, 254, 346–354.
27. Liang, Y. T.; Vijayan, B. K.; Gray, K. A.; Hersam, M. C. Minimizing Graphene Defects Enhances Titania Nanocomposite-Based Photocatalytic Reduction of CO₂ for Improved Solar Fuel Production. *Nano Lett.* 2011, 11, 2865–2870.
28. Tsai, C. W.; Chen, H. M.; Liu, R. S.; Asakura, K.; Chan, T. S.; Ni@NiO Core–Shell Structure-Modified Nitrogen-Doped InTaO₄ for Solar-Driven Highly Efficient CO₂ Reduction to Methanol. *J. Phys. Chem. C* 2011, 115, 10180–10186.
29. Izumi, Y. Recent Advances in the Photocatalytic Conversion of Carbon Dioxide to Fuels with Water and/or Hydrogen Using Solar Energy and Beyond. *Coord. Chem. Rev.* 2013, 257, 171–186.
30. Aurian-Blajeni, B.; Halmann, M.; Manassen, J. Electrochemical Measurement on the Photoelectrochemical Reduction of Aqueous Carbon Dioxide on p-Gallium Phosphide and p-Gallium Arsenide Semiconductor Electrodes. *Sol. Energy Mater.* 1983, 8, 425–440.
31. Halmann, M. Photoelectrochemical Reduction of Aqueous Carbon Dioxide on p-type Gallium Phosphide in Liquid Junction Solar Cells. *Nature* 1978, 275, 115.
32. Kaneco, S.; Katsumata, H.; Suzuki, T.; Ohta, K. Photoelectrochemical Reduction of Carbon Dioxide at p-type Gallium Arsenide and p-type Indium Phosphide Electrodes in Methanol. *Chem. Eng. J.* 2006, 116, 227–231.
33. Choi, S., Drese, J.H., & Jones, C.W., Adsorbent Materials for Carbon Dioxide Capture from Large Anthropogenic Point Sources. *Chemsuschem* 2 (9), 796-854 (2009).
34. Wolf, G.H., Chizmeshya, A.V.G., Diefenbacher, J., & McKelvy, M.J., In situ observation of CO₂ sequestration reactions using a novel microreaction system. *Environmental Science & Technology* 38 (3), 932-936 (2004).

35. Rubin, E. S., A. B. Rao, et al. (2004). Comparative Assessment of Fossil Fuel Power Plants with CO₂ Capture and Storage. 7th International Conference on Greenhouse Gas Control Technologies, Vancouver, Canada.
36. Danckwerts, P. V. (1979). "The Reaction of Carbon Dioxide with Ethanolamines." *Chem. Engr. Sci.* 34: 443.
37. National Energy Technology Laboratory Report, Research and Development Goals for CO₂ Capture Technology, DOE/NETL-2009/1366 (2011).
38. Mizen, M.B. & Wrighton, M.S., Reductive Addition of Co₂ to 9,10-Phenanthrenequinone. *Journal of the Electrochemical Society* 136 (4), 941-946 (1989).
39. Scovazzo, P., Poshusta, J., DuBois, D., Koval, C., & Noble, R., Electrochemical separation and concentration of < 1% carbon dioxide from nitrogen. *Journal of the Electrochemical Society* 150 (5), D91-D98 (2003).
40. Stern, M.C. *et al.*, Electrochemically Mediated Separation for Carbon Capture. *Energy Procedia* 4, 860-867 (2011).
41. Fischer, B.; Eisenberg, R. J. *Am. Chem. Soc.* 1980, 102, 7361
42. Tinnemans, A. H. A.; Koster, T. P. M.; Thewissen, D. H. M. W.; Mackor, A. M. *Recl. TraV. Chim. Pays-Bas.* 1984, 103, 288.
43. Pearce, D. J.; Pletcher, D.J. *Electroanal. Chem.* 1986, 197, 317.
44. Beley, M.; Collin, J. P.; Ruppert, R.; Sauvage, J. P.J. *Chem. Soc., Chem. Commun.* 1984, 1315.
45. Beley, M.; Collin, J. P.; Ruppert, R.; Sauvage, J. P.J. *Am. Chem. Soc.*, 1986, 108, 7461.
46. Ishida, H.; Tanaka, K.; Tanaka, T. *Chem. Lett.* 1985, 405.
47. Ishida, H.; Tanaka, H.; Tanaka, K.; Tanaka, T. *J. Chem. Soc., Chem. Commun.* 1987, 131.
48. Ishida, H.; Tanaka, K.; Tanaka, T. *Organometallics* 1987, 6, 181.

49. Yan, Y.; Gu, J.; Bocarsly, A.B.; *Aerosol and Air Quality Research*, 14: 515–521, 2014
50. G. J. Kavarnos, *Fundamentals of Photoinduced Electron Transfer*, VCH Publishers, New London, CT, 1999, p. 359.
51. Nicholas J. Turro, *Modern Molecular Photochemistry of Organic Molecules*, University Science Books, 2010. P. 418.

CHAPTER 2

1. Herkstroeter, W. G.; Gould, I. R. In *Physical Methods of Chemistry Series*, 2nd ed.; Rossiter, B., Baetzold, R., Eds.; Wiley: New York, 1993; Vol. 8, p 225.
2. Lorance, E. D.; Kramer, W. H.; Gould, I. R. *J. Am. Chem. Soc.*, 2004, 126, 14071.
3. Armarego, W. L. F.; Chai, C. L. L.; *Purification of Laboratory Chemicals*, Elsevier, 2013, p. 105

CHAPTER 3

1. a) Dell'Amico, D. B.; Calderazzo, F.; Labella, L.; Marchetti, F.; Pampaloni, G. *Chem. Rev.* 2003, 103, 3857- 3898. b) Jessop, P. G.; Joó, F.; Tai, C. C. *Coord. Chem. Rev.* 2004, 248, 2425-2442. c) Sakakura, T.; Choi, J. C.; Yasuda, H. *Chem. Rev.* 2007, 107, 2365-2387. d) Mikkelsen, M., Jorgensen, M.; Krebs, F. C. *Energy Environ. Sci.* 2010, 3, 43–81.
2. a) Kumar, B.; Llorente, M.; Froehlich, J.; Dang, T.; Sathrum, A.; Kubiak, C. P. *Annu. Rev. Phys. Chem.*, 2012, 63, 541-569. b) Centi, G.; Perathoner, S. *Catal. Today* 2009, 148, 191–205.
3. a) Aresta, M. *Carbon Dioxide Recovery and Utilization*; Kluwer Academic Publishers: Dordrecht, 2010. b) Metz, B., Davidson, O., De Coninck, H., Loos, M. & Meyer, L. *Carbon Dioxide Capture and Storage*; Cambridge University Press: Cambridge UK, 2005.
4. a) Villiers, C.; Dognon, J.-P.; Pollet, R.; Thuory, P.; Ephritikhine, M. *Angew. Chem. Int. Ed.* 2010, 49, 3465 –3468. b) Ma, J.; Zhang, X.; Zhao, N.; Al-Arifi, A. S. N.; Aouak, T.; Al-Othman, Z. A.; Xiao, F.; Wei, W.; Sun, Y. *J. Mol. Catal. A* 2010, 315, 76-81. c) McGhee, W.; Riley, D.; Christ, K.; Pan, Y.; Parnas, B. *J. Org. Chem.* 1995, 60, 2820–2830. d) McGhee, W.; Riley, D. *J. Org. Chem.*

- 1995, 60, 6205-6207. e) Hooker, J. M.; Reibel, A. T.; Hill, S. M.; Schueller, M. J.; Fowler, J. S. *Angew. Chem. Int. Ed.* 2009, 48, 3482-3485.
5. Morris, A. J.; Meyer, G. J.; Fujita, E. Molecular Approaches to the Photocatalytic Reduction of Carbon Dioxide for Solar Fuels. *Acc. Chem. Res.* 2009, 42, 1983–1994
 6. Fujita, E. Photochemical Carbon Dioxide Reduction with Metal Complexes. *Coord. Chem. Rev.* 1999, 185, 373–384.
 7. Takeda, H.; Ishitani, O. Development of Efficient Photocatalytic Systems for CO₂ Reduction Using Mononuclear and Multinuclear Metal Complexes Based on Mechanistic Studies. *Coord. Chem. Rev.* 2010, 254, 346–354.
 8. Liang, Y. T.; Vijayan, B. K.; Gray, K. A.; Hersam, M. C. Minimizing Graphene Defects Enhances Titania Nanocomposite-Based Photocatalytic Reduction of CO₂ for Improved Solar Fuel Production. *Nano Lett.* 2011, 11, 2865–2870.
 9. Tsai, C. W.; Chen, H. M.; Liu, R. S.; Asakura, K.; Chan, T. S.; Ni@NiO Core–Shell Structure-Modified Nitrogen-Doped InTaO₄ for Solar-Driven Highly Efficient CO₂ Reduction to Methanol. *J. Phys. Chem. C* 2011, 115, 10180–10186.
 10. Izumi, Y. Recent Advances in the Photocatalytic Conversion of Carbon Dioxide to Fuels with Water and/or Hydrogen Using Solar Energy and Beyond. *Coord. Chem. Rev.* 2013, 257, 171–186.
 11. Aurian-Blajeni, B.; Halmann, M.; Manassen, J. Electrochemical Measurement on the Photoelectrochemical Reduction of Aqueous Carbon Dioxide on p-Gallium Phosphide and p-Gallium Arsenide Semiconductor Electrodes. *Sol. Energy. Mater.* 1983, 8, 425–440.
 12. Halmann, M. Photoelectrochemical Reduction of Aqueous Carbon Dioxide on p-type Gallium Phosphide in Liquid Junction Solar Cells. *Nature* 1978, 275, 115.
 13. Kaneco, S.; Katsumata, H.; Suzuki, T.; Ohta, K. Photoelectrochemical Reduction of Carbon Dioxide at p-type Gallium Arsenide and p-type Indium Phosphide Electrodes in Methanol. *Chem. Eng. J.* 2006, 116, 227–231.

14. a) Barton, E. E.; Rampulla, D. M.; Bocarsly, A. B. *J. Am. Chem. Soc.* 2008, *130*, 6342–6344. b) Barton Cole, E.; Lakkaraju, P. S.; Rampulla, D. M.; Morris, A. J. Abelev, E.; Bocarsly, A. B. *J. Am. Chem. Soc.* 2010, *132*, 11539–11551. c) Morris, A. J.; McGibbon, R. T.; Bocarsly, A. B. *ChemSusChem*, 2011, *4*, 191–196.
15. Armarego, W. L. F.; Chai, C. L. L.; *Purification of Laboratory Chemicals*, Elsevier, 2013, p. 105
16. Ebersson, L. E. *Electron Transfer Reactions in Organic Chemistry*; Springer-Verlag: New York, 1988.
17. Sakakura, T., Choi, J.-C.; Yasuda, H. *Chem. Rev.* 2007, *107*, 2365–2387.
18. Keith, J. A.; Carter, E. A.; *J. Am. Chem. Soc.* 2012, *134*, 7580–7583
19. a) Ashby, E.C. *Acc. Chem. Res.*, 1988, *21* (11), pp 414–421. b) Rossi, R. A. *Acc. Chem. Res.* 1982, *15*, 164-170. c) Bunnett, J. F.; Kim, J. K. *J. Am. Chem. Soc.* 1970, *92*, 7463-7464.

CHAPTER 4

1. a) Dell'Amico, D. B.; Calderazzo, F.; Labella, L.; Marchetti, F.; Pampaloni, G. *Chem. Rev.* 2003, *103*, 3857- 3898. b) Jessop, P. G.; Joó, F.; Tai, C. C. *Coord. Chem. Rev.* 2004, *248*, 2425-2442. c) Sakakura, T.; Choi, J. C.; Yasuda, H. *Chem. Rev.* 2007, *107*, 2365-2387. d) Mikkelsen, M., Jorgensen, M.; Krebs, F. C. *Energy Environ. Sci.* 2010, *3*, 43–81.
2. a) Kumar, B.; Llorente, M.; Froehlich, J.; Dang, T.; Sathrum, A.; Kubiak, C. P. *Annu. Rev. Phys. Chem.*, 2012, *63*, 541-569. b) Centi, G.; Perathoner, S. *Catal. Today* 2009, *148*, 191–205.
3. a) Aresta, M. *Carbon Dioxide Recovery and Utilization*; Kluwer Academic Publishers: Dordrecht, 2010. b) Metz, B., Davidson, O., De Coninck, H., Loos, M. & Meyer, L. *Carbon Dioxide Capture and Storage*; Cambridge University Press: Cambridge UK, 2005.
4. a) Villiers, C.; Dognon, J.-P.; Pollet, R.; Thuory, P.; Ephritikhine, M. *Angew. Chem. Int. Ed.* 2010, *49*, 3465 –3468. b) Ma, J.; Zhang, X.; Zhao, N.; Al-Arifi, A. S. N.; Aouak, T.; Al-Othman, Z. A.; Xiao, F.; Wei, W.; Sun, Y. *J. Mol. Catal. A*

- 2010, 315, 76-81. c) McGhee, W.; Riley, D.; Christ, K.; Pan, Y.; Parnas, B. J. *Org. Chem.* 1995, 60, 2820–2830. d) McGhee, W.; Riley, D. *J. Org. Chem.* 1995, 60, 6205-6207. e) Hooker, J. M.; Reibel, A. T.; Hill, S. M.; Schueller, M. J.; Fowler, J. S. *Angew. Chem. Int. Ed.* 2009, 48, 3482-3485.
5. Metz, B. *IPCC Special Report on Carbon Dioxide Capture and Storage*; Cambridge University Press: Cambridge, 2005.
 6. Freguia, S.; Rochelle, G. T. *AIChE J.* 2003, 49, 1676– 168. b) Kim, I.; Svendsen, H. F. *Ind. Eng. Chem. Res.* 2007, 46, 5803-5809. c) Davison, J. *Energy* 2007, 32, 1163– 1176.
 7. a) Barton, E. E.; Rampulla, D. M.; Bocarsly, A. B. *J. Am. Chem. Soc.* 2008, 130, 6342–6344. b) Barton Cole, E.; Lakkaraju, P. S.; Rampulla, D. M.; Morris, A. J. Abelev, E.; Bocarsly, A. B. *J. Am. Chem. Soc.* 2010, 132, 11539–11551. c) Morris, A. J.; McGibbon, R. T.; Bocarsly, A. B. *ChemSusChem*, 2011, 4, 191–196.
 8. Keith, J. A.; Carter, E. A. *J. Am. Chem. Soc.*, 2012, 134, 7580-7583.
 9. a) Constantine, C.; Saveant, J.-M. *Chem. Soc. Rev.* 2013, 42, 2423-2436. b) Gattrell, M.; Gupta, N.; Co, A. *J. Electroanal. Chem.* 2006, 594, 1-19. c) Hori, Y. in *Modern Aspects of Electrochemistry*, Vol. 42; Vayenas, C.; White, R. E.; Gamboa-Adelco, M. E. (Eds.), Springer: New York, 2008, p. 89. d) Qiao, J.; Liu, Y.; Hong, F.; Zhang, J. *Chem. Soc. Rev.* 2014, 43, 631-675.
 10. a) Wayner, D. D.; McPhee, D. J.; Griller, D. *J. Am. Chem. Soc.* 1988, 110, 132-137. b) Griller, D.; Wayner, D. D. M. *Pure Appl. Chem.* 1989, 61, 717-724.
 11. a) Poizat, O.; Buntinx, G.; Valat, P.; Wintgens, V.; Bridoux, M. *J. Phys. Chem.* 1993, 97, 5905-5910. b) Poizat, O.; Buntinx, G.; Ventura, M.; Lautie, M. F. *J. Phys. Chem.* 1991, 95, 1245-1253. c) Buntinx, G.; Valat, P.; Wintgens, V.; Poizat, O. *J. Phys. Chem.* 1991, 95, 9347-9352.
 12. Wosinska, Z. M.; Stump, F. L.; Ranjan, R.; Lorange, E. D.; Finley, G. N.; Patel, P. P.; Khawaja, M. A.; Odom, K. L.; Kramer, W. H.; Gould, I. R. *Photochem. Photobiol.*, 2014, 90, 313-328.
 13. Sakakura, T., Choi, J.-C.; Yasuda, H. *Chem. Rev.* 2007, 107, 2365–2387.

14. Zheng, J. J.; Zhao, Y.; Truhlar, D. G. *J. Chem. Theory Comput.*, 5, (2009) 808–821.
15. Moore, J. W.; Pearson, R. G. *Kinetics and Mechanism*, 3rd ed.; John Wiley: New York, 1981.
16. Gould, I. R.; Lenhard, J. R.; Farid, S. *J. Phys. Chem A*. 2004, 108, 10949-10956.
17. a) Lorance, E. D., Hendrickson, K., Gould, I. R. *J. Org. Chem.*, 2005, 70, 2014-2020. b) Lorance, E. D.; Gould, I. R. *J. Phys. Chem. A*. 2005, 109, 2912. c) Lorance, E. D.; Kramer, W. H.; Gould, I. R. *J. Am. Chem. Soc.*, 2004, 126, 14071. d) Gould, I. R.; Shukla, D.; Giesen, D.; Farid, S. *Helv. Chim. Acta*, 2001, 84, 2796-2812.
18. Appetecchi G. B.; Scaccia S.; Tizzani C.; Alessandrini F.; Passerini S. *J. Electrochem. Soc.* 2006, 153, A1685–A1691.
19. Gaussian 09, Revision A.02, M. J. Frisch, G. W. Trucks, H. B. Schlegel, G. E. Scuseria, M. A. Robb, J. R. Cheeseman, G. Scalmani, V. Barone, B. Mennucci, G. A. Petersson, H. Nakatsuji, M. Caricato, X. Li, H. P. Hratchian, A. F. Izmaylov, J. Bloino, G. Zheng, J. L. Sonnenberg, M. Hada, M. Ehara, K. Toyota, R. Fukuda, J. Hasegawa, M. Ishida, T. Nakajima, Y. Honda, O. Kitao, H. Nakai, T. Vreven, J. A. Montgomery, Jr., J. E. Peralta, F. Ogliaro, M. Bearpark, J. J. Heyd, E. Brothers, K. N. Kudin, V. N. Staroverov, R. Kobayashi, J. Normand, K. Raghavachari, A. Rendell, J. C. Burant, S. S. Iyengar, J. Tomasi, M. Cossi, N. Rega, J. M. Millam, M. Klene, J. E. Knox, J. B. Cross, V. Bakken, C. Adamo, J. Jaramillo, R. Gomperts, R. E. Stratmann, O. Yazyev, A. J. Austin, R. Cammi, C. Pomelli, J. W. Ochterski, R. L. Martin, K. Morokuma, V. G. Zakrzewski, G. A. Voth, P. Salvador, J. J. Dannenberg, S. Dapprich, A. D. Daniels, O. Farkas, J. B. Foresman, J. V. Ortiz, J. Cioslowski, and D. J. Fox, Gaussian, Inc., Wallingford CT, 2009.
20. Zhao, Y.; Truhlar, D. G. *Theor. Chem. Acc.* 2008, 120, 215-241.

21. Dunning, T. H. *J. Chem. Phys.* 1989, *90*, 1007-1023. b) Kendall, R. A.; Dunning, T. H.; Harrison, R. J. *J. Chem. Phys.* 1992, *96*, 6796-806. c) Woon, D. E.; Dunning, T. H. *J. Chem. Phys.* 1993, *98*, 1358-1371. d) Peterson, K. A.; Woon, D. E.; Dunning, T. H. *J. Chem. Phys.* 1994, *100*, 7410-7415. e) Wilson, A. K.; van Mourik, T.; Dunning, T. H. *J. Mol. Struct. (Theochem)* 1996, *388*, 3393-49. f) Davidson, E. R. *Chem. Phys. Lett.* 1996, *260*, 514-518.
22. a) Truhlar, D. G.; Pliego, J. R. in *Continuum Solvation Models in Chemical Physics: From Theory to Applications*, Mennucci, B.; Cammi, R. (Eds.); Wiley: Chichester, 2008. p.338-365 (esp. 357-8). b) Raspert, G.; Nguyen, M. T.; Kelly, S.; Hegarty, A. F. *J. Org. Chem.* 1998, *63*, 9669-9677. c) Cavalli, A.; Masetti, M.; Recantini, M.; Prandi, C.; Guarna, A.; Occhiato, E. G. *Chem. Eur. J.* 2006, *12*, 2836-2845.

CHAPTER 5

1. a) Holy, N. L. *Chem. Rev.*, 1974, *74*, 243-277. b) Ebersson, L. *Adv. Phys. Org. Chem.* 1982, *18*, 79-185. c) Born, M.; Ingemann, S.; Nibbering, N. M. M. *Mass Spec. Revs.* 1997, *16*, 181-200
2. See, for example: a) Dorfman, L. M. *Acc. Chem. Res.* 1970, *3*, 224-230. b) Hayano, S., Fujihira, M. *Bull. Chem. Soc. Jpn* 1971, *44*, 1496. c) Levin, G.; Sutpohen, C.; Szwarc, M. *J. Am. Chem. Soc.* 1972, *94*, 2652. d) Levanon, H.; Neta, A.; Trozzolo, A. M. *Chem. Phys. Letts.* 1978, *54*, 181-185. e) Cliffel, D. E.; Bard, A. J. *J. Phys. Chem.* 1994, *98*, 8140-8143.
3. Smith, M. M. *March's Advanced Organic Chemistry, 7th Edition*, Wiley: New York, 2013, p 1253.
4. Peters, K. S. *Acc. Chem. Res.* 2009, *42*, 89-96.
5. a) Marcus, R. A. *J. Phys. Chem.* 1969, *91*, 7224-7225. b) Creutz, C.; Sutin, N. *J. Am. Chem. Soc.* 1988, *110*, 2418-2427. c) Albery, W. J. *Ann. Rev. Phys. Chem.* 1980, *31*, 227-263.
6. a) Kiefer, P. M.; Hynes, J. T. *J. Phys. Chem. A* 2004, *108*, 11809- 11818. b) Kiefer, P. M.; Hynes, J. T. *J. Phys. Chem. A* 2004, *108*, 11793- 11808. c) Kiefer, P. M.; Hynes, J. T. *J. Phys. Chem. A* 2003, *107*, 9022- 9039. d) Kiefer, P. M.; Hynes, J. T. *J. Phys. Chem. A* 2002, *106*, 1850-1861. e) Kiefer, P. M.; Hynes, J. T. *J. Phys. Chem. A* 2002, *106*, 1834-1849.

7. a) Peters, K. S.; Cashin, A.; Timbers, P. *J. Am. Chem. Soc.* 2000, *122*, 107-113. b) Peters, K. S.; Kim, G. *J. Phys. Chem. A* 2001, *105*, 4177-4181. c) Heeb, L. R.; Peters, K. S. *J. Phys. Chem. A* 2006, *110*, 6408-6414.
8. Andrieux, C. P.; Gamby, J.; Hapiot, P.; Saveant, J. M. *J. Am. Chem. Soc.* 2003, *125*, 10119-10124.
9. Funston, A. M.; Lyman, S. V.; Saunders-Price, B.; Czapski, G.; Miller, J. R. *J. Phys. Chem. B*, 2007, *111*, 6895-6902.
10. Ranjan, R.; Olson, J.; Lorance, E. D.; Buttry, D. A.; Gould, I. R. *J. Am. Chem. Soc.*, submitted.
11. a) Barton, E. E.; Rampulla, D. M.; Bocarsly, A. B. *J. Am. Chem. Soc.* 2008, *130*, 6342-6344. b) Barton C., E.; Lakkaraju, P. S.; Rampulla, D. M.; Morris, A. J.; Abelev, E.; Bocarsly, A. B. *J. Am. Chem. Soc.* 2010, *132*, 11539-11551. c) Morris, A. J.; McGibbon, R. T.; Bocarsly, A. B. *ChemSusChem*. 2011, *4*, 191-196.
12. Ranjan, R.; Lorance, E. D.; Gould, I. R., manuscript in preparation.
13. a) Naumov, S.; von Sonntag, C. *Rad. Res.*, 2008, *169*, 355-363. b) Naik, D. B.; Mukherjee, T. *Rad. Phys. Chem.*, 2006, *75*, 42-47. c) Singh, A. K.; Palit, D. K.; Mukherjee, T. *J. Phys. Chem. A*, 2002, *106*, 6084-6093. d) Mohan, H.; Srividya, N.; Ramamurthy, P. *Res. Chem. Inter.* 2000, *26*, 455-467. e) Takacs, E.; Dajka, K.; Wojnarovits, L.; Emmi, S. S. *Phys. Chem. Chem. Phys.*, 2000, *2*, 1431-1433. f) Telo, J. P.; Shohoji, M.; Candida B. L. *J. Chem. Soc. Perkin 2*, 1998, 711-714. g) Shoute, L. C. T.; Mittal, J. P. *J. Phys. Chem.*, 1993, *97*, 8630-8627. h) Parker, V. D.; Tilset, M.; Hammerich, O. *J. Am. Chem. Soc.* 1987, *109*, 7905-6. i) Amatore, C.; Guidelli, R.; Moncelli, M. R.; Saveant, J. M. *J. Electroanal. Chem.*, 1983, *148*, 25-49. j) Neta, P.; Behar, D. *J. Am. Chem. Soc.* 1980, *102*, 4798-802. k) Tolbert, L. M. *J. Am. Chem. Soc.* 1980, *102*, 6808-13. l) Hayon, E.; Simic, M. *J. Am. Chem. Soc.* 1973, *95*, 2433-9.
14. a) Jaworski, J. S. *J. Chem. Soc., Perkin Trans. 2* 1999, 2755-2760. b) Jaworski, J. S.; Cembor, M. *Tetrahedron Lett.* 2000, *41*, 7267-7270. c) Jaworski, J. S.; Cembor, M. *J. Phys. Org. Chem.* 2003, *16*, 655-660.
15. Lorance, E. D.; Kramer, W. H.; Gould, I. R. *J. Am. Chem. Soc.* 2004, *126*,

14071.

16. a) Poizat, O.; Buntinx, G.; Valat, P.; Wintgens, V.; Bridoux, M. *J. Phys. Chem.* 1993, *97*, 5905-5910. b) Poizat, O.; Buntinx, G.; Ventura, M.; Lautie, M. F. *J. Phys. Chem.* 1991, *95*, 1245-1253. c) Buntinx, G.; Valat, P.; Wintgens, V.; Poizat, O. *J. Phys. Chem.* 1991, *95*, 9347-9352.
17. Gould, I. R.; Mueller, L. J.; Farid, S. *Z. Phys. Chem.* 1991, *170*, 143-157.
18. a) Olmstead, W. N.; Margolin, Z.; Bordwell, F. G. *J. Org. Chem.* 1980, *45*, 3295-3299. b) Bordwell, F. G.; McCallum, R. J.; Olmstead, W. N. *J. Org. Chem.* 1984, *49*, 1424-27.
19. Bordwell, F. G. *Acc. Chem. Res.* 1988, *21*, 456-463.
20. Murov, S. L.; Carmichael, I.; Hug, G. L. *Handbook of Photochemistry, 2nd Edition*; CRC Press: Boca Raton, FL, 1993, p. 207.
21. a) Van Duyne, R. P.; Fischer, S. F. *Chem. Phys.* 1974, *5*, 183. b) Ulstrup, J.; Jortner, J. *J. Chem. Phys.* 1975, *63*, 4358. c) Siders, P.; Marcus, R. A. *J. Am. Chem. Soc.* 1981, *103*, 741.
22. a) Closs, G. L.; Johnson, M. D.; Miller, J. R.; Piotrowiak, P. *J. Am. Chem. Soc.* 1989, *111*, 3751. b) Gould, I. R.; Noukakis, D.; Goodman, J. L.; Young, R. H.; Farid, S. *J. Am. Chem. Soc.* 1993, *115*, 3830. c) Wasielewski, M. R.; Niemcxyk, M. P.; Svec, W. A.; Pewitt, M. B., *J. Am. Chem. Soc.* 1985, *107*, 1080.
23. Sandros, K. *Acta Chem. Scand.* 1964, *18*, 2355
24. a) Scandola, F.; Balzani, V.; Schuster, G. B. *J. Am. Chem. Soc.* 1981, *103*, 2519. b) Farid, S.; Dinnocenzo, J. P.; Merkel, P. B.; Young, R. H.; Shukla, D. *J. Am. Chem. Soc.* 2011, *133*, 4791-4801.
25. North, N. M. *Quart. Rev. Chem. Soc.* 1966, *20*, 421. b) Evans, T. R. *J. Am. Chem. Soc.* 1971, *93*, 2081.

26. Gould, I. R.; Farid, S. *Acc. Chem. Res.* 1996, 29, 522.
27. Keith, J. A.; Carter, E. A. *J. Am. Chem. Soc.* 2012, 134, 7580–7583.